https://doi.org/10.5194/egusphere-2025-1467
Preprint. Discussion started: 15 April 2025


# Reviews and Syntheses: Best practices for the application of marine GDGTs as proxy for paleotemperatures: sampling, processing, analyses, interpretation, and archiving protocols

Peter K. Bijl[1]*, Kasia K. Śliwińska[2]*, Bella Duncan[3], Arnaud Huguet[4], Sebastian Naeher[5,6], Ronnakrit Rattanasriampaipong[7,8], Claudia Sosa-Montes de Oca[9], Alexandra Auderset[10], Melissa A. Berke[11], Bum Soo Kim[12,13], Nina Davtian[14], Tom Dunkley Jones[15], Desmond D. Eefting[16], Felix J. Elling[17], Lauren O'Connor[1], Richard D. Pancost[9], Francien Peterse[1], Pierrick Fenies[18], Addison Rice[1], Appy Sluijs[1], Devika Varma[19], Wenjie Xiao[20], Yige Zhang[21]

[1]Department of Earth Sciences, Faculty of Geosciences, Utrecht University, Utrecht, the Netherlands. ORCID 000-000-002-1710-4012 (Bijl) 0000-0003-1872-1853 (O'Connor) 0000-0001-8781-2826 (Peterse) 0000-0002-4507-6717 (Rice) 0000-0003-2382-0215 (Sluijs)
[2]Geological Survey of Denmark and Greenland (GEUS), Department of geoenergy and storage, Copenhagen, Denmark. ORCID 0000-0001-5488-8832
[3]Antarctic Research Centre, Victoria University of Wellington, Wellington, New Zealand. ORCID 0000-0003-1108-6033
[4]Sorbonne Université, CNRS, EPHE, PSL, UMR METIS, Paris, 75005, France. ORCID 0000-0002-6124-2922
[5]GNS Science, Lower Hutt, New Zealand; ORCID 0000-0002-5336-6458
[6]School of Geography, Environment and Earth Sciences, Victoria University of Wellington, Wellington, New Zealand, ORCID 0000-0002-5336-6458
[7]University Corporation for Atmospheric Research, Boulder, CO, 80307 USA. ORCID 0000-0002-1425-8737
[8]Department of Geosciences, The University of Arizona, Tucson, AZ, 85721 USA
[9]Organic Geochemistry Unit, School of Earth Sciences, School of Chemistry, The Cabot Institute for the Environment, University of Bristol, Bristol, UK. ORCID 0000-0003-4451-6458 (Sosa-Montes de Oca) ORCID: 0000-0003-0298-4026 (Pancost)
[10]School of Ocean and Earth Science, University of Southampton, Southampton SO14 3ZH, United Kingdom. ORCID: 0000-0002-6316-4980
[11]Department of Civil and Environmental Engineering and Earth Sciences, University of Notre Dame, Notre Dame IN 46556, USA. ORCID: 0000-0003-4810-3773
[12]Astromaterials Research and Exploration Science Division, NASA Johnson Space Center, Houston, TX 77058, USA.
[13]Amentum, JSC Engineering and Technical Support (JETS) Contract, NASA Johnson Space Center, Houston, TX 77058, USA. ORCID: 0000-0002-0533-1330
[14]CEREGE, Aix-Marseille Université, CNRS, IRD, INRAE, Collège de France, Technopôle de l'Arbois, 13545 Aix-en-Provence, France. ORCID: 0000-0002-3047-6064
[15]School of Geography, Earth and Environmental Sciences, University of Birmingham, B15 2TT, United Kingdom. ORCID 0000-0002-9518-8143
[16]GeoLab, Faculty of Geoscience, Utrecht University, Utrecht, the Netherlands
[17]Leibniz-Laboratory for Radiometric Dating and Isotope Research, Christian-Albrechts-University of Kiel, 24118 Kiel, Germany. ORCID: 0000-0003-0405-4033
[18]Institute of Oceanography, National Taiwan University, No. 1, Sec. 4, Roosevelt Road, 10617 Taipei, Taiwan. ORCID: 0000-0002-1183-9704
[19]Department of Marine Microbiology and Biogeochemistry, NIOZ Royal Netherlands Institute for Sea Research, Den Burg, the Netherlands. ORCID 0000-0001-9707-6690 (Varma)

https://doi.org/10.5194/egusphere-2025-1467
Preprint. Discussion started: 15 April 2025


[20]Department of Biology, HADAL & Nordcee, University of Southern Denmark, 5230 Odense M, Denmark. ORCID: 0000-0002-4734-683X
[21]Guangzhou institute of Geochemistry, Chinese Academy of Sciences, Guangzhou, China. 0000-0001-7331-1246

** Both contributed equally to this work*
*Correspondence to*: Peter K. Bijl (p.k.bijl@uu.nl) and Kasia K. Sliwinska (kksl@geus.dk)

**Abstract.** Marine glycerol dialkyl glycerol tetraethers (GDGTs) are used in various proxies (such as $TEX_{86}$) to reconstruct past ocean temperatures. Over 20 years of improvements in GDGT sample processing, analytical techniques, data interpretation and our understanding of proxy functioning have led to the collective development of a set of best practices in all these areas. Further, the importance of Open Science in research has increased the emphasis on the systematic documentation of data generation, reporting and archiving processes for optimal reusability of data. In this paper, we provide protocols and best practices for obtaining, interpreting and presenting GDGT data (with a focus on marine GDGTs), from sampling to data archiving. The purpose of this paper is to optimize inter-laboratory comparability of GDGT data, and to ensure published data follows modern open access principles.

**Acronyms**:
APCI: atmospheric pressure chemical ionization
AOM: anaerobic methane oxidation
ASE: accelerated solvent extraction
BIT: branched and isoprenoid tetraether
brGDGT: branched glycerol dialkyl glycerol tetraether
CCSF: core composite depth below sea floor
CL: core lipid
CN: cyano column
Cren: crenarchaeol
CSF: core depth below sea floor
DCM: dichloromethane
GP: gaussian process
GDGT: glycerol dialkyl glycerol tetraether
GDD: glycerol dialkyl diether
GMGT: glycerol monoalkyl glycerol tetraether
GTGT: glycerol trialkyl glycerol tetraether
HPLC: high-performance liquid chromatography
HPLC-APCI-MS: high performance liquid chromatography-atmospheric pressure chemical ionisation-mass spectrometry
IODP: International Ocean Discovery Program
IPL: intact polar lipid
isoGDGT: isoprenoid glycerol dialkyl glycerol tetraether
LC-MS: liquid chromatography-mass spectrometry
MI: Methane Index
MeOH: methanol
OH-GDGT: hydroxylated glycerol dialkyl glycerol tetraether
$OM_{soil}$: soil organic matter

https://doi.org/10.5194/egusphere-2025-1467
Preprint. Discussion started: 15 April 2025


PFTE: polytetrafluoroethylene (commonly known as Teflon)
RI: ring index
RSE: relative standard error
SIM: selected ion monitoring
SPM: suspended particulate matter
SST: sea surface temperature
subT: subsurface temperature
$TEX_{86}$: tetraEther index of 86 carbon atoms
TLE: total lipid extract
TOC: total organic carbon

## 1 Introduction

Glycerol Dialkyl Glycerol Tetraethers (GDGTs) are membrane lipids that are widely applied as indicators of past water and air temperature, soil organic matter ($OM_{soil}$) input in marine settings, as well as soil pH (Schouten et al., 2013a; Fig. 1). They are synthesized by a group of archaea (Nitrososphaerota; formerly Thaumarchaeota and Crenarchaeota) (De Rosa and Gambacorta, 1988; Koga et al., 1993) and bacterial groups (Weijers et al., 2006b), including Acidobacteria and likely additional sources (Weijers et al., 2009; 2010; Sinninghe Damsté et al., 2011; Halamka et al., 2021; 2023; Chen et al., 2022). The GDGT 'pool' includes isoprenoid (isoGDGTs), and branched GDGTs (brGDGTs). Although iso- and brGDGTs are synthesized in both terrestrial and marine settings, isoGDGTs are typically associated to marine production (Schouten et al., 2000) and brGDGTs to terrestrial sedimentary settings (Sinninghe Damsté et al., 2000). The isoGDGTs are characterized by their isoprenoid carbon skeleton and includes isoGDGTs-0 to -8 (where numerals refer to the number of cyclopentane moieties), crenarchaeol, which has four cyclopentane rings and one cyclohexane moiety (De Rosa and Gambacorta, 1988; Sinninghe Damste et al., 2002b). Next to these, hydroxylated GDGTs (OH-GDGTs) were recognized (Liu et al., 2012c) as well as the much less studied glycerol trialkyl glycerol tetraethers (GTGTs; e.g., De Rosa and Gambacorta, 1988), glycerol dialkyl diethers (GDDs; which is not a membrane-spanning lipid (Mitrović et al., 2023; Hingley et al., 2024; Coffinet et al., 2015), and glycerol monoalkyl glycerol tetraethers (GMGTs), also known as H-shaped GDGT (Morii et al., 1998; Naafs et al., 2018; Baxter et al., 2019). It has been shown that the level of cyclization in marine isoGDGTs is correlated to mean annual sea surface or subsurface temperature (Schouten et al., 2002), and represents a powerful paleotemperature proxy. BrGDGTs have an alkyl backbone to which a total of four to six methyl branches can be attached. They are typically produced in terrestrial settings and therefore much less common in marine settings than the isoGDGTs. BrGDGTs from soils are used to reconstruct continental air temperatures and soil pH (De Jonge et al., 2024), also after transport to and deposition in marine depositional settings (e.g., Weijers et al., 2007a; Pross et al., 2012; Pancost et al., 2013; Śliwińska et al., 2014; De Jonge et al., 2014b; Willard, 2019; Bijl et al., 2018; 2021; Dearing Crampton-Flood et al., 2019). The relative abundance of brGDGTs in marine

https://doi.org/10.5194/egusphere-2025-1467
Preprint. Discussion started: 15 April 2025


sediments is further used to reconstruct input of soil material to the marine environment (Hopmans et al., 2004), albeit with care for marine brGDGT contributions (Peterse et al., 2009; Sinninghe Damsté, 2016).

The correlation between isoGDGTs and SST in marine sediments was first described by Schouten et al. (2002), who proposed the TetraEther indeX consisting of 86 carbon atoms, known as the $TEX_{86}$ index, to quantify the degree of cyclization of isoGDGTs. The shape of the relationship between $TEX_{86}$ and SST has been explored using a growing dataset of isoGDGTs in core top sediments spanning the modern ocean (Fig. 1), and temperatures of the overlying sea surface and subsurface waters (Schouten et al., 2002; Liu et al. 2009; Kim et al., 2010). Together with other geochemical proxies, both organic (alkenones, diols) and calcite ($\delta^{18}O$, $\Delta47$ and Mg/Ca measured on planktic foraminifera) -based, $TEX_{86}$ is widely applied as SST proxy. Paleo-applications of the proxy focus on the analysis of core lipids (CLs), i.e., GDGTs without their polar head groups. In contrast, investigations of water and surface sediment sample investigations also include the analysis of intact polar lipids (IPLs), i.e., with the polar headgroup still in place, indicating that these lipids are derived from living microbial cells (e.g., Harvey et al., 1986). Recently, OH-GDGTs have shown to have higher sensitivity in a lower temperature range than isoGDGTs (Huguet et al., 2013; Lü et al., 2015; Varma et al., 2024a, b).

The analysis of GDGTs requires sensitive analytical equipment, capable of measuring small quantities (sub-micrograms) of sample material. The relatively low concentration of GDGTs in environmental samples and geological archives can make their analysis sensitive to contributions from contamination during sampling, sample preparation and analysis or workup, and thus affect the reliability of GDGT-based paleoenvironmental reconstructions. Therefore, to optimize study-to-study intercomparisons it is imperative to standardize the sampling, processing, and analytical procedures between laboratories, and share best practices. In this paper we focus primarily on the isoGDGTs that are found in marine sediments and used for reconstruction of past sea surface temperature, but where relevant, brGDGTs and IPLs will be discussed as well.

Several approaches have been used for GDGT extraction, workup, analysis, and data processing. Here, we describe and compare these approaches and to assess their strengths and weaknesses. Through this study, combined with round robin studies (Schouten et al., 2009; 2013b; De Jonge et al., 2024), we propose standardized procedures to ensure inter-laboratory comparability, minimize the risk for contamination, maximize the reusability of processed sample material, and optimize data reporting for a reliable generation of palaeoenvironmental reconstructions.

https://doi.org/10.5194/egusphere-2025-1467
Preprint. Discussion started: 15 April 2025


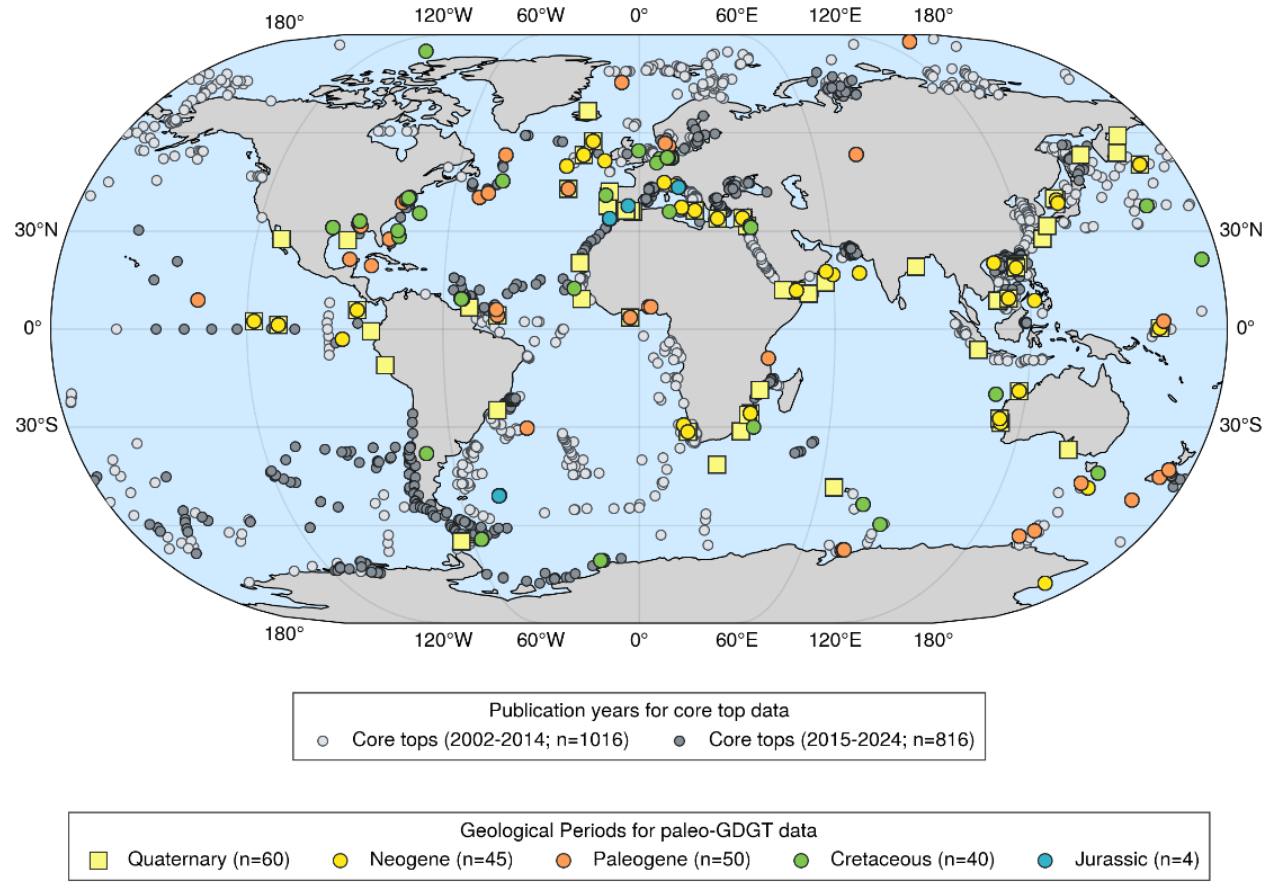


**Figure 1: Global map of core top samples for isoprenoid GDGTs is now comprise of data retrieved from previous major compilation efforts (i) published during 2002-2014 (light grey) (Kim et al., 2008; 2010; Tierney and Tingley, 2014; 2015 and references therein) and (ii) published since 2015 (dark grey) (Rodrigo-Gámiz et al., 2015; Kusch et al., 2016; Richey and Tierney, 2016; Jaeschke et al., 2017; Ceccopieri et al., 2018; Chen et al., 2018; Schukies, 2018; Lamping et al., 2021; Harning et al., 2019; Sinninghe Damsté et al., 2022; Hagemann et al., 2023; Varma et al., 2024b)—along with the location of all $TEX_{86}$ records in PhanSST (Judd et al., 2022 and references therein) in the colour of the dominant geologic time interval represented.**

Developments in Open Science in academia have increased awareness of scientific integrity in data reporting. The best-practice of reporting scientific data follows FAIR (Findable, Accessible, Interoperable, and Reusable; Wilkinson et al., 2016) open science principles, which were later translated into specific open access guidelines and objectives for the geosciences community into ICON (Integrated, Coordinated, Open and Networked; Goldman et al., 2022). The advantages of applying these principles are profound: they systematize the presentation of generated data that is connected to publications and ensure that the right kind of data (including metadata) are correctly reported. In the longer term, the availability of properly archived

https://doi.org/10.5194/egusphere-2025-1467
Preprint. Discussion started: 15 April 2025


data facilitates and stimulates its reuse by stakeholders, both in- and outside academia, with the generation of new insights far into the future. A clear example of such an effort is the SST data compilation PhanSST (Judd et al., 2022; Fig. 1). The FAIR Open Science principles greatly add value to the generated data and have ramifications for how the community best report them. We however conclude that for isoGDGT analyses, the community has yet to agree on the common framework for data presentation, and this paper is an important step towards that ambition.

The most common workflow in GDGT analysis consists of:

1. Sample selection and collection,
2. Sample storage,
3. Generation of the total lipid extract (TLE), including GDGTs, using various techniques,
4. TLE clean up procedures – column chromatography,
5. GDGT analysis using (Ultra) High Pressure Liquid Chromatography–Mass Spectrometry ((U)HPLC–MS),
6. GDGT peak integration,
7. Data interpretation,
8. Data reporting and archiving.

In this paper, we review and summarize best practices to generate, report and archive marine GDGT data, following the steps above. We base our review on examples from the literature, empirical studies, and provide data that underpins over 20 years of experience in the biomarker community. The purpose of this paper is to optimize inter-laboratory comparability of marine GDGT data, and to ensure published data follows modern FAIR open access principles.

## 2 Sampling

### 2.1 Types of samples

Marine sediment samples for GDGT analysis can be obtained from sediment cores - mainly drill cores, piston/gravity cores, multicore samples, grab samples - or outcrops. For studies on modern GDGTs, water column sampling is commonly undertaken using sediment traps or with Niskin bottles and laboratory filtration, or using *in situ* pumps to collect Suspended Particulate Matter (SPM) from the water column. As this paper focuses on sedimentary GDGTs, we do not discuss this further.

Surface marine sediment and shallow subsurface sampling (coring) happens via local/national marine cruises and expeditions, whereas the International Ocean Discovery Program (IODP) and its legacy programs Deep Sea Drilling Project (DSDP) and Ocean Drilling Program (ODP), are the only research programs to have recovered fully cored marine stratigraphic records (up

https://doi.org/10.5194/egusphere-2025-1467
Preprint. Discussion started: 15 April 2025


to 2 km of sediment) across a full range of ocean depths (up to 8 km water depth). The IODP uses dedicated research vessels and extensive international collaborations (e.g., the IODP Science plan: https://www.iodp.org/science-plan/127-low-resolution-pdf-version/file and the 2050 IODP science framework: https://www.iodp.org/docs/iodp-future/1086-2050-science-framework-full-document/file). Depending on the location of the drilling, IODP cores are stored and curated at specific repositories at the University of Bremen (Germany), Gulf Coast Repository at Texas A&M University (USA) and Kochi Core Center at Kochi University/JAMSTEC (Japan), see *www.iodp.org/resources/core-repositories*). In all three repositories sediment cores are stored in a reefer (refrigerated storage area) maintained at a temperature of +4°C and controlled humidity (*www.iodp.org/resources/core-repositories*). These repositories ensure availability of high-quality core material to member states long after the completion of each expedition. Many national research facilities have repositories of cores and marine samples as well, but the storing capacity and conditions can vary. Moreover, most sediment core repositories are not really equipped to curate processed subsets of core samples, which leaves the responsibility for curating lipid biomarker fractions and TLEs to the respective geochemistry laboratories that processed the material.

In order to study marine successions on land, two options are possible: onshore drilling for obtaining a continuous core record or hand-sampling from outcrops. Sampling outcrops for marine GDGTs may lead to challenges related to the preservation of the compounds. Sedimentary deposits on land, as in well-ventilated ocean basins, are typically exposed to various degrees of oxic degradation (Huguet et al., 2008; Lenger et al., 2013). Furthermore, outcrop exposure can alter the autochthonous GDGT signal through inputs from modern GDGTs (from e.g., modern soils) to an unknown amount, but this has never been quantified. For outcrop sampling it is thus crucial to retrieve fresh sediment material that is unaffected by weathering.

Moreover, deposits can be affected by variable degrees of heating and pressure which, if too intense, could affect GDGT preservation. GDGTs have been shown to thermally degrade at temperatures >260°C (Schouten et al., 2004), making the thermal history of especially older sediments an important consideration in the interpretation of their GDGT content. The reaction kinetics of GDGTs are mainly governed by temperature and the duration of heating, making older sediments more susceptible to the effects of thermal alteration. An understanding of the thermal history, including contact metamorphism from igneous intrusions or lava flows, is possible through an estimation of the thermal maturity of organic matter in sediment samples by using either optical (e.g., Thermal Alteration Index, vitrinite reflectance) or geochemical analysis of organic matter (e.g., RockEval Pyrolysis), or an assessment of the hopane composition, and their stereochemical configuration (e.g., Schouten et al., 2004).

In thermally mature sediments, the concentration of the original/autochthonous GDGT pool may either i) become biased due to preferential preservation of GDGTs, with $TEX_{86}$ decreasing with increasing maturity (Schouten et al., 2004; Schouten et al., 2013a), where brGDGTs are preserved preferentially over isoGDGTs thus affecting the BIT index (Huguet et al., 2008;

https://doi.org/10.5194/egusphere-2025-1467
Preprint. Discussion started: 15 April 2025


Schouten et al., 2013a), or ii) may decrease to below detection limit, even when the total organic carbon (TOC) content remains high (Schouten et al., 2004). As temperature and pressure increases with burial depth, there is a risk that GDGTs degrade at too deep depths. To date, the deepest-buried GDGTs were retrieved from North Atlantic Deep Sea Drilling Project Sites 398 and 603, from immature Lower Cretaceous sediments at depths of over 1.5 km below sea floor (Littler et al., 2011; Naafs and Pancost, 2016). This provides evidence that GDGTs can be preserved even in relatively deeply buried strata, as long as sediments do not surpass the temperature threshold (see above).

### 2.2 Contamination, storage, and initial processing of environmental samples

Sampling best practice seeks to avoid any addition of organic biomarkers or compounds to the target sample from external sources (e.g., Brocks et al., 1999). Although this paper only concerns GDGTs, sample integrity should be maintained for all lipid biomarkers where possible. When coring sediments using drilling mud/fluid, organic geochemists, whether present on-site or on-board a drilling vessel, are recommended to sample and process drill fluid as a reference where possible. Many drilling muds might not contain biomarkers or GDGTs, but to minimize contamination risk, it is strongly recommended to avoid using the external part of the core that has been in contact with drilling mud/fluids. Even though oil-contamination may not have an effect on GDGTs, it might affect other lipid biomarkers, in other fractions. For legacy cores, it is recommended to remove the outermost part of the core (which could have been contaminated with recirculating drilling mud/fluid). Once the samples/cores are obtained, they need to be sealed from oxygen exposure and, to limit microbial activity, ideally stored in a cold room (4ºC), or better yet, in a freezer (-20ºC), or freeze-dried immediately. One example that underlines the importance of this comes from a recent study (Frieling et al., 2023), where the same lithological formation was sampled from an outcrop and from a year-old sediment cores, located 3 km apart. The outcrop samples were collected recently, while the core which was drilled 50 years ago, and stored in a non-refrigerated, uninsulated storage facility in Australia. GDGT extractions carried out on age-equivalent samples from both outcrop and cores revealed orders of magnitude differences in their GDGT yield (see data files connected to Frieling et al., 2023). It was concluded that the 5 decades of aerial exposure to temperature and humidity swings had degraded the organic matter (the dinoflagellate cysts (Frieling et al., 2018) as well as the GDGT concentrations (Frieling et al., 2023)) in the old cores, to the extent that dinocyst assemblages were significantly altered and GDGTs were no longer quantifiable. Albeit extreme, this example highlights the fact that proper storage is crucial for the longevity of the preservation of GDGTs in sample material.

Once collected from the core/outcrop, sediment samples are often stored in plastic bags, but this is not recommended for samples taken for biomarker analyses. Plastic contamination (Grosjean and Logan, 2007) can be even more problematic with older sample material, where plastic bags can disintegrate with time into microscopic flakes and mix with the sediment. Although contamination from plastic will not necessarily be an issue for analysing GDGTs since it is done in selective ion

https://doi.org/10.5194/egusphere-2025-1467
Preprint. Discussion started: 15 April 2025


monitoring mode (SIM) (i.e., coelution of contaminants will not be shown), it can cause analytical complications in other fractions (e.g., Smith et al., 1993), and thus it limits reuse of extracts for analyses of non-polar biomarkers. We recommend that new samples are either i) wrapped in aluminum foil and stored in a regular plastic sample bag, but note that aluminum foil also disintegrates over time or ii) stored in a plasticizer-free sample bag dedicated to storage of samples for organic geochemistry.

In order to minimize contamination, all metal tools. extraction cells, glassware, aluminum foil, aluminum oxide, silica, $Na_4SO_2$, and glass wool must be furnaced at 450°C for 2 to 6 hours. If not furnaced, glassware and metal tools need to be cleaned, dried and rinsed (3 times) with solvents before use.

Another potential contamination could come from non-pure solvents. The workup procedure of GDGT analyses requires occasional dry-down of solvents, which has the potential to concentrate contaminants. Routine checks of batches of solvents are therefore key to ensure that solvents are not contaminated. Procedural blank samples should be added to each sample batch to confirm the absence of laboratory contamination. We recommend implementing a blank at the beginning of the laboratory workflow; at lipid extraction (Soxhlet, microwave, accelerated solvent extractor, ultrasonic extraction, see section 3.3) and at column separation, where different fractions are separated.

## 3 Processing samples for GDGTs

### 3.1 Drying samples

Prior to lipid extraction, any moisture or water content in the sediment sample is recommended to be removed for maximizing the extraction efficiency (i.e., it will allow solvents to better penetrate sediments during extraction) while preventing the loss of polar compounds bound to the water. Two sample drying methods are typically used when processing marine sediment samples: i) freeze drying - samples are dried under vacuum and below -60ºC until dry; and ii) oven drying - samples are placed in a laboratory oven (or drying device) for overnight or longer. Even though GDGTs will not be affected by temperatures above 40 ºC, it is recommended to not exceed 40 ºC when drying samples in the oven, to prevent the degradation of sensitive compounds that might occur at higher temperatures (Wiltshire and Du Preez, 1994; Rosengard et al., 2018). Freeze-drying is the preferred option (Rosengard et al., 2018).

https://doi.org/10.5194/egusphere-2025-1467
Preprint. Discussion started: 15 April 2025


### 3.2 Powdering samples

Aggregated or lithified sample materials, such as marine sediments, are usually homogenized (i.e., making sample materials into powder) to increase surface area, maximizing lipid extraction efficiency. Powdering of the sediment can be done either by hand in an agate mortar or ball mill. In both methods it is crucial to clean the mortar/mill between every sample (using either: i) DCM/MeOH, ii) acetone, or iii) by grinding quartz sands that have been cleaned via combustion followed by a rinse with solvents) to minimize cross-over contamination. Experience shows that the extraction efficiency increases when samples are powdered to a finer size, although this has not been formally quantified.

### 3.3 Extractions of lipids

The extraction of organic compounds (including lipids) from natural samples (sediment, biomass, etc) is a crucial first step in the analysis of biomarkers for paleoclimate research. The TLEs may contain thousands of various organic compounds, and several of them can be used as proxies for seawater temperature reconstructions, such as long-chain ($C_{37}$) ketones (alkenones) ($U_K'^{37}$; Brassell et al., 1986), long chain diols (e.g., Rampen et al., 2012) and GDGTs (Schouten et al., 2002). Sample preparation steps for all these lipids-based proxies, including marine GDGT analysis, usually consists of lipid extraction followed by column separation. The amount of sediment to be extracted is generally inversely correlated to TOC content, i.e., smaller amounts are required from higher TOC samples. The sample size can therefore play a role in selecting the optimal extraction technique (see below), as there is large overlap in solvent volume associated with each extraction method. The most common protocols used in GDGT-targeted studies (which are also commonly applied for other biomarkers analysis) are summarized below.

#### 3.3.1 Accelerated Solvent Extraction (ASE)

ASE is widely used to automatize lipid extraction from sediments. The typical sample size is between 8 and 50 grams (up to 100 ml), depending on the TOC content and sample type. Powdered sediments are typically mixed with either combusted quartz sand, diatomaceous earth, or glass wool (e.g., Huguet et al., 2010), to allow a better solvent flow through the cell and avoid clumping. Subsequently samples are packed into a metal extraction cell. Total lipids are extracted from the sample using a mixture of solvents, most commonly dichloromethane (DCM) and methanol (MeOH) in proportions 9 to 1 (vol:vol) under high temperature (commonly 100 °C) and high pressure (>7.6 × 106 Pa; Huguet et al., 2006). Higher temperatures are used to enhance the efficiency and speed of the extraction process. Samples can be extracted multiple times to optimize the extraction yield (e.g., Lengger et al., 2012). The advantage of ASE is that it is a fully automated and fast extraction technique, but it uses relatively large volumes of solvent for extraction and requires proper cleaning procedures for the extraction cells (see best

https://doi.org/10.5194/egusphere-2025-1467
Preprint. Discussion started: 15 April 2025


practices in cleaning in Section 2.2). Notably, the method set for the extraction of GDGTs using ASE may destroy ladderane fatty acids (due to the relatively high temperature and pressure).

### 3.3.2 Microwave-assisted extraction oven

The microwave-assisted extraction technique relies on the use of microwave energy applied to heat pressurized vessels containing solvent and powdered sediment. Samples, typically between ~5 and 7 g, are placed into glass vials held by Teflon tubes, before adding a mixture of DCM and MeOH (most commonly 9:1 or 3:1 (vol:vol); Schouten et al., 2013b), as for the ASE. The microwave is programmed for the extraction, with controlled heating of the solvent and sediment followed by cooling (e.g., Huguet et al., 2010 for examples of conditions). Like ASE, microwave extraction is fully automated, but it has an advantage using less solvent and reducing carry-over contamination as it does not require tubing between samples. The main disadvantage of microwave extraction relative to ASE is the additional step required to separate the solvent carrying total lipid extract (TLE) from the sediment. For smaller models of microwaves, the glass vials containing sediment and solvent - TLE mixture can be placed in a centrifuge to separate the aliquot from the sediment. In the case of larger microwave models, the aliquot can be either transferred into a vial compatible with centrifugation or separated from the sediment by e.g., gently pipetting the aliquot or pouring the aliquot into a clean vial. The second option will however require some extra time (1 to several hours) to allow the sediment to settle.

ASE and microwave extraction methods yield similar results for GDGTs in terms of biomarker yield and extraction quality (see Supplementary Table S1). However, it should be noted that specific settings of each method may impact the outcomes. Comparisons between ASE and microwave extractions (Frieling et al., 2023) give comparable GDGT yield and quality with a microwave heat setting of 70ºC, For the microwave-assisted extraction, significant biases in $TEX_{86}$ indices (higher by <0.2 units) can occur when the temperature is set at 100-110ºC (see Supplementary Table S1). For both extraction methods, repeated extractions of the same sample increases extraction yield.

### 3.3.3 Soxhlet

Soxhlet extraction is usually performed on larger samples (typically ~25–30 g, but not more than 100 g) compared to the previously described methods. The powdered sediment, sometimes with an admixture of quartz to prevent channeling, is placed into a pre-extracted cellulose thimble which is loaded into a Soxhlet apparatus; solvent is then heated until boiling (normally less than 70°C for DCM:MeOH (2:1, v/v) mixture) under reflux for several hours/days (commonly 24 hrs; (e.g., Huguet et al., 2010; Naeher et al., 2014b) or more (up to 48 hrs) for old sediment or low TOC) and flows through the sample, allowing the extraction of lipids. As for the other techniques, the solvent mixture usually consists of DCM and MeOH (Schouten et al., 2013b). The advantage of this technique is that extraction can be performed ultra-clean. The disadvantage is that the setup

https://doi.org/10.5194/egusphere-2025-1467
Preprint. Discussion started: 15 April 2025


takes considerable amount of space and solvent for extraction and cleaning, is relatively slow (one instrument is used for extraction of between one to ten samples between 24 and 48 hours), and complete recovery of all extracted lipids tedious, making it less efficient than ASE or microwave for large batches of samples.

#### 3.3.4 Ultrasonic extraction

Ultrasonic extraction method is usually applied for smaller samples (< 15 g) using an ultrasonic bath at ambient temperature, to avoid overheating solvents. Samples are commonly mixed with solvent (typically a DCM/MeOH mixture) for a short time (10–15 minutes, Yang et al., 2018) and subjected to centrifugation to retrieve the supernatant. The extraction is usually repeated (3 to 5 times) and the supernatants are combined, forming the total lipid extract containing GDGTs (e.g., Zhang et al., 2012; Yang et al., 2018). The final step includes a transfer of the TLE via a small $Na_2SO_4$ column (pipette) into a pre-weighed vial. GDGT core lipids are traditionally extracted using the techniques mentioned above. The efficiency of these different extraction techniques has been compared in multiple studies (e.g., Huguet et al., 2010; Lengger et al., 2012; Schouten et al., 2013b). Schouten et al. (2007) compared Soxhlet, ultrasonic, and ASE extraction techniques for CL while Lengger et al. (2012) compared Soxhlet, Bligh–Dyer (i.e., ultrasonic extraction modified from Bligh and Dyer (1959)) and ASE for extraction of both IPL and CL. Both studies showed that the extraction efficiency of these methods for CL were not significantly influenced by the allied method. In contrast, Huguet et al., (2010) suggested that CL GDGTs may be more efficiently extracted with ultrasonic or Soxhlet extraction than with ASE. Nevertheless, an extensive round robin study of $TEX_{86}$ and BIT analyses involving 35 laboratories (Schouten et al., 2013b) revealed that neither $TEX_{86}$ nor BIT index are substantially impacted by sediment workup (extraction and processing), indicating that any of the aforementioned techniques could be used for the determination of marine CL GDGT distributions.

Notably, in contrast to CL, IPL extraction usually follows a gentler method of an ultrasonic extraction modified from Bligh and Dyer (1959). GDGT extraction efficiency in IPL was also suggested to be highly dependent on the applied extraction technique (Huguet et al., 2010). The extraction yield for archaeal IPLs in cultures and environmental samples based on the commonly used Bligh and Dyer protocol was reported to be low (e.g., Huguet et al., 2010; Weber et al., 2017). The modification of the extraction protocol including the use of detergent was shown to increase the yield of archaeal lipids in cultures and marine suspended particulate matter compared to the Bligh and Dyer methodology, even though no obvious change in extraction efficiency was observed for marine sediments (Evans et al., 2022). It commonly uses a solvent mixture of MeOH, DCM, and an aqueous buffer (2:1:0.8; v/v/v). Protocols for the extraction of IPL GDGTs based on the Bligh and Dyer method were compared (e.g., Huguet et al., 2010; Evans et al., 2022) and yielded accurate comparative data for different extraction methods. If the intact polar lipids need to be separated from core lipids, a modified protocol is needed (Pitcher et

https://doi.org/10.5194/egusphere-2025-1467
Preprint. Discussion started: 15 April 2025


al., 2009; Lengger et al., 2012), where first the CL fraction is eluted with hexane/ethyl acetate 1:2 (v/v), followed by the IPL fraction with MeOH.

The final step of the extraction is to evaporate the excess solvent mixture, in order to quantify the total lipid extract. As exposure to oxygen at this step is to be avoided, drying of the solvent is typically done under flowing $N_2$. For large volumes of solvent, the solvent can be retrieved using a distillation setup under vacuum (Rotavap), whereas for smaller quantities the solvent is evaporated under flowing $N_2$ (Turbovap). In both cases it is recommended that the temperature, that serves as a heat source, does not exceed 25°C. Notably, higher temperatures (up to 40°C) and long drying under N2 may not affect GDGTs, but can cause the loss of volatile and semi-volatile compounds (e.g., pristane, phytane, short-chain alkanes and fatty acids).

### 3.4 Cleaning up - column separation techniques

In some cases, the TLE may contain traces of residue (might happen with microwave-assisted extraction). In this case it may be necessary to filter the TLE over a pipette with either i) extracted cotton wool; ii) $Na_2SO_4$ column, or a iii) extracted paper filter in a funnel. However, if the TLE is further separated into various fractions using column chromatography, the remaining sediment fraction will stay on the column and be separated from the lipid extract. In that case, removing the residue may not be strictly necessary, although the weight of the TLE will be overestimated due to the presence of the residue.

In extracts from anoxic marine sediments, elemental sulfur needs to be removed. To remove elemental sulfur from the TLE, acid-activated copper is added (Smith et al., 1984); either i) to the solvent (DCM:MeOH) in the beginning to Soxhlet extraction, or ii) to the TLE and stirred overnight, right after the ASE, microwave or ultrasonic extractions. However, this step can also be applied after the separation of the TLE into fractions (see below), and then to the specific fraction that contains the elemental sulfur.

In order to minimize the degradation of the LC column as well as to concentrate and analyze the abundance of GDGTs it is optimal to separate the polar fraction from the total lipid extract using column chromatography. The polar fraction usually contains alcohols, including isoGDGTs, brGDGTs (Section 8.2) and OH-GDGTs (Section 8.1) (Fig. 3). The separation is typically achieved by passing the TLE over either activated alumina (e.g., Huguet et al., 2006) or partly deactivated silica column (e.g., Naeher et al., 2014a) as the stationary phase.

However, underivatized fatty acids will be lost when using an activated alumina column. A silica column can also absorb FAs if they are not derivatized first. Therefore, one option is to derivatise TLEs with diazomethane, the less hazardous trimethylsilyldiazomethane or boron trifluoride methanol to convert free FAs into methyl esters prior to column separation.

https://doi.org/10.5194/egusphere-2025-1467
Preprint. Discussion started: 15 April 2025


Alternatively, fatty acid fractions can be separated through saponification from neutral fractions, which also contain GDGTs and which can further be separated from other neutral compounds following the same silica or alumina column separation (e.g., Naeher et al., 2012). In brief, TLEs are saponified using 6% KOH in MeOH and neutrals extracted by liquid-liquid extraction with n-hexane. FAs are then recovered the same way following acidification with HCl. This procedure also leads to the cleavage of wax esters, so in addition to clean separation of FAs from other compounds, this is also a suitable approach to study FAs and alcohols that are released by saponification of intact plant waxes, particularly in samples dominated by terrestrial OM. An alternative approach to saponification is the separation of free FAs (without wax ester decomposition) from other compounds using NH2 columns (Hinrichs et al., 2003).

Commonly applied solvents are hexane or hexane/DCM (9:1 vol:vol) to obtain an apolar fraction and DCM/MeOH (1:1 vol:vol) to obtain a polar fraction. Depending on other compounds that may be of interest, additional fractions can be eluted. For instance, an intermediately polar fraction is eluted using hexane/DCM 1:1 or 1:2 (vol:vol) to obtain ketones (e.g., Grant et al., 2023), in particular long-chain ketones or alkenones which are alternative paleoclimate proxies for sea surface temperature estimation (i.e., $U^{K'}_{37}$ index; e.g., Prahl and Wakeham, 1987; Herbert, 2014). When the polar fraction shows many co-eluting compounds, an additional fraction using an ethyl acetate/DCM solvent mixture (1:1 vol:vol) can be applied to further purify the polar fraction (e.g., Bijl et al., 2013). Deviating from these typical procedures there are numerous other fraction separation routines, all of which eventually end up with a polar fraction containing the GDGTs.

Polar fractions are most commonly stored refrigerated. However, dry storage at room temperature for up to 20 years has been shown not to affect the quality of GDGT analyses (e.g., Sluijs et al., 2020).

### 3.5 Standards

To enable quantification of GDGTs, a synthetic $C_{46}$ glycerol trialkyl glycerol tetraether (GTGT) is commonly used as an internal standard (Huguet et al., 2006; see 5.3 for further explanation), although quantification is not required for the calculation of $TEX_{86}$ and other GDGT-indices. The $C_{46}$ GTGT, or any other standard, can be added in known amount, either (i) to the sediment before the lipid extraction (e.g., Ceccopieri et al., 2019), (ii) to the total lipid extract (Huguet et al., 2006), or (iii) just before the analysis of the polar fraction obtained after column separation. Since lipids can be lost during the extraction process, it is important to be explicit in the methodology section about when the standard is added, and to keep this consistent throughout the workup for all samples in a dataset. This ensures clarity and reproducibility in the experimental procedures (see also in Section 5.3 on quantification).

https://doi.org/10.5194/egusphere-2025-1467
Preprint. Discussion started: 15 April 2025


### 3.6 Filtering of the polar fraction

Not all polar lipids that eluted from the column using DCM:MeOH dissolve in the solvent mixture that is used during UHPLC-MS analysis (in *n*-hexane-isopropanol 99:1 vol:vol). In order to remove any particulates before analysis, the polar fraction obtained after column separation and containing the GDGTs is classically filtered through a 0.45 µm pore size PTFE (polytetrafluoroethylene) filter prior to injection (Huguet et al., 2006). This is done using the solvent mixture with which the analyses will be performed, so that after filtration the sample is ready to be measured. Partial dry-down to concentrate the samples is to be avoided at this stage, as it affects the solvent mixture composition of the sample, and thus the elution. We thus recommend complete dry-down and then resuspend to concentrate the sample. Therefore, the filtering is recommended with GDGTs in the required concentration. The optimal concentration of the polar fraction for the UHPLC-MS is about 1 mg $mL^{-1}$. Total dry-down of the sample at this stage requires refiltering, as occasionally polar lipids do not redissolve. Brief ultrasonication may redissolve lipids at this stage. Alternatively, the redissolved polar fraction can be centrifuged before analysis (Coffinet et al., 2014).

### 3.7 Contamination during sample processing

Carry-over of GDGTs from one sample to another, either in preparation (powdering) or in the various instruments that are used for extraction. For ASE, post-extraction cell cleaning is tedious and could introduce carry-over contamination if not done well, particularly when high-TOC samples are followed by low-TOC samples. Moreover, the system itself could induce carry-over contamination through the tubing that is used to transport the extract from cell to vial (See section 2.2). Routine measurements of blanks and strict adherence of cleaning protocols minimizes risks of carry-over.

## 4 Analysis

### 4.1 LC-MS analysis

Following sample preparation (see Section 3), the filtered polar fractions containing GDGTs are analyzed by liquid chromatography mass spectrometry (LC-MS). High performance liquid chromatography (HPLC) or ultrahigh performance liquid chromatography (UHPLC) systems are typically used to separate GDGTs. Following compound separation, single, tandem, and high-resolution mass spectrometers are suitable for the detection, identification, and quantification of different compounds (Liu et al., 2012a; Lengger et al., 2018). Round-robin interlaboratory comparison studies (Schouten et al., 2013b; De Jonge et al., 2024) have investigated the effects of sample preparation and analytical differences across various LC-MS instruments available in different laboratories worldwide. These studies found no apparent systematic impacts on GDGT-based

https://doi.org/10.5194/egusphere-2025-1467
Preprint. Discussion started: 15 April 2025


indices, despite differing extraction and analysis protocols. However, minor discrepancies in absolute GDGT concentrations were noted due to several factors such as instrumentation settings and human error (i.e., manual integration).

The most commonly applied method for the analysis of GDGTs in marine sediments is reported in Hopmans et al. (2016), sometimes with minor modifications. In brief, the separation of GDGTs is achieved using two UHPLC silica columns (Acquity BEH HILIC columns, 2.1 × 150 mm, 1.7 µm; Waters) that are fitted in series and use a guard column of the same material (Acquity BEH HILIC pre-column, 2.1 × 5 mm; Waters). Normal phase separation of GDGTs is based on mixtures of *n*-hexane and isopropanol. The mobile phase is typically composed of mixtures of solvent A, which is 100% *n*-hexane, with solvent mixture B comprising *n*-hexane/isopropanol (9:1, vol:vol). Typically, GDGTs are eluted isocratically for 25 min with 18% B, followed by a linear gradient to 35% B in 25 min, then a linear gradient to 100% B in 30 min. The flow rate is low with 0.2 ml/min and the column temperature is maintained at 30°C. The typical runtime is 90 min but might be adjusted depending on user requirements (e.g., maximizing peak resolution, required target compounds to be determined, throughput efficiency). About 20 min should be included at the end of each run to return to the initial solvent mixture prior to injection of the next sample, to prevent contamination and to ensure equilibration of the composition of the mobile phase. It was shown that injection volume should not be too high (max 50 µL) when *n*-hexane-isopropanol (99:1, v/v) is the sample solvent (Wang et al., 2022). Any remaining polar fraction after the LC-MS analysis should be dried under $N_2$, properly labeled and stored.

Overall, this method achieves the separation of isoGDGTs, which elute first, followed by branched GDGTs (brGDGTs) and then hydroxylated GDGTs (OH-GDGTs; see Fig. 3). The maximum operating pressure for these columns is approximately 600 bar, but analysis is usually undertaken at much lower operating pressures, commonly ramping up from ca. 180 to 220 bar. The method described by Hopmans et al. (2016) has largely replaced previous approaches using cyano (CN) columns which did not achieve the same degree of separation of several isomers (Hopmans et al., 2000; Schouten et al., 2013b). However, since this development does require some investment, not all laboratories have yet adopted the double-column technique. Based on the new analytical developments, new indices and new paleoclimate calibrations have been proposed that yield lower analytical errors in temperature reconstructions using GDGT-based proxies (e.g., Hopmans et al., 2016). Therefore, it is recommended to use the newer approaches and proxies.

Following column separation, the eluting compounds are ionised by atmospheric pressure chemical ionisation (APCI) using positive polarity mode, which yields protonated molecular ions ($[M+H]^+$) of the target compounds. In single quadrupole systems, the spray chamber is operated with gas and vaporizer temperatures of 200°C and 400°C, respectively. The drying gas flow is typically set to 6.0 L $min^{-1}$ and the nebula pressure to 60 psig. However, all these settings may differ depending on the instrument used and may require individual modifications. The quadrupole temperature is usually set to 100°C.

https://doi.org/10.5194/egusphere-2025-1467
Preprint. Discussion started: 15 April 2025


The mass selective detector is either a single quadrupole, tandem or high-resolution mass spectrometers. However, only one-dimensional MS mode is typically used to obtain diagnostic $M^+$ ions of different GDGT homologues and isomers. The abundances of GDGTs are monitored using selective ion monitoring mode (SIM), compounds are identified by comparing mass spectra and retention times with those in the literature. For isoGDGTs, selected ion fragmentograms are *m/z* 1302.3 (GDGT-0), 1300.3 (GDGT-1 and -1'), 1298.3 (GDGT-2 and -2'), 1296.3 (GDGT-3 and -3'), 1294.3 (GDGT-4 and -4', not commonly targeted since not in the $TEX_{86}$ index, but should be) and 1292.3 (Crenarchaeol and stereoisomer - cren') (Hopmans et al., 2016; Schouten et al., 2013a). In some environments, isoGDGT homologues up to isoGDGT-8 (*m/z* 1286), particularly in hydrothermal and extremophilic environments (e.g., Schouten et al., 2013). For brGDGTs, target ions are *m/z* 1050.0, 1048.0, 1046.0, 1036.0, 1034.05, 1032.0, 1022.0, 1020.0, 1018.0 (De Jonge et al., 2014a; Hopmans et al., 2016), as well as brGMGTs at 1048.0, 1034.0 and 1020.0 (e.g., Baxter et al., 2019; Sluijs et al., 2020; Bijl et al., 2021). OH-isoGDGTs are monitored using their $M^+$ ions at *m/z* 1318.3, 1316.3 and 1314.3, and as well as dehydrated ions at *m/z* 1300.3, 1298.3 and 1296.3 for OH-GDGT-0, -1 and -2 respectively (Liu et al., 2012c; Fietz et al., 2016; Varma et al., 2024b). The $C_{46}$ GTGT standard is monitored at m/z 743.8. For all ions, a mass window of 1.0 is generally maintained.

The analysis of the large number and diversity of GDGT derivatives and related ether lipids, such as GDDs, GMGTs, GTGTs, can be analyzed with similar LC-MS methods, commonly adapted from the GDGT method of Hopmans et al. (2016). This method can be shortened or extended dependent on which of these compounds are targeted and mainly differ based on the target ions that need to be recorded for identification and quantification (e.g., Coffinet et al., 2015; Naafs et al., 2018; Baxter et al., 2019; Mitrović et al., 2023; Hingley et al., 2024). For instance, H-isoGDGTs, if present in sample, are already recorded in the mass fragmentograms of isoGDGTs, which are *m/z* 1300 (H-isoGDGT-0), 1298 (H-isoGDGT-1), 1296 (H-isoGDGT-2), 1294 (H-isoGDGT-3), 1292 (H-isoGDGT-4) and eluted later than isoGDGTs using the Hopmans et al. (2016) method. For isoprenoid GDDs (isoGDDs), the following mass fragmentograms are used: *m/z* 1246 (isoGDD-0), 1244 (isoGDD-1), 1242 (isoGDD-2), 1240 (isoGDD-3), 1238 (isoGDD-4) and 1236 (isoGDD-Cren), which corresponds to a mass difference of 56 relative to the equivalent isoGDGTs. Similarly, for branched GDDs (brGDDs), target ions are *m/z* 966 (brGDD-Ia), 964 (brGDD-Ib), 962 (brGDD-Ic), 980 (brGDD-IIa), 978 (brGDD-IIb), 976 (brGDD-IIc), 994 (brGDD-IIIa), 992 (brGDD-IIIb) and 990 (brGDD-IIIc). IsoGDDs and brGDDs elute later than isoGDGTs and brGDGTs if samples are analysing as reported in Hopmans et al. (2016). In contrast, up to three different isomers of bacterial GMGTs can be detected in each selected ion fragmentogram using *m/z* 1020, 1034 and 1048, which elute elute after brGDGTs.

Instrument performance (e.g., solvent purity and aging, leaks, blockages, pump functions and pressure control, etc) should be regularly checked and the use of check tunes to regularly evaluate the mass spectrometer performance is recommended. Blanks (processing blanks in each sample batch and clean solvent injections), laboratory standards and known reference samples should be regularly analyzed as part of sample sequences to ensure precision and accuracy of the obtained results. As an

https://doi.org/10.5194/egusphere-2025-1467
Preprint. Discussion started: 15 April 2025


example, routine in-house reference sample (Arabian Sea extract mixed with Rowden soil extract) measurements since 2019 on the same instrument ("LC1") in the GeoLab of Utrecht University, show the variability of $TEX_{86}$ (Fig. 2; data in Supplementary Table S2). The reference sample measurements during 'normal' performance of the UHPLC-MS (we removed measurements during maintenance) have a standard deviation that is much smaller than the calibration error, and also smaller than any paleoceanographic signal that is reconstructed (0.005 $TEX_{86}$ units and 0.008 BIT index units). This doesn't come by itself, and is the result of finetuning and constant monitoring of machine performance. The routine analysis of the reference sample ensures reproducibility and allows monitoring of machine drift, so that when needed machine settings can be adjusted. Ideally, laboratories use more than one reference sample for robust calibration of the analytical error, and analyse it in replicate over a short time span. Also, for optimal machine intercalibration, different labs should use the same reference samples so that machines are optimally tuned to each other. Note also the absence of user (i.e., integrator) difference in the results (Fig. 2), this reflects in part the strict in-house training and intercalibration. integration results between integrators can differ considerably, particularly when integration "hygiene" (i.e., how the peak tails are trimmed) is inconsistent. Integration intercomparisons between analysts is strongly recommended when datasets from different integrators are combined. Combining datasets from different machines require at least the cross comparison of a few samples on each machine, to ensure both machines give comparable results for the same samples. Long-term trends in the standard data are probably the result of tuning changes, performance of the pump system and column replacements. Although Fig. 2 demonstrates that the impact of such adjustments to the equipment on GDGT analyses are small, it is recommended that adjustments to the machine are carefully logged.

https://doi.org/10.5194/egusphere-2025-1467
Preprint. Discussion started: 15 April 2025


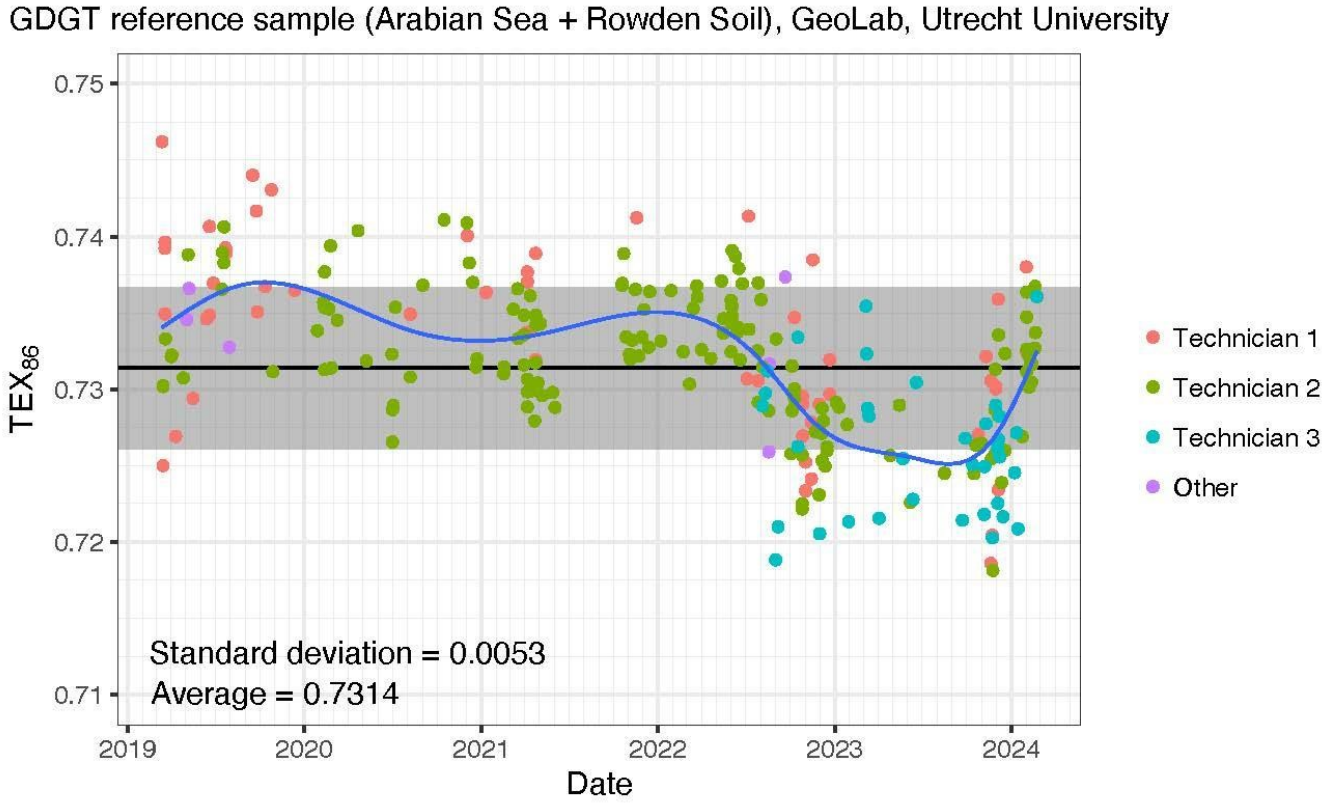


**Figure 2: The $TEX_{86}$ results of over 250 routine analyses of the internal GDGT reference sample (Arabian Sea + Rowden soil) in the Geolab of Utrecht University, over the past 5 years. Colour represents the name of the integrator of the results. Blue line represents a loess smooth through the data, black horizontal line represents the average result of the internal standard, grey bar represents the 1 sigma of all measurements. The standard deviation in $TEX_{86}$ index units equates to about 0.3°C in mid-range temperatures for all calibrations. Measurements of standards during UHPLC-MS maintenance were deleted from this dataset. For BIT results (see section 6 for details about BIT), relative abundances of individual GDGTs and their standard deviation, see data in Supplementary Table S2.**

## 5 GDGT peak integration

### 5.1 Integration guidelines

Integrating GDGT peak areas is the first step in interpreting GDGT data. Here, we provide an integration guide, with examples from seafloor core top sediments in basins with both warm (above 26 °C/77 °F, typical for tropical and subtropical regions)

https://doi.org/10.5194/egusphere-2025-1467
Preprint. Discussion started: 15 April 2025


and cold (below 10 °C/50 °F, typical for polar and subpolar regions) surface waters, to illustrate temperature-dependent differences in chromatograms and their impact on integration (Figure 3). Traditionally, GDGT-0 through to GDGT-3, crenarchaeol and cren', along with at least the three brGDGTs used in the calculation of the BIT index (see section 6.1), have been reported for marine samples (see Section 8.2). The utility of a wider array of GDGT-like compounds, including an extended array of brGDGTs, OH-GDGTs, GMGTs, GTGTs (see Section 8 for details) is increasingly recognized, and we recommend that these are reported where possible, and that it is explicitly stated if not possible (i.e., where abundances of compounds are below detection limit). Figure 3 also demonstrates integrations for GDGT-4 and OH-GDGTs.

Several criteria are in use to determine the detection limit of GDGTs, e.g., below (or above) which quantification of the GDGT is no longer reliable. On the lower end, a signal-to-background noise ratio of 3 is commonly applied, while other laboratories use a minimum peak area cutoff ($10^3$). On the higher end, cutoffs are less well-defined, but in general samples with peaks with 'blunt' maxima are to be diluted and rerun.

Multiple software packages are currently available for automate peak integration (e.g., Dillon and Huang, 2015; Fleming and Tierney, 2016). The pilot results of these programs are impressively close to human integration. These automated approaches can systematize objective choices for the baseline and tail cutoff, can save considerable amount of time when handling large datasets, and reduce the risk of human error in data integration and transfer. However, it is important to note that the inspection of chromatograms for potential coelutions and the verification of proper GDGT concentrations should still be performed manually by an expert.

https://doi.org/10.5194/egusphere-2025-1467
Preprint. Discussion started: 15 April 2025


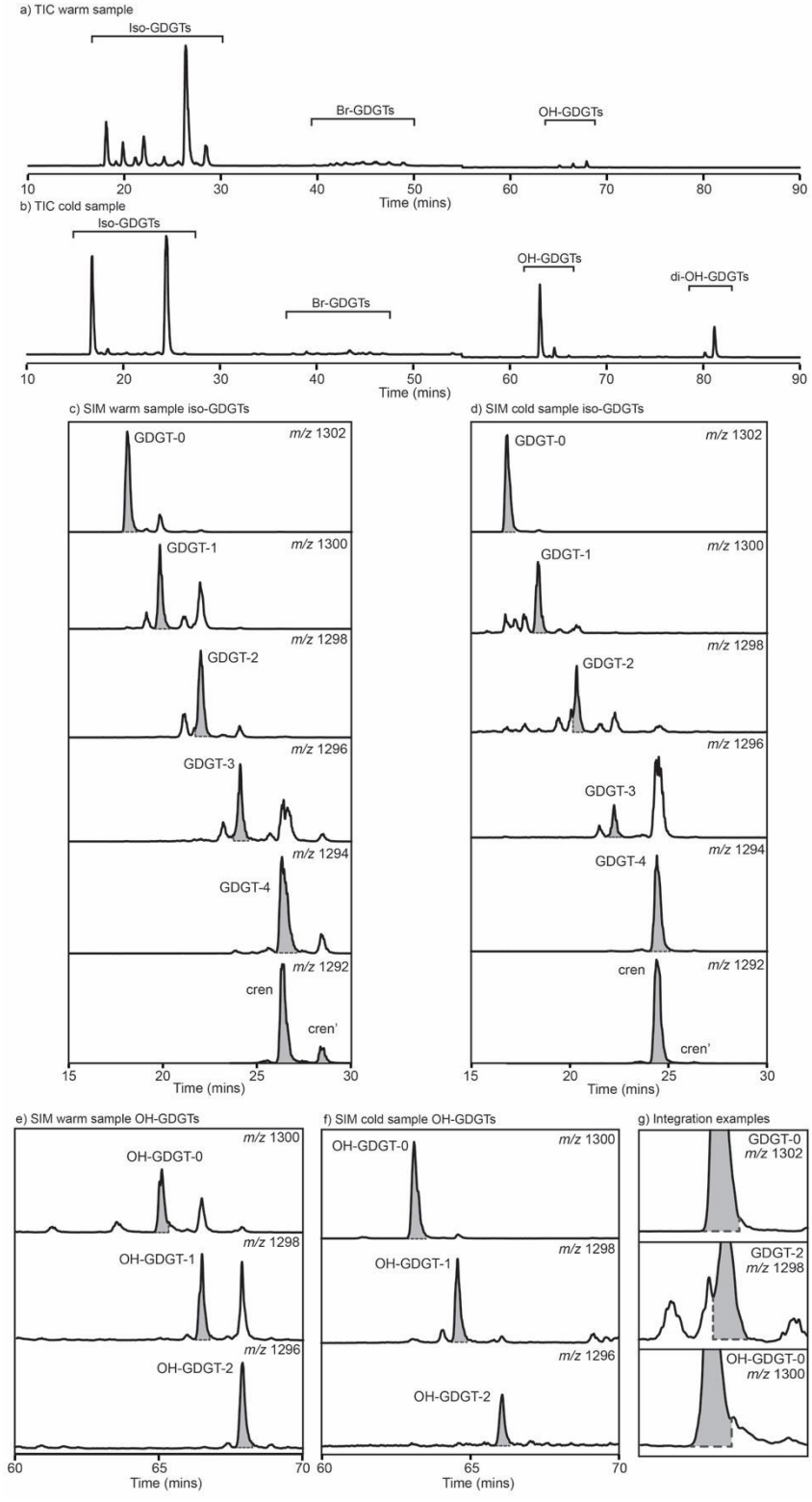


**Figure 3: Example chromatogram and integration guide for two modern samples analyzed using the method described by Hopmans et al. (2016): a) a warm sea surface temperature site (mean annual SST ~26.5 °C) in the Coral Sea, and b) a cold sea surface temperature site (mean annual SST ~-1°C) in the Ross Sea. a) and b) display the total ion current (TIC) for each sample. The mass chromatograms (derived from selective ion monitoring (SIM)) for the six commonly integrated isoGDGTs, as well as GDGT-4 are displayed for the site with warm surface water in c) and for the site with cold surface water in d) (note further discussion on the integration of GDGT-4 in Section 8.3). Mass chromatograms for the three integrated OH-GDGTs are displayed for the site with warm surface water in e) and for the site with cold surface water in f). Grey shaded panels in c), d), e) and f) represent the recommended integration for each GDGT. g) Zoom-in on the baseline of 3 isoGDGTs showing how the tails of these peaks should be trimmed.**

https://doi.org/10.5194/egusphere-2025-1467
Preprint. Discussion started: 15 April 2025


### 5.2 Possible challenges in peak integration

In addition to temperature, the distributions of GDGTs (and likely also GMGTs) can be impacted by spatial variations in archaeal communities, occasionally leading to unusual or challenging peaks to integrate. An example of this is GDGT-2, particularly observed in sediment samples from the Southern Ocean and Antarctica, where an isomer of GDGT-2 can precede and partially coelute with the main isomer peak (Fig. 3e), leading to a shoulder or double peak. This can be seen in the mass chromatogram for the sample collected from the cold SST site in Figure 3. We recommend that this peak/shoulder should be excluded from integration of the main isomer peak and be noted in the methods section.

In samples where overall GDGT abundances, or abundances of a specific GDGT, are below detection limit it is recommended to report the area limit at which quantification is no longer possible (where detection limit is defined as the point at which a peak is indistinguishable from background noise). Different laboratories are likely to have an area value (i.e., an area of 3000) or signal-to-noise ratio (i.e., >3) as cutoffs, and while these values will vary between LC systems and software we recommend that integration limits are stated in publications. Below this limit, it is recommended to refer to a peak as NQ, standing for non-quantifiable, to indicate that the peak may still be present but is not abundant enough to be confidently integrated.

### 5.3 Quantification of GDGTs

GDGTs can be quantified by comparing their peak areas to those of a standard (Huguet et al., 2006; see also Section 3.6). Typically, this is expressed in ng/g, by comparing either to the dry weight of extracted sediment (ng/g dry weight) or to TOC (ng/g TOC) data. Quantification of GDGTs helps in identifying shifts in GDGT concentration and preservation, which is important given that preservation changes could qualitatively affect the GDGT results (Ding et al., 2013). Although a linear response of the mass spectrometer for all GDGT compounds for quantification is generally assumed, studies on the reproducibility of $TEX_{86}$ and BIT analysis between different MS systems (Escala et al., 2009) and different laboratories (Schouten et al., 2009; 2013b) reveal that this response varies substantially with MS settings. Further, quantifications using $C_{46}$ or any non-authentic standard will be semi-quantitative, as the response between $C_{46}$ and GDGT can vary over time and between instruments. This leads to large interlaboratory offsets particularly in the BIT index, as this proxy comprises compounds over a large *m/z* range (Table 1) (Schouten et al., 2009). Similarly, laboratory-specific MS settings are assumed to cause large (several orders of magnitude) differences in the absolute quantification of GDGTs between laboratories worldwide (De Jonge et al., 2024). These interlaboratory comparison studies have called for the introduction of a community-wide standard mixture with established GDGT proxy values that can be used to calibrate MS instruments (Escala et al. 2009; Schouten et al., 2009; 2013b; De Jonge et al., 2024). Until this has been accomplished, laboratories should perform regular

https://doi.org/10.5194/egusphere-2025-1467
Preprint. Discussion started: 15 April 2025


reruns of an in-house GDGT standard mixture to monitor the stability of their MS instrument, and consistency in integration performance, and thus the accuracy of their measurements (see Section 4.3). Note, however, that the offsets between instruments in the quantification of GDGTs does not impact individual records generated on the same instrument, i.e., individual instruments, when maintained well, show high/sufficient accuracy and precision in both $TEX_{86}$ and BIT estimations (see Section 4.2).

## 6 Data interpretation: non-thermal overprints

Along with sea surface temperature, marine sedimentary GDGT distributions are governed by a range of factors that provide insight into past environments but can confound simple interpretation of only one environmental parameter. For example, marine GDGT-based paleothermometry is complicated by a range of sources for isoGDGTs beyond near-surface ammonia-oxidizing Nitrososphaerota. Various screening mechanisms and indices (Table 1) have been developed to assess the impact of non-thermal effects or contributions from alternative sources of isoGDGTs. These screening methods typically focus on identifying additional non-surface Nitrososphaerota contributions to sedimentary GDGTs, e.g., methanogens or anaerobic oxidisers of methane (methane index; MI) or terrestrial inputs (BIT). The impact of degradation on GDGT distributions (and associated indices) are not as well developed. However, degradation impacts appear to be minimal, with no evidence that degradation of GDGTs alters their distribution or $TEX_{86}$ values during herbivory (Huguet et al., 2006), in the water column (Kim et al., 2009), or in sediments deposited under different redox conditions (Schouten et al., 2004). The most obvious impact of degradation, therefore, is that the pelagic signal is diluted relative to sedimentary archaeal or soil contributions (Huguet et al., 2009). For example, Hou et al. (2023) and Kim and Zhang (2023) showed that high values of the MI, Delta Ring index ($\Delta RI$) and BIT index corresponded with an interval of lower absolute concentrations of GDGTs, and in particular a disproportionate decline in the concentration of crenarchaeol. Because these impacts remain incompletely understood or perhaps offer additional environmental insights, we recommend that samples that are removed by screening should still be reported in the data report but excluded from the subsequent temperature reconstruction. Bijl et al. (2021) provided an R script that follows standardized steps in GDGT data evaluation and interpretation. Although these screening methods have clearly defined cutoff values, we recommend careful consideration of the depositional setting when these screening methods are used. Specifically, concentration changes of GDGTs must be considered for those samples whereby screening methods suggest non-thermal impacts.

**Table 1: Summary of screening methods assessing anomalous GDGT distributions.**

| Index to identify | Equation | Description | Reference |
|---|---|---|---|

https://doi.org/10.5194/egusphere-2025-1467
Preprint. Discussion started: 15 April 2025


| **anomalous sample** | | | |
|---|---|---|---|
| Branched and Isoprenoid tetraether (BIT) index | $BIT = \frac{[brGDGT-I]+[II]+[III]}{[brGDGT-I]+[II]+[III]+[cren]}$ | Indicates organic matter derived from soil ($OM_{soil}$) input into a marine environment where 0 implies no $OM_{soil}$ and 1 is no crenarchaeol. Higher values may cause temperature bias from $OM_{soil}$-derived isoGDGTs. | Hopmans et al. (2004) |
| Methane Index (MI) | $MI = \frac{[GDGT-1]+[2]+[3]}{[GDGT-1]+[2]+[3]+[cren]+[cren']}$ | Indicates contribution of methanotrophic Archaea, where higher values (>0.3–0.5) indicate larger contribution. | Zhang et al. (2011) |
| %GDGT-0 | $\%[GDGT-0] = \left(\frac{[GDGT-0]}{[GDGT-0]+[cren]}\right) \times 100$<br>$[GDGT-0]/[cren]$ | Indicates contribution of methanogenic Euryarchaeota, where values >67% or ([GDGT-0])/([Cren]) >2 indicate larger potential methanogenic input. | Blaga et al. (2009), Sinninghe Damsté et al. (2012a) |
| Δ Ring Index (ΔRI) | $\Delta RI = RI_{TEX} - RI_{Sample}$<br>Where:<br>$RI_{TEX} = -0.77 \times TEX_{86} + 3.32 \times (TEX_{86})^2 + 1.59$<br>And<br>$RI_{Sample} = 0 \times [GDGT-0] + 1 \times [GDGT-1] + 2 \times [GDGT-2] + 3 \times [GDGT-3] + 4 \times [cren] + 4 \times [cren']$<br>And:<br>$TEX_{86} = \frac{[GDGT-2]+[GDGT-3]+[cren']}{[GDGT-1]+[GDGT-2]+[GDGT-3]+[cren']}$ | $TEX_{86}$ and RI correlate with temperature. ΔRI measures if a sample's GDGT distribution deviates from the modern ocean $TEX_{86}$-RI relationship. If ΔRI lies outside the 95% confidence interval of the modern regression (±0.3 ΔRI units), then non-thermal factors are indicated. | Zhang et al. (2016) |
| GDGT-2/GDGT-3 | $\frac{[GDGT-2]}{[GDGT-3]}$ | Elevated values (>5) indicate greater contribution from subsurface GDGTs. | Taylor et al. (2013) (see also Hurley et al., 2018) |
| fcren | $f_{cren':cren'+cren} = \frac{[cren']}{[cren]+[cren']}$ | High values (>0.25) indicate anomalous GDGT distribution impacted by non-thermal factors. | O'Brien et al. (2017) |
| $\%GDGT_{RS}$ | $\%GDGT_{RS} = \left(\frac{[cren']}{[GDGT-0][+[cren']}\right) \times 100$ | >30% Identifies a 'Red Sea-type' distribution, but this cannot be distinguished from a high temperature signal | Inglis et al. (2015) |
| $D_{nearest}$ | Distance metric based on a Gaussian Process emulator covariance matrix | High values (>0.5) indicate a GDGT distribution substantially different from the "nearest neighbour" within the calibration data set (i.e., non-analogue to modern core tops) | Dunkley Jones et al. (2020) |

630

https://doi.org/10.5194/egusphere-2025-1467
Preprint. Discussion started: 15 April 2025


### 6.1 Terrestrial input

IsoGDGTs form a minor component in terrestrial/aquatic GDGT distributions (e.g., Blaga et al., 2009), but in settings with significant soil organic matter input into the marine realm, terrestrially derived isoGDGTs have been shown to bias reconstructed temperatures based on $TEX_{86}$ values (Weijers et al., 2006a). The Branched and Isoprenoid Tetraether (BIT) index was developed to assess the contribution of GDGTs from terrestrial soils transported by rivers into marine sediments (Hopmans et al., 2004). It is based on the abundance of the three dominant brGDGTs (brGDGT-I, brGDGT-II, brGDGT-III) compared to crenarchaeol, which is predominantly produced in marine settings (Hopmans et al., 2004). An index value of 0 implies no brGDGT input, while a value of 1 represents no crenarchaeol input. The BIT index is useful in marginal marine and lake sediments (Hopmans et al., 2004). A study on the marine surface sediments of the Congo Fan found that in samples where BIT exceeded 0.3, temperature estimates were biased by >2°C, implying that terrestrial isoGDGT contributions affect the marine sedimentary isoGDGT pool (Weijers et al., 2006a).

There are however many complications with the use of BIT for terrestrial input. Firstly, BIT index values are not consistent between laboratories (see 5.3; Schouten et al., 2009). Secondly, the application of a threshold above which temperature bias is likely to occur is locality dependent because 1) it is influenced by the difference between the $TEX_{86}$ values of terrestrially sourced isoGDGTs, and marine sourced GDGTs, and 2) the abundance of crenarchaeol, which is typically more abundant at higher temperature, also influences the BIT index (Schouten et al., 2013a). Albeit typically in small amounts, marine production of brGDGTs can impact BIT index values, although the molecular composition of marine-produced brGDGTs differs strongly from those produced in soils (Peterse et al., 2009; Sinninghe Damsté, 2016). Various indices have been developed to assess marine or terrestrial brGDGT production (see section 8.2) (Huguet et al., 2008; Weijers et al., 2014; Xiao et al., 2016). Furthermore, brGDGTs tends to be preferentially preserved over isoGDGTs during syn- and/or post-sedimentary oxic degradation (Peterse et al., 2009). The preferential degradation occurs in particular under anoxic conditions. As a compromise, some studies chose to discard $TEX_{86}$ as SST proxy when BIT and $TEX_{86}$ values correlate, and a location-specific threshold has been established if a correlation existed, or if substantial scatter or anomalous values in $TEX_{86}$ occurs above a certain BIT threshold (e.g., Schouten et al., 2009; Bijl et al., 2013; Schouten et al., 2013b; Davtian et al., 2019). Other studies question the use of the BIT index for estimating marine vs. terrestrially derived organic matter, as samples from an increasing range of environments are found to have *in situ* produced brGDGTs (e.g., Peterse et al., 2009; Dearing Crampton-Flood et al., 2019; Bijl et al., 2021). A study of the Mississippi River Delta has also shown that river-derived brGDGTs are not transported far into the marine system (Yedema et al., 2023). Moreover, brGDGTs detected in marine sediments, even those close to shore, show distributions that are fundamentally different from those in modern soils or peats (Sinninghe Damste, 2016; Hollis et al., 2019; Bijl et al., 2021). With the documentation of isoGDGT contributions from land, and the production of brGDGTs in the

https://doi.org/10.5194/egusphere-2025-1467
Preprint. Discussion started: 15 April 2025


marine system, the BIT index proxy as purely indicative of terrestrial organic matter input becomes problematic. We recommend caution in overinterpreting BIT as proxy for terrestrial input and as criterion for evaluating $TEX_{86}$, particularly when brGDGT distributions diverge from those of modern soils and peats. The degree of cyclization in the brGDGTs reflects this best, as soil-derived brGDGTs have much less cyclization than those produced in marine sediments (Sinninghe Damste, 2016; Dearing Crampton-Flood et al., 2019). This means that some of the older $TEX_{86}$ data that were discarded because of high BIT might actually accurately reflect local temperature.

### 6.2 Methanogenic input

Marine and sedimentary archaeal communities can also contain methanogenic *Euryarchaeota*, which can synthesize GDGT-0, and to a lesser extent, GDGT-1, GDGT-2, and GDGT-3 (e.g., Pancost et al., 2001; Blaga et al., 2009; Sinninghe Damsté et al., 2012a; Inglis et al., 2015). The impact of *Euryarchaeota* on a GDGT distribution can be assessed using %GDGT-0 (Table 1), where values >67% indicate that a sample contains a substantial contribution from methanogenic sourced GDGTs (Sinninghe Damsté et al., 2012a). The ratio of GDGT-0 to crenarchaeol is also sometimes used, with values above 2 indicating a methanogenic source (e.g., Blaga et al., 2009; Naeher et al., 2012; 2014b). Other indicators of methanogenic archaeal contributions include archaeol, hydroxyarchaeol, pentamethylicosenes and crocetene (and their derivatives), which can be detected using GC-MS analysis (Hinrichs et al., 2000; Niemann and Elvert, 2008; Naeher et al., 2014b). The impact of methanogenic input on a sedimentary GDGT distribution likely varies by depositional and oceanographic setting, and has typically only been found to have a minor impact in marine sediments (i.e., Inglis et al., 2015; O'Brien et al., 2017). In any case, the likelihood of a methanogenic overprint in a specific oceanographic setting must be assessed when screening to detect non-thermal overprints in GDGTs.

### 6.3 Methanotrophic input

Post-depositional production of isoGDGTs also occurs during anaerobic oxidation of methane by anaerobic methanotrophic archaea (Zhang et al., 2011). Methanotrophic archaea, especially those of group ANME-1, preferentially produce GDGT-1, GDGT-2 and GDGT-3, and can bias reconstructed temperatures in sediments where they are active, such as around cold seeps or areas with gas hydrate occurrences (Pancost et al., 2001; Zhang et al., 2011). The Methane Index (MI; Table 1) assesses the relative contribution of methanotroph-produced GDGTs to those produced in the water column by non-methanotrophic *Nitrososphaera* (Zhang et al., 2011). A range of >0.3–0.5 is considered to indicate a significant contribution from a source other than normal marine production (Zhang et al., 2011; Kim and Zhang, 2023). We recommend that samples with MI values >0.3 are used with caution when estimating SST, acknowledging that similar to the BIT (see above), the MI value may be locality dependent and should be used as a guideline rather than a firm cut off. The sensitivity of the MI has been debated,

https://doi.org/10.5194/egusphere-2025-1467
Preprint. Discussion started: 15 April 2025


with it previously unclear whether small amounts of diagenetic methane in porewater could impact MI values, or if a high flux of methane associated with gas hydrates was required to elevate MI levels (Weijers et al., 2011; Kim and Zhang, 2023). Recent research indicates that MI is quantitatively related to sedimentary methane diffusive flux, with high MI values strongly associated with high methane fluxes and shallow depths of the sulfate-methane transition zone, where the activity of anaerobic methane oxidation is mostly concentrated (Kim and Zhang, 2023). MI values at the lower end of the range (i.e., >0.3) appear to be associated with high methane flux in polar settings, while this value is closer to >0.5 in non-polar regions (Kim and Zhang, 2023). Additional indicators of methanotrophic archaea include archaeal lipids described in 6.2, which are distinguished from methanogenic sources by their $^{13}C$-depleted composition ($\delta^{13}C$ values ranging from -40 to low as -120‰; e.g., Hinrichs et al., 2000; Niemann and Elvert, 2008; Naeher et al., 2014b). Furthermore, methanotrophic bacteria commonly occur in conjunction with methanotrophic archaea and are distinguished from heterotrophic bacteria by $^{13}C$-depleted signature of bacterial biomarkers such as fatty acids and hopanoids (Hinrichs et al., 2003; Birgel and Peckmann, 2008; Naeher et al., 2014b). Therefore, MI may not be an effective indicator at sites with additional sources of GDGTs, such as soil-derived GDGTs in coastal settings (Zhang et al., 2011). In these instances, $\delta^{13}C$ measurements of bacterial biomarkers such as hopanes (Pancost, 2024), or, in a more elaborate workup scheme, directly on the GDGTs (Pearson et al., 2016; Keller et al., 2025) could be used to assess methanotrophic contributions.

### 6.4 Ring index and Δ Ring Index

Different strains of archaea have been found to display variable $TEX_{86}$ values, despite having been cultured at the same temperatures (Elling et al., 2015; Qin et al., 2015). This suggests that growth temperature is not the sole control on changes in the $TEX_{86}$ ratio, and that other factors including Thaumarchaeal community composition can play an important role. A more linear relationship was found between growth temperature and the Ring Index (RI, Table 1), which measures the weighted average of cyclopentyl moieties, across all strains of archaea in culture experiments (Elling et al., 2015; Qin et al., 2015). The slope and strength of this relationship varies between Thaumarchaeal strains, suggesting that community composition can still impact the relationship between RI and temperature (Elling et al., 2015). Higher values of RI indicate higher temperatures. In the modern ocean, $TEX_{86}$ and RI are correlated, and RI can be calculated from $TEX_{86}$ using a regression (Zhang et al., 2016). If a sample's RI deviates from the calculated RI outside of the 95% confidence interval of the modern regression (±0.3 ΔRI units), then the $TEX_{86}$ value for that sample is considered to be potentially influenced by non-thermal factors and/or deviates from modern analogues. These factors include the impact of GDGTs derived from soil, methanogenic and methanotrophic archaea as described above, variations in community composition, or potentially other non-thermal impacts on GDGT biosynthesis such as archaeal growth rates (Zhang et al., 2016).

https://doi.org/10.5194/egusphere-2025-1467
Preprint. Discussion started: 15 April 2025


### 6.5 Surface vs subsurface GDGT production (GDGT-2/GDGT-3 ratio)

One of the known complications of the GDGT-based temperature proxy relates to the depth of GDGT production and export. *Nitrososphaerota* live throughout the water column, are most abundant near the nutricline, and less abundant in the uppermost ~50 meters of the water column (Wuchter et al., 2005; Hurley et al., 2018). Sedimentary GDGTs have typically been considered to best represent surface or shallow subsurface conditions (Schouten et al., 2002), possibly due to preferred export of *Nitrososphaerota* from these depths in aggregates like fecal pellets, as speculated in Wuchter et al., (2005). Evidence for this includes the observation that sedimentary $TEX_{86}$ values statistically best fit surface temperature (Kim et al., 2008; although below we explain that this might be a statistical artefact caused by the fact the total temperature range is larger in the surface than in the subsurface), and that those sedimentary relationships are only slightly offset from those derived from SPM of surface water (<100 m) (Wuchter et al., 2005; Taylor et al., 2013; Schouten et al., 2013a).

The GDGT literature suffers from imprecise definition of the qualitative terms surface and (shallow) subsurface. Sediment trap work has indicated that most GDGTs are exported from the surface (e.g., Wuchter et al., 2005). However, in such studies the uppermost trap is typically located at 500 meters of depth, proving nothing more than dominant export from the upper 500 meters of the water column, which includes mixed layer and thermocline. For proxy calibration and application, the major factor is whether GDGTs are exported from above, within or below the (permanent) thermocline. Because in many ocean regions the thermocline and nutriclines are related, we might expect that a portion of GDGT export might occur from close to the thermocline rather than only from above.

Interestingly, two dominant clades of Nitrososphaerota are present in the water column, of which one is present in the upper ~200 of the water column (shallow clade), and other resides typically deeper than 100 m (Francis et al., 2005; Villanueva et al., 2015). The GDGT distribution in the membranes of the shallow clade adjusts to temperature, but GDGTs from below 100 m water depth do not in the same way (Hurley et al., 2018; Schouten et al., 2002; Taylor et al., 2013; Turich et al., 2007; Wuchter et al., 2005; Zhu et al., 2016). GDGTs derived from the deeper clade thus affect the temperature signal preserved in marine sediments. The two clades are distinctive in their ratio of GDGT-2/GDGT-3: SPM collected from above the permanent pycnocline are typically <5 (e.g., Hernández-Sánchez et al., 2014; Hurley et al., 2018), while deeper SPM has values up to 40. The exact GDGT-2/GDGT-3 value of deep clade Nitrososphaerota remains elusive, however, as SPM also includes organic matter exported from the surface ocean. Nonetheless, the essentially bimodal distinction between the two clades, also encountered in the water depth domain, implies that GDGT-2/GDGT-3 ratio values can be used to differentiate between contribution from 'shallow' (~0-200 m depth) and 'deep' (> ~100 m depth) clades of archaea (Hurley et al., 2018; Rattanasriampaipong et al., 2022). The ratio of GDGT-2/GDGT-3 can thus be used as a method of assessing whether a

https://doi.org/10.5194/egusphere-2025-1467
Preprint. Discussion started: 15 April 2025


sediment sample displays a contribution from archaea living in or below the surface waters and this shows that many (notably deep ocean) samples in the calibration data set includes contributions from the deep clade (e.g., Taylor et al., 2013; Kim et al., 2015; van der Weijst et al., 2022). This implies that calibration to surface ocean temperature has likely led to an overestimate of the proxy response slope and that integrated (shallow) subsurface calibrations are more appropriate (Ho and Laepple, 2015) Yet, in many oceanographic settings, there is a strong correlation between SST and subT variability through time (e.g., Ho and Laepple, 2015) which implies that $TEX_{86}$ – calibrated to an integrated shallow subsurface depth – may still serve as a proxy for surface temperature variability, if this assumption can be substantiated (Fokkema et al., 2024).

### 6.6 Other non-thermal overprints (fcren and Red Sea-type)

Crenarchaeol and cren' are produced by marine Nitrososphaerota. Some studies (Sinninghe Damsté et al., 2012a; O'Brien et al., 2017) suggested that a substantial increase in the proportion of the cren' relative to crenarchaeol, referred to as fcren, could indicate a non-thermal impact on a GDGT distribution. For instance, Group I.1a Nitrososphaerota produce much less cren' (compared to crenarchaeol) than Group I.1b Nitrososphaerota (Pitcher et al., 2010), which means that community changes in Nitrososphaerota will have impact on the GDGT distributions (and thus overprint values and $TEX_{86}$) irrespective of temperature, and overprint values. In the modern core-top dataset, fcren values vary between 0 and 0.16. If a sample displays higher values (i.e., >0.25) it could indicate shifts in archaeal communities. This ratio might be a useful indicator of non-thermal overprints in settings which are warmer than the basins with the warmest sea temperature today. In cultures, fcren variations are strongly temperature controlled, but archaeal ecology might also play a role (Bale et al., 2019).

Core-top samples collected from the modern Red Sea display unusual GDGT distributions and $TEX_{86}$ values that do not align with observed temperatures, potentially caused by an endemic Nitrososphaerota clade (Trommer et al., 2009). Distributions in this highly saline, warm, and low nutrient environment are typically characterized by a low abundance of GDGT-0 relative to the cren' leading Inglis et al. (2015) to suggest that 'Red Sea-type' distributions in the geological past could be detected by the abundance of cren' relative to that of GDGT-0 ($\%GDGT_{RS}$). Values of $\%GDGT_{RS}$ >30 could indicate 'Red Sea-type' distributions, although Inglis et al. (2015) note that these values are also expected to also occur under very high temperature (>30 °C) surface waters. In the Red Sea surface samples, where ecological factors are at play, fcren is high as well, but the fact that the basin water is also hot makes it impossible to separate an ecology effect from a temperature effect.

### 6.7 D_nearest

The OPTiMAL method of calibrating GDGT paleothermometry (Dunkley Jones et al., 2020; Table 1) uses a Gaussian process (GP) emulator to determine the relationship between sea surface temperature and all six of the main isoGDGTs (GDGT-0, -1,

https://doi.org/10.5194/egusphere-2025-1467
Preprint. Discussion started: 15 April 2025


-2, -3, cren and cren'). This study also quantifies how similar a fossil GDGT assemblage is to the modern core top calibration data set. OPTiMAL measures the distance between the fossil assemblage and its nearest neighbours within the modern calibration data, in GDGT space. This distance is small if the fossil assemblage is "within" the modern calibration space and will grow the further the fossil assemblage is outside the modern calibration. The weighting coefficients learned by the GP emulator allow for a measurement of this "distance" - termed $D_{nearest}$. If a GDGT input coordinate has a minimal effect on temperature prediction (it is relatively insensitive to temperature), then points with a large absolute difference in GDGT-values from this coordinate will still be near in $D_{nearest}$ space. If, however, a GDGT coordinate is more significant in temperature prediction, differences between samples in that coordinate will contribute more to $D_{nearest}$. A threshold $D_{nearest}$ value of 0.5 was proposed, above which fossil samples are considered to be significantly 'non-analogue' with the modern calibration, on the basis of the inflection point of rapidly increasing uncertainty in the GP estimator of temperature (Dunkley Jones et al., 2020). As noted in Dunkley Jones et al. (2020) there are two (not exclusive) potential categories of non-analogue GDGT samples; the first consists of samples with anomalous GDGT distributions, such as fossil samples with one or more of high BIT, ΔRI, MI and/or %GDGT-0, that also show high $D_{nearest}$; and the second consists of GDGT assemblages that formed at temperatures beyond the temperature range of the modern calibration. For a GP emulator that is agnostic about the form of the temperature - GDGT relationship, there is 'no information' outside of the modern calibration space and it can make no meaningful temperature prediction for samples in this category. However, calibrations that are confident about the form of the GDGT-temperature relationship, and its conservation at temperatures >30ºC, would use this as the basis for temperature prediction at higher $D_{nearest}$ values. Even in these cases, $D_{nearest}$ is a means of checking how far these extrapolations have gone beyond the constraints of the calibration data. However, OPTiMAL is not applicable outside the modern range and has therefore no use in paleoclimate studies outside of the modern temperature range.

## 7 Temperature calibrations

### 7.1 GDGT core top dataset

GDGT distributions in samples from a global core top dataset have been critical in calibrating GDGT relationships with temperature. The calibration dataset was initially composed of 44 core top samples (Schouten et al., 2002) and has been expanded several times since then (Kim et al., 2008; 2010), to the most recent iteration of 1095 samples in Tierney and Tingley (2015). More core top data points/sites have been reported since 2015, in some cases substantially expanding some areas of the global ocean that are underrepresented in the data set of Tierney and Tingley (2015), for example from the Mediterranean Sea, Southern Ocean and Antarctica (e.g., Kim et al., 2015; Jaeschke et al., 2017; Lamping et al., 2021) (Fig. 1). However, despite these efforts, several regions of the global ocean remain poorly represented: subtropical gyres, deep water settings and other areas of the open ocean distal from land (Fig. 1). On top of this, core top data was assembled while the proxy was still

https://doi.org/10.5194/egusphere-2025-1467
Preprint. Discussion started: 15 April 2025


in the development phase. This means that it initially included only the six primary isoGDGTs (GDGT-0, GDGT-1. GDGT-2, GDGT-3, crenarchaeol and the cren') and the three brGDGTs included in the BIT index (brGDGT-I, brGDGT-II and brGDGT-III), and did not exclude core topdata with overprints. Also, it misses more recent developments in the proxies, e.g., in the interpretations of brGDGTs that are marine-*in situ* produced, and the inclusion of GDGT-4. Following our recommendations in Section 10 and in Table 4, we envision that an open access repository in which all cope top data are easy accessible and stored with metadata, will enable the community to iteratively improve the calibrations.

GDGTs are commonly applied to paleo/geological samples, where following information/data are typically generated e.g.,: sediment fraction (clay, silt), mineralogical composition, carbonate content, X-ray Fluorescence (XRF), TOC, or/and depositional setting (shallow marine, hemipelagic, etc.). To ensure better understanding of GDGT distributions in ancient and recent samples, future expansion of the core top data set as well as critical evaluation of the existing core top data should include the following information:

- Core top GDGT data should be reported as peak areas, with quantified concentrations where available, as well as the used detection limit (e.g., signal-to-noise ratio, peak area, etc). We also suggest expanding the range of GDGTs beyond those used for $TEX_{86}$ (see Section 8). This will optimize the interoperability and reusability of core top data as different indices or calibration methods are developed over time, that include more than the six primary isoGDGTs applied in the first top core calibration in 2002.
- Samples displaying unusual distributions (i.e., that fail the screening methods described above) should still be reported but flagged as possibly impacted by non-thermal processes. As an example of how this could be done, the R-script of Bijl et al. (2021) indicates in columns with logical values which samples show unusual distributions based on threshold values for overprint criteria.
- Currently sea surface temperature and water depth to seafloor are reported for each core top site. We recommend that a larger range of environmental metadata is included, for example, distance to shore, water column structure/water mass, oxygen concentrations, and any information that can guide an interpretation of core top sediment age.
- Core-top and surface sediment is often assumed to be representative of modern conditions, but variability in sediment dynamics, bottom currents and even sampling methods may lead to these samples representing thousands of years of sediment accumulation (Mekik and Anderson, 2018). Where possible, an estimate of sediment age (i.e., based on microfossils or $^{210}Pb$ dating) should be reported.
- Surface sediment data will need to be scrutinized regarding data quality and confounding factors to arrive at proper proxy calibrations. For example, there may be some doubt regarding data quality of some samples included in the current dataset that must be overcome by data reproduction in different laboratories (i.e., round-robins). Another issue is that most surface samples from the Mediterranean Sea are compromised by large contributions of deep-dwelling

https://doi.org/10.5194/egusphere-2025-1467
Preprint. Discussion started: 15 April 2025


archaea and should possibly not be used for calibrations to SST. The community must define a way forward for defining proper analytical conditions and use of surface sediment data for the development of proxies.

### 7.2 Calibration equations

Currently, a large range of GDGT-based temperature calibrations exist, as a result of method development and improved mechanistic understanding of proxy functioning (see GDGT review paper). We summarize key developments in global calibrations, and when/how to use these calibrations in Table 2. We note that the current understanding of GDGT synthesis and taphonomy prevents choosing one calibration that suits all purposes, geologic time intervals, and geographic settings.

**Table 2. Summary of key developments in GDGT-based global calibrations (where 'n' refers to the number of coretop/surface sediment samples, RSE - residual standard error).**

| Calibration | Equation | Calibration error | Description | Reference | Status |
|---|---|---|---|---|---|
| Linear $TEX_{86}$, n=44 | $TEX_{86} = 0.015 \times T + 0.28$ Where $TEX_{86} = \frac{[GDGT-2]+[GDGT-3]+[cren']}{[GDGT-1]+[GDGT-2]+[GDGT-3]+[cre}$ And T= annual mean SST in °C. | RSE ±2.0 °C | Original linear SST calibration based on a global core top dataset | Schouten et al. (2002) | Superseded by Kim et al., (2008) |
| $TEX_{86}$' n=104 | $TEX_{86}$=0.016×SST+0.20 Where $TEX_{86}$= ([GDGT-2] +[GDGT-3] +[cren])/ ([GDGT-1] +[GDGT-2] +[cren]) | RSE: none given | Modified version of $TEX_{86}$ used in Paleogene Arctic samples with high relative abundances of GDGT-3 | Sluijs et al., (2006) | No longer in use, see discussion in Sluijs et al., (2020) |
| Updated linear $TEX_{86}$ n=223 | $SST = 56.2 \times TEX_{86} - 10.8$ | RSE ±1.7 °C | Updated linear SST calibration | Kim et al. (2008) | Superseded by Kim et al., (2010) |
| Reciprocal $TEX_{86}$ n=287 | $SST = -16.3 \times \left(\frac{1}{TEX_{86}}\right) + 50.5$ | 68.2% confidence interval | Non-linear (reciprocal), high temperature calibration | Liu et al. (2009) | Not recommended since it lacks underlying mechanistic understanding |
| $TEX_{86}^{H}$ Exponential n=255 | $TEX_{86}^{H} = log\,(TEX_{86})$ And $SST = 68.4 \times (TEX_{86}^{H}) + 38.6$ | $TEX_{86}^{H}$ | Logarithmic (Kim et al., 2010) or exponential; (Tierney and Tingley, 2014) calibrations; $TEX_{86}^{H}$ was recommended for temperature > 15°C. Surface waters (0–20m) | Kim et al. (2010) | In use, but $TEX_{86}^{H}$suffers from statistical shortcomings, notably regression dilution and residuals at the warm end of the calibration. (Tierney and Tingly, 2014) |

https://doi.org/10.5194/egusphere-2025-1467
Preprint. Discussion started: 15 April 2025


| | | | | | |
|---|---|---|---|---|---|
| $TEX_{86}^{L}$ and Exponential<br><br>n=396 | $TEX_{86}^{L} = log\left(\frac{[GDGT-2]}{[GDGT-1]+[GDGT-2]+[GDGT-3]}\right)$<br>And<br>$SST = 67.5 \times (TEX_{86}^{L}) + 46.9$ | RSE ±4.0 °C for $TEX_{86}^{L}$ ±2.5°C | $TEX_{86}^{L}$ was recommended for temperature below 15°C. Surface waters (0–20m) | Kim et al. (2010) | $TEX_{86}^{L}$ has mechanistic flaws and is no longer recommended for use. |
| Linear $TEX_{86}^{H}$<br>n=21 | $T = 52.0 \times (TEX_{86}^{H}) + 42.0$ | RSE ±3.4 °C | Linear calibration of $TEX_{86}^{H}$ in mesocosms. | Kim et al. (2010) | Not used because of the lack of analogy between mesocosm and core top GDGT distributions |
| BAYSPAR<br><br>n=1095<br><br>(samples north<br><br>of 70° N<br><br>removed) | Bayesian, spatially varying regression based on $TEX_{86}$ | 90th percent confidence intervals | Linear calibration. Used in 'Standard' or 'Analogue' mode depending on whether oceanographic conditions at the site were analogue to modern. Can reconstruct SST or SubT (weighted 0–200 m water depth, weights given by gamma probability density function). | Tierney and Tingley (2014, 2015) | In use, particularly for applications in modern-like temperature ranges and analogue settings |
| Subsurface<br><br>$TEX_{86}^{H}$<br><br>n=255; >15°C | $T = 40.8 \times (TEX_{86}^{H}) + 22.3$ | 95% confidence intervals | Recalibration of $TEX_{86}^{H}$. A least squared regression was performed for depth-integrated temperatures between 0-1000m water depth, and an ensemble (SUBCAL) derived for a subsurface temperature calibration. | Ho and Laepple (2016) | In use by the community because the paper presents a useful range of integrated export depths. The assumption of deeper export reduces the proxy response slope and dampens variability in downcore records. |
| OPTiMAL | Machine learning-based Gaussian process regression model | 95% confidence intervals, root mean square uncertainty ±3.6 °C | SST model based on machine learning using relative abundances of all 6 isoGDGTs. | Dunkley Jones et al. (2020) | In use, but assumes surface signal. It cannot be used to predict temperatures outside of the modern calibration range of SSTs (>30 °C). |

https://doi.org/10.5194/egusphere-2025-1467
Preprint. Discussion started: 15 April 2025


An initial calibration between GDGTs and temperature was developed by Schouten et al. (2002) on a core top dataset of 44 samples (Table 2). They found the best correlation with annual mean SST was a linear regression using the $TEX_{86}$ ratio, which includes GDGT-1, GDGT-2, GDGT-3 and cren', but excludes the abundant GDGT-0 and crenarchaeol to avoid these compounds having an overwhelming influence on the index. This was also driven by concerns that GDGT-0 had many alternative sedimentary sources (see Section 6). Nonetheless, Zhang et al. (2015) confirmed a strong relationship between SST and the weighted average RI. A modified version of $TEX_{86}$, termed $TEX_{86}$', based on an expanded data set of 104 core top sites, was used by Sluijs et al. (2006) for samples from the Paleogene succession from the Arctic which contained high relative abundances of GDGT-3, possibly related to high terrestrial input. This index removed GDGT-3 from the denominator of $TEX_{86}$, but proportionally high GDGT-3 was not commonly found in other sample sets, and the index is no longer in use (Sluijs et al., 2020).

The linear $TEX_{86}$-based calibration of Schouten et al. (2002) was subsequently updated by Kim et al. (2008) based on an expanded global core top data set of 223 samples (Table 2). Kim et al. (2008) noted that the core top samples from high latitude sites showed significant scatter, and that the $TEX_{86}$ calibration had limited utility below 5°C. Liu et al. (2009) expanded on the concepts introduced by Schouten et al. (2002) acknowledging the challenges in extrapolating the core top calibration above the limit of the modern day (i.e., above ~30°C and $TEX_{86}$ values of ~0.73) (Table 2). Liu et al. (2009) developed a calibration based on the reciprocal of $TEX_{86}$ that reduced the slope of the $TEX_{86}$-temperature relationship for samples from warm water pool.

The modern core top data set was expanded further by Kim et al. (2010), who also observed the relative insensitivity of $TEX_{86}$ to temperature in cold regions and investigated variations in GDGT ratios to improve the calibration at both the cold and warm ends of the spectrum (Table 2). The authors concluded that a logarithmic form of $TEX_{86}$, referred to as $TEX_{86}^{H}$ was most optimal as it exhibited the highest $R^2$ and the smallest residual error (which was their prime quality criterion) for samples from sites with moderate to high surface water temperature (15–28°C) when tested on a core top dataset with subpolar and polar samples removed, and recommended this calibration was applied for sites with expected temperatures above 15°C. For the whole temperature spectrum, and especially below 15°C, the authors found a logarithmic form of a GDGT ratio without the cren' resulted in the best correlation ($TEX_{86}^{L}$). $TEX_{86}^{L}$ is still in use as a proxy for polar sea surface or subsurface temperature, as it seems to provide the most plausible absolute values (e.g., Ai et al., 2024). However the ratio used in $TEX_{86}^{L}$ does not correlate with an increase in cyclopentane rings, i.e., it lacks a physiological basis and can be easily biased by water depth-driven variations as expressed by the GDGT-2/GDGT-3 ratio (Taylor et al., 2013). Thus, this calibration of $TEX_{86}$ has been widely discarded by the community, and we recommend it not be used.

https://doi.org/10.5194/egusphere-2025-1467
Preprint. Discussion started: 15 April 2025


Kim et al. (2010) also investigated the validity of $TEX_{86}^{H}$ and $TEX_{86}^{L}$ using mesocosm experiments, and found that $TEX_{86}^{H}$ (i.e., log $TEX_{86}$) provided the strongest correlation to incubation temperatures in culture data, albeit with a slightly different intercept and slope reflecting a reduced amount of the cren' in cultures than present in core tops. Incubation studies have since highlighted that $TEX_{86}$-temperature correlations vary across archaeal strains, while RI appears to have a more linear relationship (Elling et al., 2015). Despite this, global core tope values of RI have not yet been calibrated to temperature.

Several temperature calibrations have focused on the fact that sedimentary GDGTs may represent a subsurface rather than near surface temperature signal (e.g., Taylor et al., 2013). Kim et al. (2008) statistically compared the fit of sedimentary $TEX_{86}$ to temperatures from various depths, as outlined above, and based on that proposed that $TEX_{86}$ correlates best to SST. Later, mounting evidence suggested that $TEX_{86}$ is more representative of a subsurface signal. Ho and Laepple (2016) employed a calibration ensemble between 0 and 1000 m water depth, assuming the majority of GDGTs are exported from between 100 and 350 m. Tierney and Tingley (2014, 2015) expanded the core top dataset and developed a Bayesian, spatially varying method to generate linear calibrations (BAYSPAR) to surface (0–20m) or subsurface (0–200m), and recognized a regression dilution bias in the warm end of $TEX_{86}^{H}$. An approach taken by van der Weijst et al. (2022) combines modern observations of water column structure, and additional microfossil and GDGT-based proxies (i.e., the ratio of GDGT-2/GDGT-3) to assess changes in the export depth of GDGTs through a 15 million year long equatorial Atlantic record, enabling authors to determine which depth-integrated calibration is most appropriate to use at in the investigated core site.

BAYSPAR can also spatially weight a calibration to core tops near a sample site, recognizing that archaeal communities vary through the global ocean. As well as BAYSPAR, several regional calibrations have been developed to take account of this spatial variance, with examples including a calibration for the Baltic Sea (Kabel et al. 2012) or Sea of Okhotsk (Seki et al., 2014) and a subsurface calibration for offshore Antarctica (Kim et al., 2012). More recently, improvements to low temperature calibrations have focused on the inclusion of OH-GDGTs alongside isoGDGTs (e.g., Fietz et al., 2016; Varma et al., 2024b) (see section 8.1).

Machine learning-based approaches (e.g., OPTiMAL, Dunkley Jones et al., 2020) take an agnostic view of the form of the relationship between GDGT abundances and temperatures, using a Gaussian Process emulator to optimize temperature estimation from the modern core-top calibration data set of Tierney and Tingley (2015). This approach uses the fractional abundances of all six GDGTs to reconstruct SSTs (Dunkley Jones et al., 2020) and generates prediction uncertainty estimates that include uncertainty about the learned function (Dunkley Jones et al., 2020). The disadvantage of this approach is that no SST estimations can be made outside of the range of the calibration space - the GP emulator can only make SST predictions

https://doi.org/10.5194/egusphere-2025-1467
Preprint. Discussion started: 15 April 2025


with any degree of confidence where it is constrained by data, so for SSTs >30ºC and <5 ºC. For these temperatures, other compounds such as the OH-GDGTs seem to have a higher sensitivity to temperature (Varma et al., 2024b) (see Section 8.1). Choosing the most appropriate calibration can be a complicated process, creating at least two particularly acute challenges to their interpretation (e.g., Fokkema et al., 2024). First, although evidence for a dominant subsurface signal is mounting, it remains unclear which water depths sedimentary $TEX_{86}$ exactly represents at certain oceanographic conditions. This means that this may also be spatially, or temporally varying (van der Weijst et al., 2022; Cartagena-Sierra et al., 2021). Second, although calibration choice may not strongly impact reconstructed temperatures when applied to indices that fall within the modern calibration dataset, the assumed mathematical relationship (linear or logarithmic) between $TEX_{86}$ and temperature has a profound impact when applied to ancient climates with indices higher than those observed in modern oceans. It is important to note that there is not necessarily one 'correct' calibration to use, as calibration choice will depend on factors such as a sample set location and the studied time period. It is critical to determine the mathematical relationship between temperature and GDGT distributions, including whether that is properly represented by $TEX_{86}$ at all temperatures (i.e., as opposed to a weighted averaged ring index). We must also improve our understanding of the mechanistic relationship between GDGTs and temperature (see GDGT review paper), including the effect of local oceanographic conditions, community structure, export dynamics and changes therein. Therefore, when publishing the GDGT-derived temperature record, justification of the selected calibration should be provided. Stating the rationale behind the choice of the calibration will give a better understanding for the community, who may not be experts in the study area, why a particular calibration has been deemed as the most appropriate for the given sample set. It is imperative to disclose GDGT data in full for appropriate reuse and recalibration of existing data (see section 6). Moreover, there is now abundant evidence to suggest that although several good calibration approaches calibrate GDGTs to sea surface temperature, with also good proxy-to-proxy intercomparison, the majority of GDGTs are produced in the subsurface (50–200m; Hurley et al., 2018). At the same time, dominant depth of export remains difficult to constrain, and for deeper time, substantial part of the $TEX_{86}$ proxy records are derived from settings with relatively shallow water depths (Tierney et al., 2017). Proxy records should be interpreted with that in mind; our lack of understanding about how temperature affects GDGT distributions of the Archaea living in sub-thermocline waters and responsible for unusual GDGT-2/GDGT-3 ratios. For samples from the most recent geological past, where oceanographic conditions could be assumed to be relatively similar to modern, investigating how different calibrations predict temperature for nearby core-tops may also help to inform an appropriate calibration to use. For the moment, there is no perfect calibration that could provide reliable temperature reconstructions in cold temperatures, warmer-than-modern climates, and that takes full account of the depth of production of GDGTs, also given the fact that that depth may vary per oceanographic setting and through time. Considering known overprints, depth of production and oceanographic settings that are important for reliable temperature reconstructions from GDGTs, the community has a way forward for further proxy development and improving calibrations.

https://doi.org/10.5194/egusphere-2025-1467
Preprint. Discussion started: 15 April 2025


# 8 Other marine GDGT proxies

## 8.1 OH-GDGTs

OH-GDGTs are, like isoGDGTs, widespread in marine environments. They contain one or two hydroxy groups attached to their biphytanyl chains, and were first identified in marine sediment by Liu et al. (2012). OH-GDGTs increase in abundance at higher latitudes (Huguet et al., 2013). Initially, OH-GDGTs were used to improve accuracy of the SST reconstructions in (sub)polar regions where $TEX_{86}$ residual standard error increases. Using a dataset of 77 samples collected from the water column, marine surface sediments, as well as marine and freshwater downcore sediments, Huguet et al. (2013) found that the relative abundance of OH-GDGTs compared with isoGDGTs (%OH) shows a weak negative correlation with annual SST. They reduced the dataset to marine surface samples only (n = 38; Table 3) in order to improve the correlation and reduce the error. By extending the initial dataset of Huguet et al. (2013) with sea surface sediments from the Southern Ocean (Ho et al., 2014) (n = 52) and empirically searching for a better calibration, Fietz et al. (2016) established a new temperature calibration including GDGT-1, GDGT-2, GDGT-3, the cren' and OH-GDGTs ($OH^C$) that shows a better correlation and lower residual standard error than %OH with annual SST, summer SST and SST 0 – 200m. Recently, Varma et al. (2024b) compiled OH-GDGT from an extended array of surface sediments, including data analysed at NIOZ 'NIOZ dataset' (n=575) and data analysed in other laboratories (n=297). Data that failed either the screening methods described in Section 6 (i.e., high BIT index values), or where abundances of OH-GDGT-1 and/or OH-GDGT-2 were below the detection limit, were excluded from further analysis, leaving n=469 in the NIOZ dataset. Varma et al. (2024b) found interlaboratory offsets for OH-GDGT-based proxies between the NIOZ dataset and datasets from other laboratories. The offset was especially large for indices which combine both iso- and OH-GDGTs (i.e., %OH), indicating OH-GDGT response may vary on different analytical equipment. To circumvent this, authors obtained calibration results based only on the NIOZ dataset, but suggested that a round robin study is necessary to determine the extent of interlaboratory differences. Authors found a better correlation between annual SST and %OH compared with earlier studies, but with no significant improvement for the $OH^C$ calibration. Varma et al. (2024b) also proposed a new OH-GDGT-based temperature calibration by adding OH-GDGT-0 to the denominator of the $TEX_{86}$ equation ($TEX_{86}OH$) (Table 3). This new calibration has a stronger correlation with SST than $TEX_{86}$, showing no flattening of the relationship below 15°C, remaining linear down to around 5 °C. Interestingly, the $TEX_{86}OH$ calibration has a similar correlation with ocean temperatures between 0–200 m ($R^2 = 0.89$, n = 470) as with SST ($R^2 = 0.88$, n = 513), suggesting that $TEX_{86}OH$ might be more suitable for reconstructing subsurface temperatures than surface temperatures, although as of yet it is not known where in the water column OH-GDGTs are produced.

Another approach is to generate OH-GDGT calibrations independent of isoGDGTs, also circumventing the interlaboratory differences for proxy indices that incorporate both OH-GDGTs and isoGDGTs (Varma et al., 2024b). Lü et al. (2015) analyzed

https://doi.org/10.5194/egusphere-2025-1467
Preprint. Discussion started: 15 April 2025


the correlation between OH-GDGT cyclization and SST using a dataset of 107 samples from the global dataset of Huguet et al. (2013), the Nordic Seas (Fietz et al., 2013) and new sediment samples from the South and East China Seas. Lü et al. (2015) proposed two new calibrations: RI-OH using only OH-GDGT-1 and OH-GDGT-2, recommended for SST > 15°C, and RI-OH' in which OH-0 is added to the denominator of the RI-OH equation, recommended for SST < 15°C. Subsequently, the correlation of RI-OH' with SST was improved by Fietz et al. (2020) by adding surface sediment data from the Baltic Sea (Kaiser and Arz, 2016), observing a better correlation to SST ($R^2$ = 0.76) than in the original equation ($R^2$ = 0.75) of Lü et al. (2015). Recently, Varma et al. (2024b) updated the equations of these two calibrations, improving the correlation of RI-OH with SST ($R^2$ = 0.79) but showing a poorer correlation for RI-OH' ($R^2$ = 0.64).

Although the main factor influence on OH-GDGT distributions is temperature, several studies have shown the impact of non-thermal factors. Xiao et al. (2023) observed that the production of OH-GDGTs by benthic archaea can have a large impact on RI-OH', which dictates caution to apply this proxy on sediments from deep ocean basins. Other confounding factors include: i) the influence of seasonal phenomena such as the extension of sea ice cover (Wu et al., 2020), or changes in the monsoon regime (Wei et al., 2020), ii) inputs of terrestrial sediments that often have a higher relative abundance of OH-GDGT-2 compared to marine sediments (Kang et al., 2017; He et al., 2024) iii) freshwater inputs modifying how the archaea adjust the OH-GDGT composition of their membrane (Sinninghe Damsté et al., 2022), iv) a difference in the archaeal community as a function of water column depth (Zhu et al., 2016; Lü et al., 2019; Liu et al., 2020; Varma et al., 2023; 2024a), v) changes in dissolved oxygen concentration or nutrient abundance (Harning et al., 2023; Harning and Sepúlveda, 2024) vi) seasonal biases (Lü et al., 2015; Davtian et al., 2019), and vii) difficulty in quantifying OH-GDGTs when abundance is low, especially in tropical regions with temperatures > 25°C (Varma et al., 2024a; 2024b).

As with $TEX_{86}$, selecting a calibration and an equation is a complicated process that is generally carried out on a case-by-case basis, depending on the characteristics of the study area (e.g., ice cover, variability of terrestrial inputs, depth of the nutricline, archaeal community differences) and the location of the samples (e.g., water depth, distance from the river mouth). Importantly, a brief justification of the choice of calibration is necessary to allow the reader to understand the rationale behind this decision.

**Table 3. Temperature calibrations using OH-GDGTs (RMSE - root mean square error)**

| Calibration | Equation | Error | Description | Reference |
|---|---|---|---|---|
| % OH | $\frac{\sum[OH-GDGTs]}{\sum[OH-GDGTs]+\sum[iso-GDGTs]}$<br>$SST = -0.24 \times \%OH + 8.3$ | RMSE = 9.7 °C<br>95% confidence interval | Original global linear SST calibration based on a marine surface sediment dataset of 38 samples. | Huguet et al. (2013) |

https://doi.org/10.5194/egusphere-2025-1467
Preprint. Discussion started: 15 April 2025


| | | | | |
|---|---|---|---|---|
| RI-OH | $\frac{[OH-1]+2\times[OH-2]}{[OH-1]+[OH-2]}$<br>$RI-OH = 0.018\times SST + 1.11$ | RMSE = 6 °C | Global linear calibration based on marine surface sediment dataset of 107 samples, for use above 15 °C. | Lü et al. (2015) |
| RI-OH' | $\frac{[OH-1]+2\times[OH-2]}{[OH-0]+[OH-1]+[OH-2]}$<br>$RI-OH' = 0.0382\times SST + 0.1$ | RMSE = 6 °C | Global linear calibration based on marine surface sediment dataset of 107 samples, for use below 15 °C. | (Lü et al., 2015) |
| $OH^C$ | $\frac{[GDGT-2]+[GDGT-3]+}{[GDGT-1]+[GDGT-2]+[GDGT-}$<br>$OHC = 0.0266\times SST - 0.144$ | RMSE = 3.9 °C | | Fietz et al. (2016) |
| $TEX_{86}^{OH}$ | $\frac{[GDGT-2]+[GDGT-3]+[Cren']}{[GDGT-1]+[GDGT-2]+[GDGT-3]+[Cren']+[OH}$<br>$TEX_{86}^{OH}$ = 0.023 × SST +0.03<br>$TEX_{86\,0-200\,m}^{OH}$= 0.026 × $SST_{0-200m}$+0.09<br>NIOZ dataset<br><br>$TEX_{86}^{OH}$ = 0.021 × SST +0.08<br>$TEX_{86\,0-200\,m}^{OH}$= 0.025 × $SST_{0-200m}$+0.11<br>Complete dataset | Standard deviation of residuals (NIOZ dataset): 3.2 °C (SST) and 2.8 °C (SST 0–200m)<br><br>Standard deviation of residuals (complete dataset): 3.7 °C (SST) and 2.9 °C (SST 0–200m) | Increases the temperature sensitivity of the index, especially for temperatures from 5 to 15°C. Two equations available: surface and subsurface (0–200m). Calibrations obtained using the NIOZ dataset and complete dataset. | Varma et al. (2024b) |
| $RI-OH'^{\square}_{WD}$ | SST = 15.2 × $RI-OH'^{\square}_{200m}$ + 5.0<br>for SST reconstruction between 0 – 200 m | RMSE = 2.1 °C | The contribution of deep-water archaea may alter OH-GDGT distributions, with increased OH-GDGT-0 production at greater depths due to colder temperatures. This effect is more pronounced in low latitudes, where the surface-to-bottom water temperature gradient is stronger. The RI-OH' equations proposed here attempt to consider the impact of water depth. | Xiao et al. (2023) |
| | $SST = 21.2\times RI-OH'^{\square}_{Global-FOD} + 0.0013\times Water\ Depth - 0.3$ | RMSE = 5.2 °C | | |

https://doi.org/10.5194/egusphere-2025-1467
Preprint. Discussion started: 15 April 2025


### 8.2 Branched GDGTs

The distribution of brGDGTs in terrestrial environments is mainly linked to changes in temperature and pH (Weijers et al., 2007b). As brGDGTs are predominantly produced in terrestrial environments, their presence in marine sediments is often associated with the input of terrigenous material, notably soils (Hopmans et al., 2004; Schouten et al., 2013a). However, studies carried out in a variety of environments including open oceans (Weijers et al., 2014), fjords (Peterse et al., 2009), continental shelves and rivers (Zhu et al., 2011; Zell et al., 2014), and the deepest hadal trenches (Xiao et al., 2020) showed significant differences in the distribution of brGDGTs between terrestrial and marine sediments, leading to the hypothesis of *in situ* marine production. The distribution of *in situ* brGDGTs in marine environments remains however poorly understood. Currently, three approaches are used to differentiate the origin of brGDGTs in marine sediments: the abundance of hexamethylated (sum of hexamethylated brGDGTs- ΣIIIa) over pentamethylated (ΣIIa) brGDGTs (ΣIIIa/ΣIIa) (Xiao et al., 2016), the degree of cyclisation of tetramethylated brGDGTs (#rings$_{tetra}$) (Sinninghe Damsté, 2016) and comparison of the relative abundance of tetramethylated, pentamethylated and hexamethylated brGDGTs (Sinninghe Damsté, 2016).

The ΣIIIa/ΣIIa ratio was derived from a global dataset comprising 1,354 terrestrial and 589 marine samples. Notably, 90% of marine sediments exhibited a ΣIIIa/ΣIIa >0.92, while 90% of terrestrial sediments had ΣIIIa/ΣIIa of <0.59 (Xiao et al., 2016). In their study, Xiao et al. (2016) combined IIIa and IIIa' as the majority of the available data at that time did not distinguish between the isomers. As a result, the proposed proxy was predominantly based on data lacking isomer separation. With improved compound separation achieved by the HPLC method of Hopmans et al. (2016), now both 5- and 6-methyl brGDGTs are incorporated in the calculation.

The #rings$_{tetra}$ approach is based on the comparison between the global soil dataset and sediments from a variety of open sea, coastal and river environments, which shows that the #rings$_{tetra}$ value in soils is always <0.7, suggesting that brGDGTs in marine sediments with values >0.7 have a purely marine origin (Sinninghe Damsté, 2016). It was also observed that the relative abundance of tetra-, penta- and hexamethylated brGDGTs in soils followed a clear trend when plotted in a triplot, and that datapoints derived from (coastal) marine sediments plot increasingly offset from this trend depending on the contribution of *in situ* produced brGDGTs in marine sediments (Sinninghe Damsté, 2016). The observed discrepancies in the degree of methylation and cyclisation of brGDGTs in marine sediments and soils have been attributed to pH differences between soils and marine waters, and to colder temperatures in the deep ocean than in soils (Sinninghe Damsté, 2016; Xiao et al., 2016). These new approaches supplement the use of the BIT index as a tracer of terrestrial brGDGT inputs to marine sediments (see Terrestrial inputs), particularly in coastal regions where primary productivity is controlled mainly by nutrient inputs from rivers, for example, in Chinese coastal seas (Liu et al., 2021). In this configuration, the increase in marine isoGDGTs

https://doi.org/10.5194/egusphere-2025-1467
Preprint. Discussion started: 15 April 2025


production due to increased Nitrososphaerota productivity offsets the terrestrial brGDGTs inputs from the rivers, resulting in a low BIT index despite high inputs from land (Liu et al., 2021).

Identifying the source of brGDGTs in marine environments is crucial for applying both terrestrial or marine paleothermometers. In the case of significant *in situ* marine production of brGDGTs in marine settings, the MBT'$_{5ME}$ index should be applied with care (cf., De Jonge et al., 2014b), or corrected for the marine contribution prior to reconstructing mean annual air temperatures from marine sediments (Dearing-Crampton-Flood et al., 2018). Although *in situ* production of brGDGTs in marine environments complicates their use as proxies for terrestrial environmental conditions, recent studies suggest that their distribution can provide information about other marine environmental conditions, such as oxygen conditions (Liu et al., 2014; Xiao et al., 2024).

### 8.3 GDGT-4

Although GDGT-4 is produced by marine Nitrososphaera, it is rarely quantified and reported with other GDGTs because it is not included in the $TEX_{86}$ equation. However, its presence in various environments, including cultures (Pitcher et al., 2010; Elling et al., 2015; 2017; Bale et al., 2019), SPM (Zhu et al., 2016; Hurley et al., 2018; Besseling et al., 2019), core tops (Wei et al., 2011), ancient sediments (Zhang et al., 2014; Zhuang et al., 2017; De Bar et al., 2019; Crouch et al., 2020; Cavalheiro et al., 2021) and hydrothermal systems (Hernández-Sánchez et al., 2024) suggests that GDGT-4 contributes to membrane adaptation, and may be an important component of membrane lipids, especially in warm climates. Although GDGT-4 is not currently included in GDGT-derived indices, quantifying it and including it in the core top database will future-proof data for potential inclusion in future indices. Accurate quantification of GDGT-4 hinges on full chromatographic separation of crenarchaeol (or any crenarchaeol isomer) and GDGT-4. If crenarchaeol and GDGT-4 are not chromatographically separated, correction of the apparent GDGT-4 peak area is needed, which may be done by subtracting the isobaric interference of the +2 Da isotope peak of crenarchaeol (1294.2601), which occurs at 45.97% of the intensity of crenarchaeol (1292.2444) at natural isotopic abundance (Sinninghe Damste et al., 2012b).

### 8.4 GTGTs, GMGTs and GDDs

Glycerol trialkyl glycerol tetraethers (GTGTs) and glycerol dialkanol diethers (GDDs) have been identified in cultured archaea (e.g., Bauersachs et al., 2015; Elling et al., 2014; 2017) and marine sediments (Liu et al., 2012b; Liu et al., 2018; Xu et al., 2020). GDD have been speculated to be either biosynthetic intermediates (e.g., Meador et al., 2014) or degradation products (Coffinet et al., 2015). In fact, a degradation pathway was proposed by Liu et al. (2016) suggesting that isoGDDs are formed from isoGDGTs. Recent discoveries in the isoGDGT biosynthetic pathway (Zeng et al., 2019; Lloyd et al., 2022) do not

https://doi.org/10.5194/egusphere-2025-1467
Preprint. Discussion started: 15 April 2025


consider the involvement of GDDs as intermediates in the biosynthesis, giving further support to GDDs as degradation products. Alternatively, it has been shown that GDDs could be degradation products of GDGTs (Coffinet et al., 2015; Naafs et al., 2018; Baxter et al., 2019; Mitrović et al., 2023; Hingley et al., 2024). Glycerol monoalkyl glycerol tetraethers (GMGTs; also known as H-shaped GDGTs (H-GDGTs) were first identified in a hyperthermophilic methanogen (Morii et al., 1998), but later appeared to also occur in sediments from low-temperature marine and lacustrine environments (e.g., Schouten et al., 2008; Liu et al., 2012c), where they were inferred to possibly be derived from Euryarchaeota. Their relative increase with temperature in marine hydrothermal sediments suggests that they may play a role in thermal regulation for their archaeal source organism (Sollich et al., 2017; Hernández-Sánchez et al., 2024), as recently supported by a mechanism linking GMGTs to high temperatures using molecular dynamics simulations (Garcia et al., 2024; Zhou and Dong, 2024). Next to isoGMGTs, branched GMGTs (brGMGTs) also exist, and are found in marine sediments of modern (Liu et al., 2012c) to late Cretaceous (e.g., Bijl et al., 2021), where their distributions, including methylation, strongly, but not consistently, vary in response to environmental change, likely temperature and/or water column oxygenation (Sluijs et al., 2020; Bijl et al., 2021; Kirkels et al., 2022) although in all these applications, brGMGTs have a different relationship to temperature. BrGMGTs furthermore occur in oxygen minimum zone SPM from the eastern Pacific (Xie et al., 2014), which agrees with the identification of the enzyme that synthesizes GMGTs, which is associated with obligate anaerobic archaea in oxygen-deficient ($O_2$ < 25 µM) environments (Li et al., 2024). While GTGTs, GDDs, and GMGTs are currently not commonly investigated or reported in marine sediments, future research may explore their potential applications in paleoclimate studies.

## 9 Best practices for sample, site and proxy intercomparisons and the presentation of error and uncertainty

Studies using GDGTs for temperature reconstruction can span or compile multiple sites (e.g., O' Brien et al., 2020; Auderset et al., 2022; Hou et al., 2023), or different depositional settings within an individual study site, e.g., fully marine to shallow marine or glaciomarine (e.g., Śliwińska et al., 2019; Duncan et al., 2022). It is important to consider variability in the depositional setting through a record, or in multi-site compilations, as this can influence GDGT preservation, or the water depth GDGTs have been exported from (e.g., Huguet et al., 2008; Taylor et al., 2013; Duncan et al., 2022). Integration of GDGT distributions and screening indices with the wider sedimentological and depositional history of a site should play an important role in interpreting a GDGT record. Likewise, other proxy methods for environmental reconstruction, such as those based on microfossils or other molecular fossils, can serve to support or help interpret a GDGT temperature record.

While the analytical error in GDGT-based temperature proxies is very small (see Figure 2), the calibration error imposes uncertainty on the absolute reconstructed SST values. This calibration error includes variability caused by known factors which could bias $TEX_{86}$ and its relationship to temperature, such as overprints, water column factors etc. One way to reduce the

https://doi.org/10.5194/egusphere-2025-1467
Preprint. Discussion started: 15 April 2025


calibration error is by more careful selection of subsets from the core top calibration that, based on what we now know, most accurately reflects temperature (e.g., as in Fokkema et al., 2024). In any case, we recommend that graphs wherein GDGT-based temperature records are presented should indicate the calibration error. We note that the calibration error is occasionally taken to represent the uncertainty in the reconstructed SST from sample to sample, and interpreted to mean that only SST shifts larger than the calibration error can be interpreted from any proxy record, whereas this error addresses the uncertainty of the record as a whole. In fact, many available reconstructions show predictable (e.g., relative to other temperature proxies) sample-to-sample $TEX_{86}$ variability, well within the range of the calibration error (e.g., Bijl et al., 2021; Hou et al., 2023). This distinction is important, because despite some level of uncertainty in the absolute temperature reconstruction derived from GDGTs, the temperature trends and sample-to-sample variability within the calibration error still hold paleoceanographic significance. One way to assess the significance of predictable or expected (e.g., relative to other temperature proxies or sites subject to similar conditions) temperature trends is to examine downcore variations in temperature proxy values and compare them with the analytical error before proxy conversion into SST. Indeed, the cumulative effect of all non-thermal effects at the spatial scale (e.g., global or regional) of the selected calibration may not apply to one specific site, so the calibration error should be viewed as an upper-bound of the uncertainty attributable to the non-thermal effects relevant to this site (Davtian et al., 2019). Therefore, applying the calibration error as uncertainty on all samples (e.g., via an envelope, or by a temperature error bar on each sample) gives the false impression that downcore trends within the calibration error might not be significant. We therefore recommend visualizing the calibration error separate from the individual data points, e.g., as bars in the corner of the plot.

# 10 Data reporting and archiving

## 10.1 Towards a common approach in GDGT data reporting and archiving

Since the development of the high performance liquid chromatography-mass spectrometry (HPLC-MS) technique for analysis of GDGTs (Hopmans et al., 2000), research into the environmental occurrence of GDGTs synthesized by archaea and bacteria has greatly expanded. To date, tens of thousands of GDGTs determined from laboratory experiments (cultures and mesocosms), modern environmental archives (marine waters and sediments), and ancient sedimentary sequences, have been reported in published literature. Additionally, the recent improvement of analytical techniques and methodology in lipid determination allowed scientists to discover newer classes of GDGT compounds.

Published temperature records derived from GDGTs are largely accompanied by raw data. Researchers commonly use online archiving systems like World Data Center for Paleoclimatology and Pangaea to make their data publicly available. However, data reporting and accessibility have never been fully systematized. To date, there is no agreed-upon standard for reporting

https://doi.org/10.5194/egusphere-2025-1467
Preprint. Discussion started: 15 April 2025


GDGT information upon publication. As the number of GDGT measurements carried out by the community has grown over the years, the effort to analyze, integrate, and/or synthesize such large datasets requires a significant amount of time to manually compile and vet each data record individually (cf. Judd et al., 2022; PhanSST database). In this section, we aim to provide a list of recommended items for reporting GDGT information in publications. The recommendations are based on the Linked Paleo Data (LiPD; Mckay and Emile-Geay, 2016) data standards and architecture, ensuring adherence to FAIR open access principles and facilitating the interchange.

### 10.2 Data components

Following LiPD data reporting framework, six possible types of information should be included when reporting GDGT data in any publications, including (1) root metadata, (2) geographic metadata, (3) publication metadata, (4) funding metadata, (5) paleodata information, and (6) geochronological information (e.g., age-depth models). Scientific journals and/or online archiving systems may require some data components during the peer review process, making sure to have all the data components listed here available at publication will ensure the integrity of the data for future use. Table 4 provides further descriptions of each data component.

**Table 4: Description of data components needed to be considered when reporting GDGT information. Please note that the list provided here is not exhaustive.**

https://doi.org/10.5194/egusphere-2025-1467
Preprint. Discussion started: 15 April 2025


| No. | Data Component | Description(s) | Elements in each component | | Level of Importance (Required, Preferred, Optional) |
|---|---|---|---|---|---|
| 1 | Root Metadata (Dataset Metadata) | This contains basic information of the reporting dataset, including but not limited to: | i | Dataset name | Required |
| | | | ii | Author(s)/Investigator(s) | Required |
| | | | iii | Sample request number(s)/ID(s) | Required |
| | | | iv | Cruise name/ID | Required |
| | | | v | Link(s) to published dataset(s) | Required - This information will be available after the author(s) publishing the dataset with an online archive, such as PANGAEA online database |
| 2 | Geographic Metadata | This contains geographical information of study sites, including but not limited to: | i | Coordinate(s) (modern latitude/longitude) | Required |
| | | | ii | Site name(s) | Required |
| | | | iii | Descriptive information such as:<br>• Country, State, Province<br>• Ocean basin/region | Preferred - especially for studies with samples from geological outcrops<br><br>Optional - for marine samples, providing site names with coordinates is sufficient |
| 3 | Publication Metadata | This contains publication information of GDGT data retrieved from previously published datasets, including but not limited to:<br><br>Not all information will be required, but the authors need to make sure that the publication metadata is sufficient for readers to be able to track back to the original publications of the compiled information. | i | Author(s) | Required |
| | | | ii | Title | Preferred |
| | | | iii | Journal name | Optional |
| | | | iv | DOI | Preferred |
| | | | v | Year of publication | Required |
| | | | vi | Link(s) to original publication(s) | Optional |

https://doi.org/10.5194/egusphere-2025-1467
Preprint. Discussion started: 15 April 2025


| No. | Data Component | Description(s) | Elements in each component | | Level of Importance (Required, Preferred, Optional) |
|---|---|---|---|---|---|
| 4 | Funding Metadata | This is applicable when the research that produced the data was funded. The metadata includes: | i | Funding agency | Generally required by journal(s)/publisher(s) |
| | | | ii | Funding grant number(s)/ID(s) | |
| 5 | PaleoData Information | All measured and inferred paleoenvironmental data, including but not limited to:<br><br>Note: GDGT abundances and material information are commonly reported in data tables and/or spreadsheets. | **GDGT Abundances** | | |
| | | | i | Raw peak intensities including the standard | Required |
| | | | ii | Absolute abundances (required material information) | Optional |
| | | | iii | Fractional abundances | Optional<br><br>If reported, the authors MUST explicitly describe all the fractions used for the fractional abundance calculation, i.e., all fractions that will give the sum to 1. |
| | | | **Material Information** | | |
| | | | iv | Sample information, including:<br>● For IODP samples<br>○ Site, Hole, Core, section, interval, depth (and which depth scale), age (and whose age model)<br>● For non-IODP/outcrop samples<br>○ Hole/Core/Section/Interval | Required |
| | | | v | Sample weight(s) | Required when reported absolute abundances |
| | | | vi | Amount of spiked standard | Required when reported absolute abundances |

https://doi.org/10.5194/egusphere-2025-1467
Preprint. Discussion started: 15 April 2025


| No. | Data Component | Description(s) | Elements in each component | | Level of Importance (Required, Preferred, Optional) |
|---|---|---|---|---|---|
| | | | vii | Sample description(s) (usually optional):<br>Colour, texture, key features from core images | Optional |
| | | | **Sample Preparation Information** | | |
| | | | vii | Sample preparation information<br>Lipid extraction and purification method(s) used | Required - usually described in the “Methods and Materials” section in scientific reports/publications. See section 10.2.2 for details. |
| 6 | Geochronological Information | This contains information used to infer the age of individual GDGT samples. | i | Age-depth models<br>● Tie points<br>● Age determination approach<br>○ Linear interpolation between tie points<br>○ etc. | Required if sample age is reported. |

1138

https://doi.org/10.5194/egusphere-2025-1467
Preprint. Discussion started: 15 April 2025


### 10.2.1 Non-GDGT information (metadata)

This section includes a list of recommended metadata of non-GDGT information to be reported alongside GDGT data. We have categorized the importance of each metadata item into three levels: required, recommended, and optional. Required information must be publicly accessible at time of publication. Additionally, we discuss best practices for reporting this information and provide guidance on handling missing information from published literature when necessary.

- **Sample Name and/or Sample ID (required):** Samples must be identified with unique and unambiguous sample names and/or sample identifications (IDs). Crucially, this label must provide the explicit link between published data and vial/sampleID. For example, the double-column development in GDGT analyses on UHPLC-MS (Hopmans et al., 2016) required that previously measured GDGTs had to be re-measured, highlighting the importance of proper sample labeling and storage. GDGTs can be stored for decades in their vials, which yields an opportunity for future remeasurements when labeling is adequate and links to original datasets.
- **Sample Request Number and/or Sample Request ID (required when applicable, in e.g., IODP regime):** This provides a direct way to link GDGT data with the original source of the sample information that is curated at the core repository.
- **Sample Information (required)**. The majority of GDGT research is done on core material, for instance from the IODP regime and its predecessors, but also from piston coring expeditions with national seagoing expeditions and onshore drilling campaigns. Reporting GDGT data without sample metadata (Site, Hole, Core, Section, Interval) makes it impossible to apply an updated depth or age scale to the data, and thus limits future reuse of the data.
- **Sampling depth (required).** Depth scales can change with a revision of the splice, the stratigraphic correlation, or to correct errors. For sediment samples from ocean drilling programs, various depth scales are developed, including CSF-A, CSF-B, and CCSF (prior to stratigraphic correlation, after stratigraphic correlation, depth from the splice, etc.), and the reporting of sample depths should include a reference to the scale used (e.g., original site reports or similar), especially when using an revised post-expedition composite depth scale. More information: https://www.iodp.org/policies-and-guidelines/142-iodp-depth-scales-terminology-april-2011/file.
- **Modern water depth (recommended).**
- **Age (recommended).**

https://doi.org/10.5194/egusphere-2025-1467
Preprint. Discussion started: 15 April 2025


- Provide reference for the applied age model used and type - e.g., biostratigraphic, magnetostratigraphic, cyclostratigraphic or others
- Specify how sample ages are interpolated between tie points

- **Paleo-location (optional, but required for Bayesian calibrations).**
  - When reporting paleolatitude/longitude, authors must report plate rotation models and refer to the source of the information.

### 10.2.2 Sample Information

GDGT abundances can be reported in three different formats as described below:

- **Raw peak areas:** This format represents the area under integrated GDGT peaks (intensity x time) obtained using LC-MS.
- **Absolute concentrations:** Areas of individual peaks peak that are above a set and well-defined detection limit can be quantified when a known amount of a standard is used (i.e., the most common is a synthesized $C_{46}$ GDGT; cf. Huguet et al. (2006)) and dry weight of extracted sediment (and TOC) are reported; usually reported as nanograms of GDGT per gram of sediment dry weight (ng/g dry weight and/or per g TOC).
- **Fractional abundances:** Abundance of individual GDGTs relative to the whole suite of GDGTs of interest (i.e., six common isoGDGTs) is commonly referred to as "fractional abundances." Reporting GDGT distributions in the fractional abundance format is likely the most common approach, as we can compare GDGT distribution patterns across all samples regardless of the absolute amount of GDGTs. Franctional abundances can be reported in either a fraction (0-1) or a percentage format (0-100%). The sum of all GDGT fractional abundances should add up to 1 or 100%. It must be explicit which components are included in the fractional abundance calculations, as with the additional reporting of additional GDGT-like compounds this may become ambiguous. Moreover, reporting GDGT abundances in this format can cause subsequent biases in GDGT-based index values if the reported numbers are rounded up with too few decimal places. See a discussion on the potential impact of the decimal rounding below.

Best practices in reporting GDGT abundances:

https://doi.org/10.5194/egusphere-2025-1467
Preprint. Discussion started: 15 April 2025


- We recommend that authors always report peak areas from the LC-MS. Although these values are inherently dependent on instrument sensitivity and method settings, peak areas are the root of the analyses and as such more interoperable and reusable. The peak areas can be used for the subsequent quantification of absolute and/or fractional GDGT abundances. Although retention times of each individual peak is information that is not commonly reported in published literature, we recommend the authors to keep track of these metrics as they are useful to evaluate integration consistency, machine functioning, and column lifespan.
- Despite ongoing progress in understanding the relationship between GDGTs and temperature, the mechanistic constraints on GDGT proxies require further improvement. Therefore, we recommend reporting all available GDGT data (e.g., isoGDGTs, brGDGTs, OH-GDGTs, GTGTs, GDDs, and GMGTs, even those not currently used in indices) to enable re-evaluation in subsequent research. If these data can not be archived upon publication, the authors should as minimum make it clear which GDGT compounds have been detected and which have not.
- When reporting fractional abundances, we recommend not rounding the calculated fractions, as rounding can introduce biases in GDGT-based ratios and indices. Figure 4 illustrates the impact of varying degrees of rounding on calculated $TEX_{86}$ values. This issue derived from rounding decimals is commonly found in early studies where GDGT information is reported in printed data tables without supplementary spreadsheets. If printed data tables require significant decimal rounding due to limited space, we recommend that the authors must provide the supplementary spreadsheets where the non-rounded GDGT fractional abundances are available. We also recommend that authors explicitly describe the method used to calculate fractional abundances (i.e., which GDGTs are included in the fractional abundance calculation). A lack of information on this complicates the calculation of indices that utilize GDGT compounds from different series; for example, BIT uses isoGDGTs and brGDGTs.
- Lastly, we recommend that authors should explicitly provide remarks for compounds that are either absent or in (too) low concentration. GDGT compounds that are not analysed (i.e., "NA") should be clearly distinguished from compounds with below quantification limit compounds (i.e., "NQ").

https://doi.org/10.5194/egusphere-2025-1467
Preprint. Discussion started: 15 April 2025


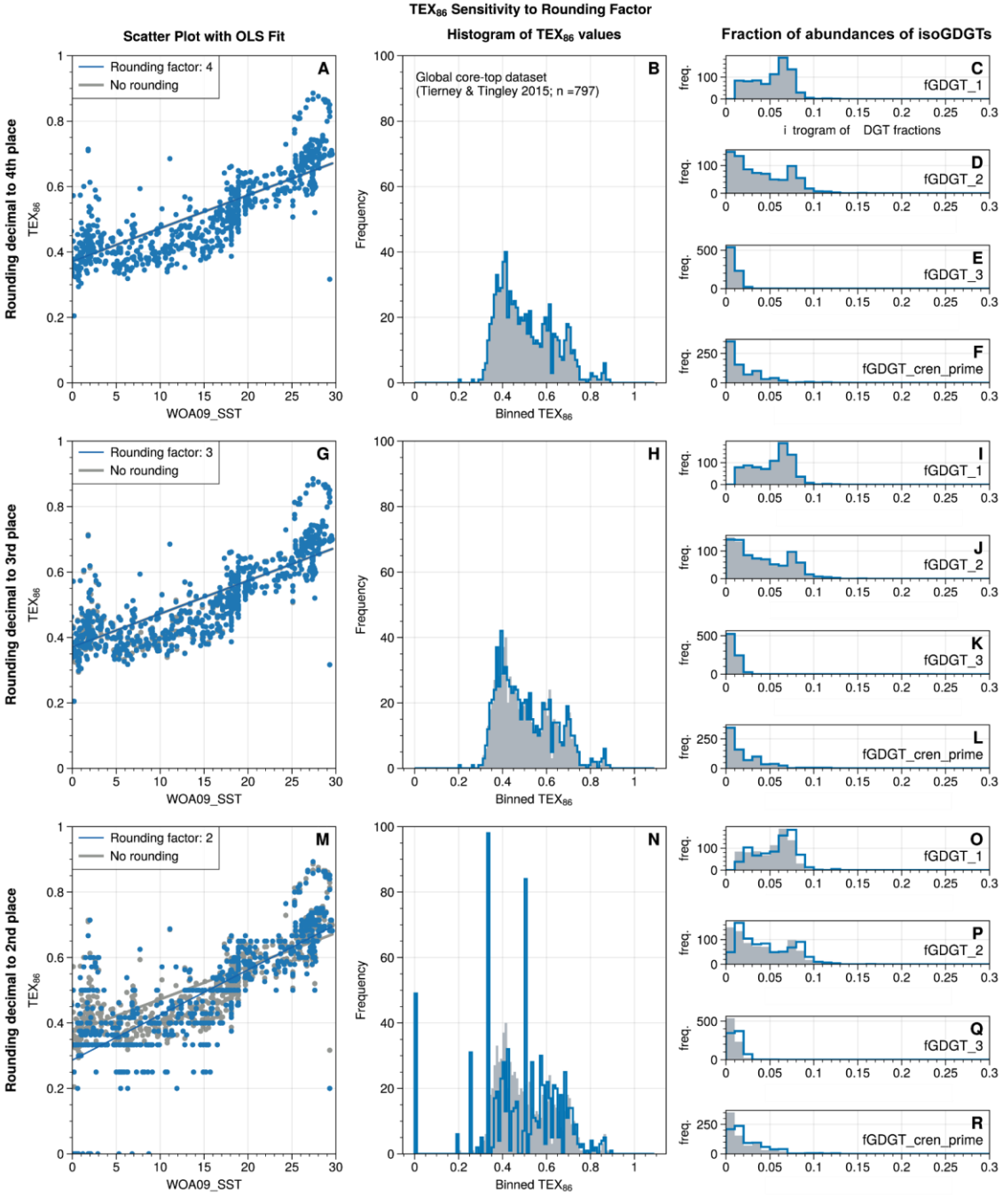

https://doi.org/10.5194/egusphere-2025-1467
Preprint. Discussion started: 15 April 2025


**Figure 4: The sensitivity of $TEX_{86}$ values to different rounding factors. The rounding factor indicates the last decimal place that the numbers are rounded up to (i.e., rounding factor of 2 means that the numbers are rounded up to the 2nd decimal place). Changes in data distribution with rounding factors of four (A–F), three (G–L), and two (M–R), are presented from top to bottom. From left to right, plots A, G, M show the scatter plots between SST from the nearest grid cells from the 2009 World Ocean Atlas database (retrieved from Tierney and Tingley, 2015) and the $TEX_{86}$ values calculated from rounded GDGT fractional abundances (blue) as well as the non-rounding original $TEX_{86}$ values (grey). Histograms of binned $TEX_{86}$ values (plots B, H, N) and each isoGDGT (plots C–F, I–L and O–R).**

### 10.3 Recommended templates for data reporting and archiving

We provide a sample template that lists all recommended column names for GDGT reporting of core tops and downcore samples (Supplementary Table S3 and S4, respectively).

## 11 Concluding remarks

This paper represents the consensus of a large part of the lipid biomarker community on the best practices, guidelines and recommendations for the entire process of generating marine GDGT data with the purpose of reconstructing past ocean temperature. Following these guidelines of analyses and reporting provides a level of certainty that data is reproducible, comparable, findable, accessible, interoperable and reusable. This maximizes the use and thus the value of the generated data, now and in the foreseeable future. This paper serves as an accessible reference for best practice in future studies.

## Supplements

Supplementary Table S1: comparison of extraction efficiency and quality between ASE and microwave extractions and with different temperature settings.
Supplementary Table S2: integration data of the UU TEX+BIT GDGT standard measurements.
Supplementary Table S3: A template for coretop samples
Supplementary Table S4: A template for downcore samples

https://doi.org/10.5194/egusphere-2025-1467
Preprint. Discussion started: 15 April 2025


## Data availability

Data that was used to draft Figure 1, 3 and 4 are available via the cited papers in the captions. Data that was used to draft Figure 2 is presented in Supplementary Table S2.

## Conflict of Interest

One of the co-authors, Sebastian Naeher, is associate editor for Biogeosciences

## Author contributions

Tier 1: PKB and KKS coordinated the compilation of the paper, assembled and coordinated with the writing teams for the sections, streamlined the separate sections, co-wrote Chapters 1–16; arranged alphabetically
Tier 2: BD, AH, SN, RR and CSMdO led the writing of the main sections of the paper (Chapters 2–10); arranged alphabetically
Tier 3: AA, MB, BSK, ND, TDJ, DDE, FE, LO'C, RDP, Fpe, Fpi, AR, AS, DV, WX and YZ contributed to the writing of the sections of the paper (Chapters 2–10); arranged alphabetically

Chapter 1, 11–16: all
Chapter 2: CSMdO, SN, MB, PKB, KKS
Chapter 3: AH, CSMdO, FE, ND, PKB, DE
Chapter 4: SN, CSMdO, FE, ND, PKB, DE
Chapter 5–9: BD, AR, AA, LO'C, SN, TDJ, MB, FPe, DV, FE, RR, ND, WX, RDP, KKS, YZ, FPi, BSK
Chapter 10: RR, LO'C, AS, BD, FPi, DV, ND, KKS

## Acknowledgements

This paper has been constructed after fruitful discussions during the 2nd International GDGT workshop in Zurich, 6–8 September 2023, which was organised with funding from SNSF Scientific Exchanges 2023, IZSEZ0 220372 to main organiser Cindy de Jonge. We also thank the Netherlands Earth System Science Center (NESSC; grant no. work20232-1), and the Dutch Research Council (NWO-Vidi grant no. 192.074)

https://doi.org/10.5194/egusphere-2025-1467
Preprint. Discussion started: 15 April 2025


to FP. The authors wish to thank the organisers of that workshop for facilitating these discussions. FJE acknowledges funding from the Deutsche Forschungsgemeinschaft (grant 441217575)

**References:**

Ai, X. E., Thöle, L. M., Auderset, A., Schmitt, M., Moretti, S., Studer, A. S., Michel, E., Wegmann, M., Mazaud, A., Bijl, P. K., Sigman, D. M., Martínez-García, A., and Jaccard, S. L.: The southward migration of the Antarctic Circumpolar Current enhanced oceanic degassing of carbon dioxide during the last two deglaciations, Communications Earth & Environment, 5, 58, 10.1038/s43247-024-01216-x, 2024.

Auderset, A., Moretti, S., Taphorn, B., Ebner, P.-R., Kast, E., Wang, X. T., Schiebel, R., Sigman, D. M., Haug, G. H., and Martínez-García, A.: Enhanced ocean oxygenation during Cenozoic warm periods, Nature, 609, 77-82, 10.1038/s41586-022-05017-0, 2022.

Bale, N. J., Palatinszky, M., Rijpstra, W. I. C., Herbold, C. W., Wagner, M., and Damsté, J. S. S.: Membrane Lipid Composition of the Moderately Thermophilic Ammonia-Oxidizing Archaeon “Candidatus Nitrosotenuis uzonensis” at Different Growth Temperatures, Applied and Environmental Microbiology, 85, e01332-01319, doi:10.1128/AEM.01332-19, 2019.

Bauersachs, T., Weidenbach, K., Schmitz, R. A., and Schwark, L.: Distribution of glycerol ether lipids in halophilic, methanogenic and hyperthermophilic archaea, Organic Geochemistry, 83-84, 101-108, https://doi.org/10.1016/j.orggeochem.2015.03.009, 2015.

Baxter, A. J., Hopmans, E. C., Russell, J. M., and Sinninghe Damsté, J. S.: Bacterial GMGTs in East African lake sediments: Their potential as palaeotemperature indicators, Geochimica et Cosmochimica Acta, 259, 155-169, https://doi.org/10.1016/j.gca.2019.05.039, 2019.

Besseling, M. A., Hopmans, E. C., Koenen, M., van der Meer, M. T. J., Vreugdenhil, S., Schouten, S., Sinninghe Damsté, J. S., and Villanueva, L.: Depth-related differences in archaeal populations impact the isoprenoid tetraether lipid composition of the Mediterranean Sea water column, Organic Geochemistry, 135, 16-31, https://doi.org/10.1016/j.orggeochem.2019.06.008, 2019.

Bijl, P. K., Bendle, J. A. P., Bohaty, S. M., Pross, J., Schouten, S., Tauxe, L., Stickley, C. E., McKay, R. M., Röhl, U., Olney, M., Sluijs, A., Escutia, C., and Brinkhuis, H.: Eocene cooling linked to early flow across the Tasmanian Gateway, Proceedings of the National Academy of Sciences of the United States of America, 110, 9645-9650, 2013.

Bijl, P. K., Frieling, J., Cramwinckel, M. J., Boschman, C., Sluijs, A., and Peterse, F.: Maastrichtian–Rupelian paleoclimates in the southwest Pacific – a critical re-evaluation of biomarker paleothermometry and dinoflagellate cyst paleoecology at Ocean Drilling Program Site 1172, Clim. Past, 17, 2393-2425, 10.5194/cp-17-2393-2021, 2021.

Birgel, D. and Peckmann, J.: Aerobic methanotrophy at ancient marine methane seeps: A synthesis, Organic Geochemistry, 39, 1659-1667, https://doi.org/10.1016/j.orggeochem.2008.01.023, 2008.

https://doi.org/10.5194/egusphere-2025-1467
Preprint. Discussion started: 15 April 2025


Blaga, C. I., Reichart, G.-J., Heiri, O., and Sinninghe Damsté, J. S.: Tetraether membrane lipid distributions in water-column particulate matter and sediments: a study of 47 European lakes along a north–south transect, Journal of Paleolimnology, 41, 523-540, 10.1007/s10933-008-9242-2, 2009.

Bligh, E. G. and Dyer, W. J.: A rapid method of total lipid extraction and purification, Canadian Journal of Biochemistry and Physiology, 37, 911-917, 10.1139/o59-099 1959.

Brassell, S. C., Eglinton, G., Marlowe, I. T., Pflaumann, U., and Sarnthein, M.: Molecular stratigraphy: a new tool for climatic assessment, Nature, 320, 129-133, 10.1038/320129a0, 1986.

Brocks, J. J., Logan, G. A., Buick, R., and Summons, R. E.: Archean Molecular Fossils and the Early Rise of Eukaryotes, Science, 285, 1033-1036, 1999.

Cartagena-Sierra, A., Berke, M. A., Robinson, R. S., Marcks, B., Castañeda, I. S., Starr, A., Hall, I. R., Hemming, S. R., LeVay, L. J., and Party, E. S.: Latitudinal Migrations of the Subtropical Front at the Agulhas Plateau Through the Mid-Pleistocene Transition, Paleoceanography and Paleoclimatology, 36, e2020PA004084, https://doi.org/10.1029/2020PA004084, 2021

Cavalheiro, L., Wagner, T., Steinig, S., Bottini, C., Dummann, W., Esegbue, O., Gambacorta, G., Giraldo-Gómez, V., Farnsworth, A., Flögel, S., Hofmann, P., Lunt, D. J., Rethemeyer, J., Torricelli, S., and Erba, E.: Impact of global cooling on Early Cretaceous high pCO2 world during the Weissert Event, Nature Communications, 12, 5411, 10.1038/s41467-021-25706-0, 2021.

Ceccopieri, M., Carreira, R. S., Wagener, A. L. R., Hefter, J., and Mollenhauer, G.: Branched GDGTs as Proxies in Surface Sediments From the South-Eastern Brazilian Continental Margin, Frontiers in Earth Science, 7, 2019.

Ceccopieri, M., Carreira, R. S., Wagener, A. L. R., Hefter, J. H., and Mollenhauer, G.: On the application of alkenone- and GDGT-based temperature proxies in the south-eastern Brazilian continental margin, Organic Geochemistry, 126, 43-56, https://doi.org/10.1016/j.orggeochem.2018.10.009, 2018.

Chen, J., Hu, P., Li, X., Yang, Y., Song, J., Li, X., Yuan, H., Li, N., and Lü, X.: Impact of water depth on the distribution of iGDGTs in the surface sediments from the northern South China Sea: applicability of TEX86 in marginal seas, Frontiers of Earth Science, 12, 95-107, 10.1007/s11707-016-0620-1, 2018.

Chen, Y., Zheng, F., Yang, H., Yang, W., Wu, R., Liu, X., Liang, H., Chen, H., Pei, H., Zhang, C., Pancost, R. D., and Zeng, Z.: The production of diverse brGDGTs by an Acidobacterium providing a physiological basis for paleoclimate proxies, Geochimica et Cosmochimica Acta, 337, 155-165, https://doi.org/10.1016/j.gca.2022.08.033, 2022.

Coffinet, S., Huguet, A., Williamson, D., Fosse, C., and Derenne, S.: Potential of GDGTs as a temperature proxy along an altitudinal transect at Mount Rungwe (Tanzania), Organic Geochemistry, 68, 82-89, https://doi.org/10.1016/j.orggeochem.2014.01.004, 2014.

Coffinet, S., Huguet, A., Williamson, D., Bergonzini, L., Anquetil, C., Majule, A., and Derenne, S.: Occurrence and distribution of glycerol dialkanol diethers and glycerol dialkyl glycerol tetraethers in a

peat core from SW Tanzania, Organic Geochemistry, 83-84, 170-177, https://doi.org/10.1016/j.orggeochem.2015.03.013, 2015.

Crouch, E. M., Shepherd, C. L., Morgans, H. E. G., Naafs, B. D. A., Dallanave, E., Phillips, A., Hollis, C. J., and Pancost, R. D.: Climatic and environmental changes across the early Eocene climatic optimum at mid-Waipara River, Canterbury Basin, New Zealand, Earth-Science Reviews, 200, 102961, https://doi.org/10.1016/j.earscirev.2019.102961, 2020.

Davtian, N., Ménot, G., Fagault, Y., and Bard, E.: Western Mediterranean Sea Paleothermometry Over the Last Glacial Cycle Based on the Novel RI-OH Index, Paleoceanography and Paleoclimatology, 34, 616-634, https://doi.org/10.1029/2018PA003452, 2019.

de Bar, M. W., Rampen, S. W., Hopmans, E. C., Sinninghe Damsté, J. S., and Schouten, S.: Constraining the applicability of organic paleotemperature proxies for the last 90 Myrs, Organic Geochemistry, 128, 122-136, https://doi.org/10.1016/j.orggeochem.2018.12.005, 2019.

De Jonge, C., Hopmans, E. C., Zell, C. I., Kim, J. H., Schouten, S., and Sinninghe Damsté, J. S.: Occurrence and abundance of 6-methyl branched glycerol dialkyl glycerol tetraethers in soils: Implications for palaeoclimate reconstruction, Geochimica et Cosmochimica Acta, 10.1016/j.gca.2014.06.013, 2014a.

De Jonge, C., Stadnitskaia, A., Hopmans, E. C., Cherkashov, G., Fedotov, A., and Sinninghe Damsté, J. S.: In situ produced branched glycerol dialkyl glycerol tetraethers in suspended particulate matter from the Yenisei River, Eastern Siberia, Geochimica et Cosmochimica Acta, 10.1016/j.gca.2013.10.031, 2014b.

De Jonge, C., Peterse, F., Nierop, K. G. J., Blattmann, T. M., Alexandre, M., Ansanay-Alex, S., Austin, T., Babin, M., Bard, E., Bauersachs, T., Blewett, J., Boehman, B., Castañeda, I. S., Chen, J., Conti, M. L. G., Contreras, S., Cordes, J., Davtian, N., van Dongen, B., Duncan, B., Elling, F. J., Galy, V., Gao, S., Hefter, J., Hinrichs, K.-U., Helling, M. R., Hoorweg, M., Hopmans, E., Hou, J., Huang, Y., Huguet, A., Jia, G., Karger, C., Keely, B. J., Kusch, S., Li, H., Liang, J., Lipp, J. S., Liu, W., Lu, H., Mangelsdorf, K., Manners, H., Martinez Garcia, A., Menot, G., Mollenhauer, G., Naafs, B. D. A., Naeher, S., O'Connor, L. K., Pearce, E. M., Pearson, A., Rao, Z., Rodrigo-Gámiz, M., Rosendahl, C., Rostek, F., Bao, R., Sanyal, P., Schubotz, F., Scott, W., Sen, R., Sluijs, A., Smittenberg, R., Stefanescu, I., Sun, J., Sutton, P., Tierney, J., Tejos, E., Villanueva, J., Wang, H., Werne, J., Yamamoto, M., Yang, H., and Zhou, A.: Interlaboratory Comparison of Branched GDGT Temperature and pH Proxies Using Soils and Lipid Extracts, Geochemistry, Geophysics, Geosystems, 25, e2024GC011583, https://doi.org/10.1029/2024GC011583, 2024.

De Rosa, M. and Gambacorta, A.: The lipids of archaebacteria, Progress in Lipid Research, 27, 153-175, https://doi.org/10.1016/0163-7827(88)90011-2, 1988.

Dearing Crampton-Flood, E., Peterse, F., Munsterman, D., and Sinninghe Damsté, J. S.: Using tetraether lipids archived in North Sea Basin sediments to extract North Western European Pliocene continental air temperatures, Earth and Planetary Science Letters, 490, 193-205, https://doi.org/10.1016/j.epsl.2018.03.030, 2018.

https://doi.org/10.5194/egusphere-2025-1467
Preprint. Discussion started: 15 April 2025


Dearing Crampton-Flood, E., Peterse, F., and Sinninghe Damsté, J. S.: Production of branched tetraethers in the marine realm: Svalbard fjord sediments revisited, Organic Geochemistry, 138, 103907, https://doi.org/10.1016/j.orggeochem.2019.103907, 2019.

Dillon, J. T. and Huang, Y.: TEXPRESS v1.0: A MATLAB toolbox for efficient processing of GDGT LC–MS data, Organic Geochemistry, 79, 44-48, https://doi.org/10.1016/j.orggeochem.2014.11.009, 2015.

Ding, W. H., Yang, H., He, G. Q., and Xie, S.: Effect of oxidative degradation by hydrogen peroxide on tetraethers based organic proxies, Q. Sci., 33, 39-47, 2013.

Duncan, B., McKay, R., Levy, R., Naish, T., Prebble, J. G., Sangiorgi, F., Krishnan, S., Hoem, F., Clowes, C., Dunkley Jones, T., Gasson, E., Kraus, C., Kulhanek, D. K., Meyers, S. R., Moossen, H., Warren, C., Willmott, V., Ventura, G. T., and Bendle, J.: Climatic and tectonic drivers of late Oligocene Antarctic ice volume, Nature Geoscience, 15, 819-825, 10.1038/s41561-022-01025-x, 2022.

Dunkley Jones, T., Eley, Y. L., Thomson, W., Greene, S. E., Mandel, I., Edgar, K., and Bendle, J. A.: OPTiMAL: a new machine learning approach for GDGT-based palaeothermometry, Clim. Past, 16, 2599-2617, 10.5194/cp-16-2599-2020, 2020.

Elling, F. J., Könneke, M., Lipp, J. S., Becker, K. W., Gagen, E. J., and Hinrichs, K.-U.: Effects of growth phase on the membrane lipid composition of the thaumarchaeon Nitrosopumilus maritimus and their implications for archaeal lipid distributions in the marine environment, Geochimica et Cosmochimica Acta, 141, 579-597, https://doi.org/10.1016/j.gca.2014.07.005, 2014.

Elling, F. J., Könneke, M., Mußmann, M., Greve, A., and Hinrichs, K.-U.: Influence of temperature, pH, and salinity on membrane lipid composition and TEX86 of marine planktonic thaumarchaeal isolates, Geochimica et Cosmochimica Acta, 171, 238-255, https://doi.org/10.1016/j.gca.2015.09.004, 2015.

Elling, F. J., Könneke, M., Nicol, G. W., Stieglmeier, M., Bayer, B., Spieck, E., de la Torre, J. R., Becker, K. W., Thomm, M., Prosser, J. I., Herndl, G. J., Schleper, C., and Hinrichs, K.-U.: Chemotaxonomic characterisation of the thaumarchaeal lipidome, Environmental Microbiology, 19, 2681-2700, https://doi.org/10.1111/1462-2920.13759, 2017.

Escala, M., Fietz, S., Rueda, G., and Rosell-Melé, A.: Analytical Considerations for the Use of the Paleothermometer Tetraether Index86 and the Branched vs Isoprenoid Tetraether Index Regarding the Choice of Cleanup and Instrumental Conditions, Analytical Chemistry, 81, 2701-2707, 10.1021/ac8027678, 2009.

Evans, T. W., Elling, F. J., Li, Y., Pearson, A., and Summons, R. E.: A new and improved protocol for extraction of intact polar membrane lipids from archaea, Organic Geochemistry, 165, 104353, https://doi.org/10.1016/j.orggeochem.2021.104353, 2022.

Fietz, S., Ho, S. L., and Huguet, C.: Archaeal Membrane Lipid-Based Paleothermometry for Applications in Polar Oceans, Oceanography, 33, 104-114, 2020.

https://doi.org/10.5194/egusphere-2025-1467
Preprint. Discussion started: 15 April 2025


Fietz, S., Huguet, C., Rueda, G., Hambach, B., and Rosell-Melé, A.: Hydroxylated isoprenoidal GDGTs in the Nordic Seas, Marine Chemistry, 152, 1-10, https://doi.org/10.1016/j.marchem.2013.02.007, 2013.

Fietz, S., Ho, S. L., Huguet, C., Rosell-Melé, A., and Martínez-García, A.: Appraising GDGT-based seawater temperature indices in the Southern Ocean, Organic Geochemistry, 102, 93-105, https://doi.org/10.1016/j.orggeochem.2016.10.003, 2016.

Fleming, L. E. and Tierney, J. E.: An automated method for the determination of the TEX86 and U37K′ paleotemperature indices, Organic Geochemistry, 92, 84-91, https://doi.org/10.1016/j.orggeochem.2015.12.011, 2016.

Fokkema, C. D., Agterhuis, T., Gerritsma, D., de Goeij, M., Liu, X., de Regt, P., Rice, A., Vennema, L., Agnini, C., Bijl, P. K., Frieling, J., Huber, M., Peterse, F., and Sluijs, A.: Polar amplification of orbital-scale climate variability in the early Eocene greenhouse world, Clim. Past, 20, 1303-1325, 10.5194/cp-20-1303-2024, 2024

Francis, C. A., Roberts, K. J., Beman, J. M., Santoro, A. E., and Oakley, B. B.: Ubiquity and diversity of ammonia-oxidizing archaea in water columns and sediments of the ocean, Proceedings of the National Academy of Sciences, 102, 14683-14688, doi:10.1073/pnas.0506625102, 2005

Frieling, J., Huurdeman, E. P., Rem, C. C. M., Donders, T. H., Pross, J., Bohaty, S. M., Holdgate, G. R., Gallagher, S. J., McGowran, B., and Bijl, P. K.: Identification of the Paleocene–Eocene boundary in coastal strata in the Otway Basin, Victoria, Australia, J. Micropalaeontol., 37, 317–339, https://doi.org/10.5194/jm-37-317-2018, 2018.

Frieling, J., Bohaty, S. M., Cramwinckel, M. J., Gallagher, S. J., Holdgate, G. R., Reichgelt, T., Peterse, F., Pross, J., Sluijs, A., and Bijl, P. K.: Revisiting the Geographical Extent of Exceptional Warmth in the Early Paleogene Southern Ocean, Paleoceanography and Paleoclimatology, 38, e2022PA004529, https://doi.org/10.1029/2022PA004529, 2023.

Garcia, A. A., Chadwick, G. L., Liu, X. L., and Welander, P. V.: Identification of two archaeal GDGT lipid-modifying proteins reveals diverse microbes capable of GMGT biosynthesis and modification, Proc Natl Acad Sci U S A, 121, e2318761121, 10.1073/pnas.2318761121, 2024.

Goldman, A. E., Emani, S. R., Pérez-Angel, L. C., Rodríguez-Ramos, J. A., and Stegen, J. C.: Integrated, Coordinated, Open, and Networked (ICON) Science to Advance the Geosciences: Introduction and Synthesis of a Special Collection of Commentary Articles, Earth and Space Science, 9, e2021EA002099, https://doi.org/10.1029/2021EA002099, 2022.

Grant, G. R., Williams, J. H. T., Naeher, S., Seki, O., McClymont, E. L., Patterson, M. O., Haywood, A. M., Behrens, E., Yamamoto, M., and Johnson, K.: Amplified surface warming in the south-west Pacific during the mid-Pliocene (3.3–3.0 Ma) and future implications, Climate of the Past, 19, 1359-1381, https://doi.org/10.5194/cp-19-1359-2023, 2023.

https://doi.org/10.5194/egusphere-2025-1467
Preprint. Discussion started: 15 April 2025


Grosjean, E. and Logan, G. A.: Incorporation of organic contaminants into geochemical samples and an assessment of potential sources: Examples from Geoscience Australia marine survey S282, Organic Geochemistry, 38, 853-869, https://doi.org/10.1016/j.orggeochem.2006.12.013, 2007.

Hagemann, J. R., Lembke-Jene, L., Lamy, F., Vorrath, M. E., Kaiser, J., Müller, J., Arz, H. W., Hefter, J., Jaeschke, A., Ruggieri, N., and Tiedemann, R.: Upper-ocean temperature characteristics in the subantarctic southeastern Pacific based on biomarker reconstructions, Clim. Past, 19, 1825-1845, 10.5194/cp-19-1825-2023, 2023.

Halamka, T. A., McFarlin, J. M., Younkin, A. D., Depoy, J., Dildar, N., and Kopf, S. H.: Oxygen limitation can trigger the production of branched GDGTs in culture, Geochemical Perspectives Letters, 19, 36-39, https://doi.org/10.7185/geochemlet.2132, 2021.

Halamka, T. A., Raberg, J. H., McFarlin, J. M., Younkin, A. D., Mulligan, C., Liu, X.-L., and Kopf, S. H.: Production of diverse brGDGTs by Acidobacterium Solibacter usitatus in response to temperature, pH, and O2 provides a culturing perspective on brGDGT proxies and biosynthesis, Geobiology, 21, 102-118, https://doi.org/10.1111/gbi.12525, 2023.

Harning, D. J., Andrews, J. T., Belt, S. T., Cabedo-Sanz, P., Geirsdóttir, Á., Dildar, N., Miller, G. H., and Sepúlveda, J.: Sea Ice Control on Winter Subsurface Temperatures of the North Iceland Shelf During the Little Ice Age: A TEX86 Calibration Case Study, Paleoceanography and Paleoclimatology, 34, 1006-1021, https://doi.org/10.1029/2018PA003523, 2019.

Harning, D. J., Holman, B., Woelders, L., Jennings, A. E., and Sepúlveda, J.: Biomarker characterization of the North Water Polynya, Baffin Bay: implications for local sea ice and temperature proxies, Biogeosciences, 20, 229-249, 10.5194/bg-20-229-2023, 2023.

Harning, D. J. and Sepúlveda, J.: Impact of non-thermal variables on hydroxylated GDGT distributions around Iceland, Frontiers in Earth Science, 12, 10.3389/feart.2024.1430441, 2024.

Harvey, H. R., Fallon, R. D., and Patton, J. S.: The effect of organic matter and oxygen on the degradation of bacterial membrane lipids in marine sediments, Geochimica et Cosmochimica Acta, 50, 795-804, https://doi.org/10.1016/0016-7037(86)90355-8, 1986.

He, Y., Zhao, Q., and Wang, H.: Sources and implications of hydroxylated isoprenoid GDGTs on the northwest shelf of Australia through the Pliocene-Pleistocene era, Chemical Geology, 648, 121975, https://doi.org/10.1016/j.chemgeo.2024.121975, 2024.

Herbert, T. D.: 8.15 - Alkenone Paleotemperature Determinations, in: Treatise on Geochemistry (Second Edition), edited by: Holland, H. D., and Turekian, K. K., Elsevier, Oxford, 399-433, https://doi.org/10.1016/B978-0-08-095975-7.00615-X, 2014.

Hernández-Sánchez, M. T., Woodward, E. M. S., Taylor, K. W. R., Henderson, G. M., and Pancost, R. D.: Variations in GDGT distributions through the water column in the South East Atlantic Ocean, Geochimica et Cosmochimica Acta, 132, 337-348, https://doi.org/10.1016/j.gca.2014.02.009, 2014.

https://doi.org/10.5194/egusphere-2025-1467
Preprint. Discussion started: 15 April 2025


Hernández-Sánchez, M. T., Hepburn, L., Stock, M. J., Connelly, D. P., and Pancost, R. D.: The microbial lipid signature in sediments and chimneys within a back-arc basin hydrothermal system south of the Antarctic Polar Front, Deep Sea Research Part I: Oceanographic Research Papers, 206, 104247, https://doi.org/10.1016/j.dsr.2024.104247, 2024.

Hingley, J. S., Martins, C. C., Walker-Trivett, C., Adams, J. K., Naeher, S., Häggi, C., Feakins, S. J., and Naafs, B. D. A.: The global distribution of Isoprenoidal Glycerol Dialkyl Diethers (isoGDDs) is consistent with a predominant degradation origin, Organic Geochemistry, 192, 104782, https://doi.org/10.1016/j.orggeochem.2024.104782, 2024.

Hinrichs, K.-U., Summons, R. E., Orphan, V., Sylva, S. P., and Hayes, J. M.: Molecular and isotopic analysis of anaerobic methane-oxidizing communities in marine sediments, Organic Geochemistry, 31, 1685-1701, https://doi.org/10.1016/S0146-6380(00)00106-6, 2000.

Hinrichs, K. U., Hmelo, L. R., and Sylva, S. P.: Molecular fossil record of elevated methane levels in late Pleistocene coastal waters, Science, 299, 1214-1217, 10.1126/science.1079601, 2003.

Ho, S. L., Mollenhauer, G., Fietz, S., Martínez-Garcia, A., Lamy, F., Rueda, G., Schipper, K., Méheust, M., Rosell-Melé, A., Stein, R., and Tiedemann, R.: Appraisal of TEX86 and TEX86L thermometries in subpolar and polar regions, Geochimica et Cosmochimica Acta, 131, 213-226, https://doi.org/10.1016/j.gca.2014.01.001, 2014.

Ho, S. L. and Laepple, T.: Flat meridional temperature gradient in the early Eocene in the subsurface rather than surface ocean, Nature Geoscience, 9, 606-610, 10.1038/ngeo2763, 2016.

Hollis, C. J., Dunkley Jones, T., Anagnostou, E., Bijl, P. K., Cramwinckel, M. J., Cui, Y., Dickens, G. R., Edgar, K. M., Eley, Y., Evans, D., Foster, G. L., Frieling, J., Inglis, G. N., Kennedy, E. M., Kozdon, R., Lauretano, V., Lear, C. H., Littler, K., Lourens, L., Meckler, A. N., Naafs, B. D. A., Pälike, H., Pancost, R. D., Pearson, P. N., Röhl, U., Royer, D. L., Salzmann, U., Schubert, B. A., Seebeck, H., Sluijs, A., Speijer, R. P., Stassen, P., Tierney, J., Tripati, A., Wade, B., Westerhold, T., Witkowski, C., Zachos, J. C., Zhang, Y. G., Huber, M., and Lunt, D. J.: The DeepMIP contribution to PMIP4: methodologies for selection, compilation and analysis of latest Paleocene and early Eocene climate proxy data, incorporating version 0.1 of the DeepMIP database, Geosci. Model Dev., 12, 3149-3206, 10.5194/gmd-12-3149-2019, 2019.

Hopmans, E. C., Schouten, S., Pancost, R. D., van der Meer, M. T. J., and Sinninghe Damsté, J. S.: Analysis of intact tetraether lipids in archaeal cell material and sediments by high performance liquid chromatography/atmospheric pressure chemical ionization mass spectrometry, Rapid Communications in Mass Spectrometry, 14, 585-589, https://doi.org/10.1002/(SICI)1097-0231(20000415)14:7<585::AID-RCM913>3.0.CO;2-N, 2000.

Hopmans, E. C., Weijers, J. W. H., Schefuß, E., Herfort, L., Sinninghe Damsté, J. S., and Schouten, S.: A novel proxy for terrestrial organic matter in sediments based on branched and isoprenoid tetraether lipids, Earth and Planetary Science Letters, 224, 107-116, 10.1016/j.epsl.2004.05.012, 2004.

https://doi.org/10.5194/egusphere-2025-1467
Preprint. Discussion started: 15 April 2025


Hopmans, E. C., Schouten, S., and Sinninghe Damsté, J. S.: The effect of improved chromatography on GDGT-based palaeoproxies, Organic Geochemistry, 93, 1-6, 10.1016/j.orggeochem.2015.12.006, 2016.

Hou, S., Lamprou, F., Hoem, F. S., Hadju, M. R. N., Sangiorgi, F., Peterse, F., and Bijl, P. K.: Lipid-biomarker-based sea surface temperature record offshore Tasmania over the last 23 million years, Clim. Past, 19, 787-802, 10.5194/cp-19-787-2023, 2023.

Huguet, C., Hopmans, E. C., Febo-Ayala, W., Thompson, D. H., Sinninghe Damsté, J. S., and Schouten, S.: An improved method to determine the absolute abundance of glycerol dibiphytanyl glycerol tetraether lipids, Organic Geochemistry, 37, 1036-1041, https://doi.org/10.1016/j.orggeochem.2006.05.008, 2006.

Huguet, C., de Lange, G. J., Gustafsson, Ö., Middelburg, J. J., Sinninghe Damsté, J. S., and Schouten, S.: Selective preservation of soil organic matter in oxidized marine sediments (Madeira Abyssal Plain), Geochimica et Cosmochimica Acta, 72, 6061-6068, https://doi.org/10.1016/j.gca.2008.09.021, 2008.

Huguet, C., Kim, J.-H., de Lange, G. J., Sinninghe Damsté, J. S., and Schouten, S.: Effects of long term oxic degradation on the U37K′, TEX86 and BIT organic proxies, Organic Geochemistry, 40, 1188-1194, https://doi.org/10.1016/j.orggeochem.2009.09.003, 2009.Huguet, C., Martens-Habbena, W., Urakawa, H., Stahl, D. A., and Ingalls, A. E.: Comparison of extraction methods for quantitative analysis of core and intact polar glycerol dialkyl glycerol tetraethers (GDGTs) in environmental samples, Limnology and Oceanography: Methods, 8, 127-145, https://doi.org/10.4319/lom.2010.8.127, 2010.

Huguet, C., Fietz, S., and Rosell-Melé, A.: Global distribution patterns of hydroxy glycerol dialkyl glycerol tetraethers, Organic Geochemistry, 57, 107-118, https://doi.org/10.1016/j.orggeochem.2013.01.010, 2013.

Hurley, S. J., Lipp, J. S., Close, H. G., Hinrichs, K.-U., and Pearson, A.: Distribution and export of isoprenoid tetraether lipids in suspended particulate matter from the water column of the Western Atlantic Ocean, Organic Geochemistry, 116, 90-102, https://doi.org/10.1016/j.orggeochem.2017.11.010, 2018.

Inglis, G. N., Farnsworth, A., Lunt, D., Foster, G. L., Hollis, C. J., Pagani, M., Jardine, P. E., Pearson, P. N., Markwick, P., Galsworthy, A. M. J., Raynham, L., Taylor, K. W. R., and Pancost, R. D.: Descent toward the Icehouse: Eocene sea surface cooling inferred from GDGT distributions, Paleoceanography, 30, 1000-1020, 10.1002/2014PA002723, 2015.

Jaeschke, A., Wengler, M., Hefter, J., Ronge, T. A., Geibert, W., Mollenhauer, G., Gersonde, R., and Lamy, F.: A biomarker perspective on dust, productivity, and sea surface temperature in the Pacific sector of the Southern Ocean, Geochimica et Cosmochimica Acta, 204, 120-139, https://doi.org/10.1016/j.gca.2017.01.045, 2017.

Judd, E. J., Tierney, J. E., Huber, B. T., Wing, S. L., Lunt, D. J., Ford, H. L., Inglis, G. N., McClymont, E. L., O'Brien, C. L., Rattanasriampaipong, R., Si, W., Staitis, M. L., Thirumalai, K., Anagnostou, E., Cramwinckel, M. J., Dawson, R. R., Evans, D., Gray, W. R., Grossman, E. L., Henehan, M. J., Hupp, B. N., MacLeod, K. G., O'Connor, L. K., Sánchez Montes, M. L., Song, H., and Zhang, Y. G.: The PhanSST global database of Phanerozoic sea surface temperature proxy data, Scientific Data, 9, 753, 10.1038/s41597-022-01826-0, 2022.

https://doi.org/10.5194/egusphere-2025-1467
Preprint. Discussion started: 15 April 2025


Kabel, K., Moros, M., Porsche, C., Neumann, T., Adolphi, F., Andersen, T. J., Siegel, H., Gerth, M., Leipe, T., Jansen, E., and Sinninghe Damsté, J. S.: Impact of climate change on the Baltic Sea ecosystem over the past 1,000 years, Nature Climate Change, 2, 871-874, 10.1038/nclimate1595, 2012.

Kaiser, J. and Arz, H. W.: Sources of sedimentary biomarkers and proxies with potential paleoenvironmental significance for the Baltic Sea, Continental Shelf Research, 122, 102-119, https://doi.org/10.1016/j.csr.2016.03.020, 2016.

Kang, S., Shin, K.-H., and Kim, J.-H.: Occurrence and distribution of hydroxylated isoprenoid glycerol dialkyl glycerol tetraethers (OH-GDGTs) in the Han River system, South Korea, Acta Geochimica, 36, 367-369, 10.1007/s11631-017-0165-3, 2017.

Kim, B. and Zhang, Y. G.: Methane Index: Towards a quantitative archaeal lipid biomarker proxy for reconstructing marine sedimentary methane fluxes, Geochimica et Cosmochimica Acta, 354, 74-87, https://doi.org/10.1016/j.gca.2023.06.008, 2023.

Kim, J.-H., Schouten, S., Hopmans, E. C., Donner, B., and Sinninghe Damsté, J. S.: Global sediment core-top calibration of the TEX86 paleothermometer in the ocean, Geochimica et Cosmochimica Acta, 72, 1154-1173, https://doi.org/10.1016/j.gca.2007.12.010, 2008.

Kim, J.-H., Huguet, C., Zonneveld, K. A. F., Versteegh, G. J. M., Roeder, W., Sinninghe Damsté, J. S., and Schouten, S.: An experimental field study to test the stability of lipids used for the TEX86 and U37K′ palaeothermometers, Geochimica et Cosmochimica Acta, 73, 2888-2898, https://doi.org/10.1016/j.gca.2009.02.030, 2009.

Kim, J. H., van der Meer, J., Schouten, S., Helmke, P., Willmott, V., Sangiorgi, F., Koç, N., Hopmans, E. C., and Damsté, J. S. S.: New indices and calibrations derived from the distribution of crenarchaeal isoprenoid tetraether lipids: Implications for past sea surface temperature reconstructions, Geochimica et Cosmochimica Acta, 74, 4639-4654, 10.1016/j.gca.2010.05.027, 2010.

Kim, J.-H., Crosta, X., Willmott, V., Renssen, H., Bonnin, J., Helmke, P., Schouten, S., and Sinninghe Damsté, J. S.: Holocene subsurface temperature variability in the eastern Antarctic continental margin, Geophysical Research Letters, 39, L06705--n/a, 10.1029/2012GL051157, 2012.

Kim, J.-H., Schouten, S., Rodrigo-Gámiz, M., Rampen, S., Marino, G., Huguet, C., Helmke, P., Buscail, R., Hopmans, E. C., Pross, J., Sangiorgi, F., Middelburg, J. B. M., and Sinninghe Damsté, J. S.: Influence of deep-water derived isoprenoid tetraether lipids on the TEX86H paleothermometer in the Mediterranean Sea, Geochimica et Cosmochimica Acta, 150, 125-141, https://doi.org/10.1016/j.gca.2014.11.017, 2015.

Kirkels, F. M. S. A., Usman, M. O., and Peterse, F.: Distinct sources of bacterial branched GMGTs in the Godavari River basin (India) and Bay of Bengal sediments, Organic Geochemistry, 167, 104405, https://doi.org/10.1016/j.orggeochem.2022.104405, 2022.

Koga, Y., Nishihara, M., Morii, H., and Akagawa-Matsushita, M.: Ether polar lipids of methanogenic bacteria: structures, comparative aspects, and biosyntheses, Microbiological reviews, 57 1, 164-182, 1993.

https://doi.org/10.5194/egusphere-2025-1467
Preprint. Discussion started: 15 April 2025


Kusch, S., Rethemeyer, J., Hopmans, E. C., Wacker, L., and Mollenhauer, G.: Factors influencing 14C concentrations of algal and archaeal lipids and their associated sea surface temperature proxies in the Black Sea, Geochimica et Cosmochimica Acta, 188, 35-57, https://doi.org/10.1016/j.gca.2016.05.025, 2016.

Lamping, N., Müller, J., Hefter, J., Mollenhauer, G., Haas, C., Shi, X., Maria-Elena, V., Lohmann, G., and Hillenbrand, C.-D.: Evaluation of lipid biomarkers as proxies for sea ice and ocean temperatures along the Antarctic continental margin, Climate of the Past, 17, 2305-2326, https://doi.org/10.5194/cp-17-2305-2021, 2021.

Lengger, S. K., Hopmans, E. C., Sinninghe Damsté, J. S., and Schouten, S.: Comparison of extraction and work up techniques for analysis of core and intact polar tetraether lipids from sedimentary environments, Organic Geochemistry, 47, 34-40, https://doi.org/10.1016/j.orggeochem.2012.02.009, 2012.

Lengger, S. K., Kraaij, M., Tjallingii, R., Baas, M., Stuut, J.-B., Hopmans, E. C., Sinninghe Damsté, J. S., and Schouten, S.: Differential degradation of intact polar and core glycerol dialkyl glycerol tetraether lipids upon post-depositional oxidation, Organic Geochemistry, 65, 83-93, https://doi.org/10.1016/j.orggeochem.2013.10.004, 2013.

Lengger, S. K., Sutton, P. A., Rowland, S. J., Hurley, S. J., Pearson, A., Naafs, B. D. A., Dang, X., Inglis, G. N., and Pancost, R. D.: Archaeal and bacterial glycerol dialkyl glycerol tetraether (GDGT) lipids in environmental samples by high temperature-gas chromatography with flame ionisation and time-of-flight mass spectrometry detection, Organic Geochemistry, 121, 10-21, https://doi.org/10.1016/j.orggeochem.2018.03.012, 2018.

Li, Y., Yu, T., Feng, X., Zhao, B., Chen, H., Yang, H., Chen, X., Zhang, X.-H., Anderson, H. R., Burns, N. Z., Zeng, F., Tao, L., and Zeng, Z.: Biosynthesis of GMGT lipids by a radical SAM enzyme associated with anaerobic archaea and oxygen-deficient environments, Nature Communications, 15, 5256, 10.1038/s41467-024-49650-x, 2024.

Littler, K., Robinson, S. A., Bown, P. R., Nederbragt, A. J., and Pancost, R. D.: High sea-surface temperatures during the Early Cretaceous Epoch, Nature Geoscience, 4, 169-172, 10.1038/ngeo1081, 2011.

Liu, R., Han, Z., Zhao, J., Zhang, H., Li, D., Ren, J., Pan, J., and Zhang, H.: Distribution and source of glycerol dialkyl glycerol tetraethers (GDGTs) and the applicability of GDGT-based temperature proxies in surface sediments of Prydz Bay, East Antarctica, Polar Research, 39, https://doi.org/10.33265/polar.v39.3557, 2020.

Liu, X.-L., Summons, R. E., and Hinrichs, K.-U.: Extending the known range of glycerol ether lipids in the environment: structural assignments based on tandem mass spectral fragmentation patterns, Rapid Communications in Mass Spectrometry, 26, 2295-2302, https://doi.org/10.1002/rcm.6355, 2012a.

Liu, X.-L., Lipp, J. S., Schröder, J. M., Summons, R. E., and Hinrichs, K.-U.: Isoprenoid glycerol dialkanol diethers: A series of novel archaeal lipids in marine sediments, Organic Geochemistry, 43, 50-55, https://doi.org/10.1016/j.orggeochem.2011.11.002, 2012b.

https://doi.org/10.5194/egusphere-2025-1467
Preprint. Discussion started: 15 April 2025


Liu, X.-L., Lipp, J. S., Simpson, J. H., Lin, Y.-S., Summons, R. E., and Hinrichs, K.-U.: Mono- and dihydroxyl glycerol dibiphytanyl glycerol tetraethers in marine sediments: Identification of both core and intact polar lipid forms, Geochimica et Cosmochimica Acta, 89, 102-115, https://doi.org/10.1016/j.gca.2012.04.053, 2012c.

Liu, X.-L., Zhu, C., Wakeham, S. G., and Hinrichs, K.-U.: In situ production of branched glycerol dialkyl glycerol tetraethers in anoxic marine water columns, Marine Chemistry, 166, 1-8, https://doi.org/10.1016/j.marchem.2014.08.008, 2014.

Liu, X.-L., Birgel, D., Elling, F. J., Sutton, P. A., Lipp, J. S., Zhu, R., Zhang, C., Könneke, M., Peckmann, J., Rowland, S. J., Summons, R. E., and Hinrichs, K.-U.: From ether to acid: A plausible degradation pathway of glycerol dialkyl glycerol tetraethers, Geochimica et Cosmochimica Acta, 183, 138-152, https://doi.org/10.1016/j.gca.2016.04.016, 2016.

Liu, Y., Xiao, W., Wu, J., Han, L., Zhang, H., and Xu, Y.: Source, composition, and distributional pattern of branched tetraethers in sediments of northern Chinese marginal seas, Organic Geochemistry, 157, 104244, https://doi.org/10.1016/j.orggeochem.2021.104244, 2021.

Liu, Z., Pagani, M., Zinniker, D., DeConto, R., Huber, M., Brinkhuis, H., Shah, S. R., Leckie, R. M., and Pearson, A.: Global cooling during the Eocene-Oligocene climate transition, Science, 323, 1187-1190, 10.1126/science.1166368, 2009.

Liu, Z., He, Y., Jiang, Y., Wang, H., Liu, W., Bohaty, S. M., and Wilson, P. A.: Transient temperature asymmetry between hemispheres in the Palaeogene Atlantic Ocean, Nature Geoscience, 11, 656-660, 10.1038/s41561-018-0182-9, 2018.

Lloyd, C. T., Iwig, D. F., Wang, B., Cossu, M., Metcalf, W. W., Boal, A. K., and Booker, S. J.: Discovery, structure and mechanism of a tetraether lipid synthase, Nature, 609, 197-203, 10.1038/s41586-022-05120-2, 2022.

Lü, X., Liu, X.-L., Elling, F. J., Yang, H., Xie, S., Song, J., Li, X., Yuan, H., Li, N., and Hinrichs, K.-U.: Hydroxylated isoprenoid GDGTs in Chinese coastal seas and their potential as a paleotemperature proxy for mid-to-low latitude marginal seas, Organic Geochemistry, 89-90, 31-43, https://doi.org/10.1016/j.orggeochem.2015.10.004, 2015.

Lü, X., Chen, J., Han, T., Yang, H., Wu, W., Ding, W., and Hinrichs, K.-U.: Origin of hydroxyl GDGTs and regular isoprenoid GDGTs in suspended particulate matter of Yangtze River Estuary, Organic Geochemistry, 128, 78-85, https://doi.org/10.1016/j.orggeochem.2018.12.010, 2019.

McKay, N. P. and Emile-Geay, J.: Technical note: The Linked Paleo Data framework – a common tongue for paleoclimatology, Clim. Past, 12, 1093-1100, 10.5194/cp-12-1093-2016, 2016.

Meador, T. B., Gagen, E. J., Loscar, M. E., Goldhammer, T., Yoshinaga, M. Y., Wendt, J., Thomm, M., and Hinrichs, K.-U.: Thermococcus kodakarensis modulates its polar membrane lipids and elemental composition according to growth stage and phosphate availability, Frontiers in Microbiology, 5, 10.3389/fmicb.2014.00010, 2014.

https://doi.org/10.5194/egusphere-2025-1467
Preprint. Discussion started: 15 April 2025


Mekik, F. and Anderson, R.: Is the core top modern? Observations from the eastern equatorial Pacific, Quaternary Science Reviews, 186, 156-168, https://doi.org/10.1016/j.quascirev.2018.01.020, 2018.

Mitrović, D., Hopmans, E. C., Bale, N. J., Richter, N., Amaral-Zettler, L. A., Baxter, A. J., Peterse, F., Miguel Raposeiro, P., Gonçalves, V., Cristina Costa, A., and Schouten, S.: Isoprenoidal GDGTs and GDDs associated with anoxic lacustrine environments, Organic Geochemistry, 178, 104582, https://doi.org/10.1016/j.orggeochem.2023.104582, 2023.

Morii, H., Eguchi, T., Nishihara, M., Kakinuma, K., König, H., and Koga, Y.: A novel ether core lipid with H-shaped C80-isoprenoid hydrocarbon chain from the hyperthermophilic methanogen Methanothermus fervidus, Biochimica et Biophysica Acta (BBA) - Lipids and Lipid Metabolism, 1390, 339-345, https://doi.org/10.1016/S0005-2760(97)00183-5, 1998.

Naeher, S., Smittenberg, R. H., Gilli, A., Kirilova, E. P., Lotter, A. F., and Schubert, C. J.: Impact of recent lake eutrophication on microbial community changes as revealed by high resolution lipid biomarkers in Rotsee (Switzerland), Organic Geochemistry, 49, 86-95, https://doi.org/10.1016/j.orggeochem.2012.05.014, 2012.

Naeher, S., Peterse, F., Smittenberg, R. H., Niemann, H., Zigah, P. K., and Schubert, C. J.: Sources of glycerol dialkyl glycerol tetraethers (GDGTs) in catchment soils, water column and sediments of Lake Rotsee (Switzerland) – Implications for the application of GDGT-based proxies for lakes, Organic Geochemistry, 66, 164-173, https://doi.org/10.1016/j.orggeochem.2013.10.017, 2014a.

Naeher, S., Niemann, H., Peterse, F., Smittenberg, R. H., Zigah, P. K., and Schubert, C. J.: Tracing the methane cycle with lipid biomarkers in Lake Rotsee (Switzerland), Organic Geochemistry, 66, 174-181, https://doi.org/10.1016/j.orggeochem.2013.11.002, 2014b.

Niemann, H. and Elvert, M.: Diagnostic lipid biomarker and stable carbon isotope signatures of microbial communities mediating the anaerobic oxidation of methane with sulphate, Organic Geochemistry, 39, 1668-1677, https://doi.org/10.1016/j.orggeochem.2007.11.003, 2008.

Naafs, B. D. A. and Pancost, R. D.: Sea-surface temperature evolution across Aptian Oceanic Anoxic Event 1a, Geology, 10.1130/G38575.1, 2016.

Naafs, B. D. A., McCormick, D., Inglis, G. N., and Pancost, R. D.: Archaeal and bacterial H-GDGTs are abundant in peat and their relative abundance is positively correlated with temperature, Geochimica et Cosmochimica Acta, 227, 156-170, https://doi.org/10.1016/j.gca.2018.02.025, 2018.

O'Brien, C. L., Robinson, S. A., Pancost, R. D., Sinninghe Damsté, J. S., Schouten, S., Lunt, D. J., Alsenz, H., Bornemann, A., Bottini, C., Brassell, S. C., Farnsworth, A., Forster, A., Huber, B. T., Inglis, G. N., Jenkyns, H. C., Linnert, C., Littler, K., Markwick, P., McAnena, A., Mutterlose, J., Naafs, B. D. A., Püttmann, W., Sluijs, A., van Helmond, N. A. G. M., Vellekoop, J., Wagner, T., and Wrobel, N. E.: Cretaceous sea-surface temperature evolution: Constraints from TEX86 and planktonic foraminiferal oxygen isotopes, 224–247 pp.2017.

https://doi.org/10.5194/egusphere-2025-1467
Preprint. Discussion started: 15 April 2025


O' Brien, C. L., Huber, M., Thomas, E., Pagani, M., Super, J. R., Elder, L. E., and Hull, P. M.: The enigma of Oligocene climate and global surface temperature evolution, Proceedings of the National Academy of Sciences, 117, 25302-25309, 10.1073/pnas.2003914117, 2020.

Pancost, R. D., Hopmans, E. C., and Sinninghe Damsté, J. S.: Archaeal lipids in Mediterranean cold seeps: molecular proxies for anaerobic methane oxidation, Geochimica et Cosmochimica Acta, 65, 1611-1627, https://doi.org/10.1016/S0016-7037(00)00562-7, 2001.

Pancost, R. D., Taylor, K. W. R., Inglis, G. N., Kennedy, E. M., Handley, L., Hollis, C. J., Crouch, E. M., Pross, J., Huber, M., Schouten, S., Pearson, P. N., Morgans, H. E. G., and Raine, J. I.: Early Paleogene evolution of terrestrial climate in the SW Pacific, Southern New Zealand, Geochemistry, Geophysics, Geosystems, 14, 5413-5429, https://doi.org/10.1002/2013GC004935, 2013.

Pancost, R. D.: Biomarker carbon and hydrogen isotopes reveal changing peatland vegetation, hydroclimate and biogeochemical tipping points, Quaternary Science Reviews, 339, 108828, https://doi.org/10.1016/j.quascirev.2024.108828, 2024.

Peterse, F., Kim, J.-H., Schouten, S., Kristensen, D. K., Koç, N., and Sinninghe Damsté, J. S.: Constraints on the application of the MBT/CBT palaeothermometer at high latitude environments (Svalbard, Norway), Organic Geochemistry, 40, 692-699, https://doi.org/10.1016/j.orggeochem.2009.03.004, 2009.

Pitcher, A., Hopmans, E. C., Schouten, S., and Sinninghe Damsté, J. S.: Separation of core and intact polar archaeal tetraether lipids using silica columns: Insights into living and fossil biomass contributions, Organic Geochemistry, 40, 12-19, https://doi.org/10.1016/j.orggeochem.2008.09.008, 2009.

Pitcher, A., Rychlik, N., Hopmans, E. C., Spieck, E., Rijpstra, W. I. C., Ossebaar, J., Schouten, S., Wagner, M., and Sinninghe Damsté, J. S.: Crenarchaeol dominates the membrane lipids of Candidatus Nitrososphaera gargensis, a thermophilic Group I.1b Archaeon, The ISME Journal, 4, 542-552, 10.1038/ismej.2009.138, 2010.

Prahl, F. G. and Wakeham, S. G.: Calibration of unsaturation patterns in long-chain ketone compositions for paleotemperature assessment, Nature 330, 367–369. https://doi.org/10.1038/330367a01987, 1987.

Pross, J., Contreras, L., Bijl, P. K., Greenwood, D. R., Bohaty, S. M., Schouten, S., Bendle, J. A., Röhl, U., Tauxe, L., Raine, J. I., Huck, C. E., Van De Flierdt, T., Jamieson, S. S. R., Stickley, C. E., Van De Schootbrugge, B., Escutia, C., Brinkhuis, H., Escutia Dotti, C., Klaus, A., Fehr, A., Williams, T., Bendle, J. A. P., Carr, S. A., Dunbar, R. B., Gonzèlez, J. J., Hayden, T. G., Iwai, M., Jimenez Espejo, F. J., Katsuki, K., Soo Kong, G., Mc Kay, R. M., Nakai, M., Olney, M. P., Passchier, S., Pekar, S. F., Riesselman, C. R., Sakai, T., Shrivastava, P. K., Sugisaki, S., Tuo, S., Welsh, K., and Yamane, M.: Persistent near–tropical warmth on the antarctic continent during the early Eocene epoch, Nature, 488, 73-77, 10.1038/nature11300, 2012.

Qin, W., Carlson, L. T., Armbrust, E. V., Devol, A. H., Moffett, J. W., Stahl, D. A., and Ingalls, A. E.: Confounding effects of oxygen and temperature on the TEX<sub>86</sub> signature of marine Thaumarchaeota, Proceedings of the National Academy of Sciences of the United States of America, 112, 10979-10984, 2015.

https://doi.org/10.5194/egusphere-2025-1467
Preprint. Discussion started: 15 April 2025


Rampen, S. W., Willmott, V., Kim, J.-H., Uliana, E., Mollenhauer, G., Schefuß, E., Sinninghe Damsté, J. S., and Schouten, S.: Long chain 1,13- and 1,15-diols as a potential proxy for palaeotemperature reconstruction, Geochimica et Cosmochimica Acta, 84, 204-216, https://doi.org/10.1016/j.gca.2012.01.024, 2012.

Rattanasriampaipong, R., Zhang, Y. G., Pearson, A., Hedlund, B. P., and Zhang, S.: Archaeal lipids trace ecology and evolution of marine ammonia-oxidizing archaea, Proceedings of the National Academy of Sciences, 119, e2123193119, doi:10.1073/pnas.2123193119, 2022.

Richey, J. N. and Tierney, J. E.: GDGT and alkenone flux in the northern Gulf of Mexico: Implications for the TEX86 and U37 paleothermometers, Paleoceanography, 31, 1547-1561, https://doi.org/10.1002/2016PA003032, 2016.

Rodrigo-Gámiz, M., Rampen, S. W., de Haas, H., Baas, M., Schouten, S., and Sinninghe Damsté, J. S.: Constraints on the applicability of the organic temperature proxies U<sup>K'</sup><sub>37</sub>, TEX<sub>86</sub> and LDI in the subpolar region around Iceland, Biogeosciences, 12, 6573-6590, 10.5194/bg-12-6573-2015, 2015.

Rosengard, S. Z., Lam, P. J., McNichol, A. P., Johnson, C. G., and Galy, V. V.: The effect of sample drying temperature on marine particulate organic carbon composition, Limnology and Oceanography: Methods, 16, 286-298, https://doi.org/10.1002/lom3.10245, 2018.

Schouten, S., Hopmans, E. C., Schefuß, E., and Sinninghe Damsté, J. S.: Distributional variations in marine crenarchaeol membrane lipids: a new tool for reconstructing ancient sea water temperatures?, Earth and Planetary Science Letters, 10.1016/S0012-821X(03)00193-6, 2002.

Schouten, S., Wakeham, S. G., Hopmans, E. C., and Damsté, J. S. S.: Biogeochemical Evidence that Thermophilic Archaea Mediate the Anaerobic Oxidation of Methane, Applied and Environmental Microbiology, 69, 1680-1686, doi:10.1128/AEM.69.3.1680-1686.2003, 2003.

Schouten, S., Hopmans, E. C., and Sinninghe Damsté, J. S.: The effect of maturity and depositional redox conditions on archaeal tetraether lipid palaeothermometry, Organic Geochemistry, 35, 567-571, https://doi.org/10.1016/j.orggeochem.2004.01.012, 2004.

Schouten, S., Huguet, C., Hopmans, E. C., Kienhuis, M. V. M., and Sinninghe Damsté, J. S.: Analytical Methodology for TEX86 Paleothermometry by High-Performance Liquid Chromatography/Atmospheric Pressure Chemical Ionization-Mass Spectrometry, Analytical Chemistry, 79, 2940-2944, 10.1021/ac062339v, 2007.

Schouten, S., Baas, M., Hopmans, E. C., and Sinninghe Damsté, J. S.: An unusual isoprenoid tetraether lipid in marine and lacustrine sediments, Organic Geochemistry, 39, 1033-1038, https://doi.org/10.1016/j.orggeochem.2008.01.019, 2008.

Schouten, S., Hopmans, E. C., van der Meer, J., Mets, A., Bard, E., Bianchi, T. S., Diefendorf, A., Escala, M., Freeman, K. H., Furukawa, Y., Huguet, C., Ingalls, A., Ménot-Combes, G., Nederbragt, A. J., Oba, M., Pearson, A., Pearson, E. J., Rosell-Melé, A., Schaeffer, P., Shah, S. R., Shanahan, T. M., Smith, R.

https://doi.org/10.5194/egusphere-2025-1467
Preprint. Discussion started: 15 April 2025


W., Smittenberg, R., Talbot, H. M., Uchida, M., Van Mooy, B. A. S., Yamamoto, M., Zhang, Z., and Sinninghe Damsté, J. S.: An interlaboratory study of TEX86 and BIT analysis using high-performance liquid chromatography–mass spectrometry, Geochemistry, Geophysics, Geosystems, 10, https://doi.org/10.1029/2008GC002221, 2009.

Schouten, S., Hopmans, E. C., and Sinninghe Damsté, J. S.: The organic geochemistry of glycerol dialkyl glycerol tetraether lipids: A review, Organic Geochemistry, 54, 19-61, 10.1016/j.orggeochem.2012.09.006, 2013a.

Schouten, S., Hopmans, E. C., Rosell-Melé, A., Pearson, A., Adam, P., Bauersachs, T., Bard, E., Bernasconi, S. M., Bianchi, T. S., Brocks, J. J., Carlson, L. T., Castañeda, I. S., Derenne, S., Selver, A. D., Dutta, K., Eglinton, T., Fosse, C., Galy, V., Grice, K., Hinrichs, K.-U., Huang, Y., Huguet, A., Huguet, C., Hurley, S., Ingalls, A., Jia, G., Keely, B., Knappy, C., Kondo, M., Krishnan, S., Lincoln, S., Lipp, J., Mangelsdorf, K., Martínez-García, A., Ménot, G., Mets, A., Mollenhauer, G., Ohkouchi, N., Ossebaar, J., Pagani, M., Pancost, R. D., Pearson, E. J., Peterse, F., Reichart, G.-J., Schaeffer, P., Schmitt, G., Schwark, L., Shah, S. R., Smith, R. W., Smittenberg, R. H., Summons, R. E., Takano, Y., Talbot, H. M., Taylor, K. W. R., Tarozo, R., Uchida, M., van Dongen, B. E., Van Mooy, B. A. S., Wang, J., Warren, C., Weijers, J. W. H., Werne, J. P., Woltering, M., Xie, S., Yamamoto, M., Yang, H., Zhang, C. L., Zhang, Y., Zhao, M., and Damsté, J. S. S.: An interlaboratory study of TEX86 and BIT analysis of sediments, extracts, and standard mixtures, Geochemistry, Geophysics, Geosystems, 14, 5263-5285, https://doi.org/10.1002/2013GC004904, 2013b.

Schukies, J.: Concentrations of glycerol dialkyl glycerol tetraethers (GDGTs) in core top sediments from continental slope off Newfoundland, Orphan Knoll Region, PANGAEA [dataset], 10.1594/PANGAEA.894305, 2018.

Seki, O., Bendle, J. A., Harada, N., Kobayashi, M., Sawada, K., Moossen, H., Inglis, G. N., Nagao, S., and Sakamoto, T.: Assessment and calibration of TEX86 paleothermometry in the Sea of Okhotsk and sub-polar North Pacific region: Implications for paleoceanography, Progress in Oceanography, 126, 254-266, https://doi.org/10.1016/j.pocean.2014.04.013, 2014.

Sinninghe Damsté, J. S., Hopmans, E. C., Pancost, R. D., Schouten, S., and Geenevasen, J. A. J.: Newly discovered non-isoprenoid glycerol dialkyl glycerol tetraether lipids in sediments, Chemical Communications, 1683-1684, 10.1039/B004517I, 2000.

Sinninghe Damste, J. S., Schouten, S., Hopmans, E. C., van Duin, A. C., and Geenevasen, J. A. J.: Crenarchaeol: the characteristic core glycerol dibiphytanyl glycerol tetraether membrane lipid of cosmopolitan pelagic crenarchaeota, The Journal of Lipid Research, 43, 1641-1651, 10.1194/jlr.M200148-JLR200, 2002.

Sinninghe Damsté, J. S., Rijpstra, W. I. C., Hopmans, E. C., Weijers, J. W. H., Foesel, B. U., Overmann, J., and Dedysh, S. N.: 13,16-Dimethyl Octacosanedioic Acid (iso-Diabolic Acid), a Common Membrane-Spanning Lipid of Acidobacteria Subdivisions 1 and 3, Applied and Environmental Microbiology, 77, 4147-4154, doi:10.1128/AEM.00466-11, 2011.

https://doi.org/10.5194/egusphere-2025-1467
Preprint. Discussion started: 15 April 2025


Sinninghe Damsté, J. S., Ossebaar, J., Schouten, S., and Verschuren, D.: Distribution of tetraether lipids in the 25-ka sedimentary record of Lake Challa: Extracting reliable TEX86 and MBT/CBT palaeotemperatures from an equatorial African lake, Quaternary Science Reviews, 50, 43-54, 10.1016/j.quascirev.2012.07.001, 2012a.

Sinninghe Damsté, J. S., Rijpstra, W. I., Hopmans, E. C., Jung, M. Y., Kim, J. G., Rhee, S. K., Stieglmeier, M., and Schleper, C.: Intact polar and core glycerol dibiphytanyl glycerol tetraether lipids of group I.1a and I.1b thaumarchaeota in soil, Appl Environ Microbiol, 78, 6866-6874, 10.1128/aem.01681-12, 2012b.

Sinninghe Damsté, J. S.: Spatial heterogeneity of sources of branched tetraethers in shelf systems: The geochemistry of tetraethers in the Berau River delta (Kalimantan, Indonesia), Geochimica et Cosmochimica Acta, 186, 13-31, 10.1016/j.gca.2016.04.033, 2016.

Sinninghe Damsté, J., S., Warden, L. A., Berg, C., Jürgens, K., and Moros, M.: Evaluation of the distributions of hydroxylated glycerol dibiphytanyl glycerol tetraethers (GDGTs) in Holocene Baltic Sea sediments for reconstruction of sea surface temperature: the effect of changing salinity, Climate of the Past, 18, 2271-2288, https://doi.org/10.5194/cp-18-2271-2022, 2022.

Śliwińska, K. K., Dybkjær, K., Schoon, P. L., Beyer, C., King, C., Schouten, S., and Nielsen, O. B.: Paleoclimatic and paleoenvironmental records of the Oligocene–Miocene transition, central Jylland, Denmark, Marine Geology, 350, 1-15, 10.1016/j.margeo.2013.12.014, 2014.

Śliwińska, K. K., Thomsen, E., Schouten, S., Schoon, P. L., and Heilmann-Clausen, C.: Climate- and gateway-driven cooling of Late Eocene to earliest Oligocene sea surface temperatures in the North Sea Basin, Scientific Reports, 9, 4458, 10.1038/s41598-019-41013-7, 2019.

Sluijs, A., Schouten, S., Pagani, M., Woltering, M., Brinkhuis, H., Damsté, J. S. S., Dickens, G. R., Huber, M., Reichart, G. J., Stein, R., Matthiessen, J., Lourens, L. J., Pedentchouk, N., Backman, J., Moran, K., Clemens, S., Cronin, T., Eynaud, F., Gattacceca, J., Jakobsson, M., Jordan, R., Kaminski, M., King, J., Koc, N., Martinez, N. C., McInroy, D., Moore, T. C., O'Regan, M., Onodera, J., Pälike, H., Rea, B., Rio, D., Sakamoto, T., Smith, D. C., St John, K. E. K., Suto, I., Suzuki, N., Takahashi, K., Watanabe, M., and Yamamoto, M.: Subtropical Arctic Ocean temperatures during the Palaeocene/Eocene thermal maximum, Nature, 441, 610-613, 10.1038/nature04668, 2006.

Sluijs, A., Frieling, J., Inglis, G. N., Nierop, K. G. J., Peterse, F., Sangiorgi, F., and Schouten, S.: Late Paleocene–early Eocene Arctic Ocean sea surface temperatures: reassessing biomarker paleothermometry at Lomonosov Ridge, Clim. Past, 16, 2381-2400, 10.5194/cp-16-2381-2020, 2020.

Smith, L. M., Stalling, D. L., and Johnson, J. L.: Determination of part-per-trillion levels of polychlorinated dibenzofurans and dioxins in environmental samples, Analytical Chemistry, 56, 1830-1842, 10.1021/ac00275a018, 1984.

Smith, M. B., Poynter, J. G., Bradshaw, S. A., and Eglinton, G.: High resolution molecular stratigraphy: analytical methodology, Geological Society, London, Special Publications, 70, 51-63, doi:10.1144/GSL.SP.1993.070.01.05, 1993.

https://doi.org/10.5194/egusphere-2025-1467
Preprint. Discussion started: 15 April 2025


Sollich, M., Yoshinaga, M. Y., Häusler, S., Price, R. E., Hinrichs, K.-U., and Bühring, S. I.: Heat Stress Dictates Microbial Lipid Composition along a Thermal Gradient in Marine Sediments, Frontiers in Microbiology, 8, 10.3389/fmicb.2017.01550, 2017.

Taylor, K. W. R., Huber, M., Hollis, C. J., Hernandez-Sanchez, M. T., and Pancost, R. D.: Re-evaluating modern and Palaeogene GDGT distributions: Implications for SST reconstructions, Global and Planetary Change, 108, 158-174, 10.1016/j.gloplacha.2013.06.011, 2013.

Tierney, J. E. and Tingley, M. P.: A Bayesian, spatially-varying calibration model for the TEX86 proxy, Geochimica et Cosmochimica Acta, 127, 83-106, 10.1016/j.gca.2013.11.026, 2014.

Tierney, J. E. and Tingley, M. P.: A TEX86 surface sediment database and extended Bayesian calibration, Scientific Data, 2, 150029, 10.1038/sdata.2015.29, 2015.

Tierney, J. E., Sinninghe Damsté, J. S., Pancost, R. D., Sluijs, A., and Zachos, J. C.: Eocene temperature gradients, Nature Geoscience, 10, 538-539, 10.1038/ngeo2997, 2017.

Trommer, G., Siccha, M., van der Meer, M. T. J., Schouten, S., Sinninghe Damsté, J. S., Schulz, H., Hemleben, C., and Kucera, M.: Distribution of Crenarchaeota tetraether membrane lipids in surface sediments from the Red Sea, Organic Geochemistry, 40, 724-731, https://doi.org/10.1016/j.orggeochem.2009.03.001, 2009.

van der Weijst, C. M. H., van der Laan, K. J., Peterse, F., Reichart, G. J., Sangiorgi, F., Schouten, S., Veenstra, T. J. T., and Sluijs, A.: A 15-million-year surface- and subsurface-integrated TEX86 temperature record from the eastern equatorial Atlantic, Clim. Past, 18, 1947-1962, 10.5194/cp-18-1947-2022, 2022.

van der Weijst, C. M. H., Winkelhorst, J., de Nooijer, W., von der Heydt, A., Reichart, G. J., Sangiorgi, F., and Sluijs, A.: Pliocene evolution of the tropical Atlantic thermocline depth, Clim. Past, 18, 961-973, 10.5194/cp-18-961-2022, 2022.

Varma, D., Hättig, K., van der Meer, M. T. J., Reichart, G.-J., and Schouten, S.: Constraining Water Depth Influence on Organic Paleotemperature Proxies Using Sedimentary Archives, Paleoceanography and Paleoclimatology, 38, e2022PA004533, https://doi.org/10.1029/2022PA004533, 2023.

Varma, D., van der Meer, M. T. J., Reichart, G.-J., and Schouten, S.: Impact of water depth on the distributions and proxies of isoprenoidal hydroxylated GDGTs in the Mediterranean Sea and the Red Sea, Organic Geochemistry, 194, 104780, https://doi.org/10.1016/j.orggeochem.2024.104780, 2024a.

Varma, D., Hopmans, E. C., van Kemenade, Z. R., Kusch, S., Berg, S., Bale, N. J., Sangiorgi, F., Reichart, G.-J., Sinninghe Damsté, J. S., and Schouten, S.: Evaluating isoprenoidal hydroxylated GDGT-based temperature proxies in surface sediments from the global ocean, Geochimica et Cosmochimica Acta, 370, 113-127, https://doi.org/10.1016/j.gca.2023.12.019, 2024b.

https://doi.org/10.5194/egusphere-2025-1467
Preprint. Discussion started: 15 April 2025


Villanueva, L., Schouten, S., and Sinninghe Damsté, J. S.: Depth-related distribution of a key gene of the tetraether lipid biosynthetic pathway in marine Thaumarchaeota, Environmental Microbiology, 17, 3527-3539, https://doi.org/10.1111/1462-2920.12508, 2015.

Wang, Y., Chen, J., He, X., Pang, J., Yang, J., Cui, Z., Xin, M., Cao, W., Wang, B., and Wang, Z.: Improved protocols for large-volume injection and liquid chromatography–mass spectrometry analyses enable determination of various glycerol dialkyl glycerol tetraethers in a small amount of sediment and suspended particulate matter, Chemical Geology, 595, 120793, https://doi.org/10.1016/j.chemgeo.2022.120793, 2022.

Weber, Y., Sinninghe Damsté, J. S., Hopmans, E. C., Lehmann, M. F., and Niemann, H.: Incomplete recovery of intact polar glycerol dialkyl glycerol tetraethers from lacustrine suspended biomass, Limnology and Oceanography: Methods, 15, 782-793, https://doi.org/10.1002/lom3.10198, 2017.

Wei, B., Jia, G., Hefter, J., Kang, M., Park, E., Wang, S., and Mollenhauer, G.: Comparison of the U37K′, LDI, TEX86H, and RI-OH temperature proxies in sediments from the northern shelf of the South China Sea, Biogeosciences, 17, 4489-4508, 10.5194/bg-17-4489-2020, 2020.

Wei, Y., Wang, J., Liu, J., Dong, L., Li, L., Wang, H., Wang, P., Zhao, M., and Zhang, C. L.: Spatial Variations in Archaeal Lipids of Surface Water and Core-Top Sediments in the South China Sea and Their Implications for Paleoclimate Studies, Applied and Environmental Microbiology, 77, 7479-7489, doi:10.1128/AEM.00580-11, 2011.

Weijers, J. W. H., Schouten, S., Spaargaren, O. C., and Sinninghe Damsté, J. S.: Occurrence and distribution of tetraether membrane lipids in soils: Implications for the use of the TEX86 proxy and the BIT index, Organic Geochemistry, 37, 1680-1693, 10.1016/j.orggeochem.2006.07.018, 2006a.

Weijers, J. W. H., Schouten, S., Hopmans, E. C., Geenevasen, J. A. J., David, O. R. P., Coleman, J. M., Pancost, R. D., and Sinninghe Damsté, J. S.: Membrane lipids of mesophilic anaerobic bacteria thriving in peats have typical archaeal traits, Environmental Microbiology, 8, 648-657, 10.1111/j.1462-2920.2005.00941.x, 2006b.

Weijers, J. W. H., Schouten, S., Sluijs, A., Brinkhuis, H., and Sinninghe Damsté, J. S.: Warm arctic continents during the Palaeocene–Eocene thermal maximum, Earth and Planetary Science Letters, 261, 230-238, https://doi.org/10.1016/j.epsl.2007.06.033, 2007a.

Weijers, J. W. H., Schouten, S., van den Donker, J. C., Hopmans, E. C., and Sinninghe Damsté, J. S.: Environmental controls on bacterial tetraether membrane lipid distribution in soils, Geochimica et Cosmochimica Acta, 71, 703-713, 10.1016/j.gca.2006.10.003, 2007b.

Weijers, J. W. H., Panoto, E., van Bleijswijk, J., Schouten, S., Rijpstra, W. I. C., Balk, M., Stams, A. J. M., and Damsté, J. S. S.: Constraints on the Biological Source(s) of the Orphan Branched Tetraether Membrane Lipids, Geomicrobiology Journal, 26, 402-414, 10.1080/01490450902937293, 2009.

https://doi.org/10.5194/egusphere-2025-1467
Preprint. Discussion started: 15 April 2025


Weijers, J. W. H., Wiesenberg, G. L. B., Bol, R., Hopmans, E. C., and Pancost, R. D.: Carbon isotopic composition of branched tetraether membrane lipids in soils suggest a rapid turnover and a heterotrophic life style of their source organism(s), Biogeosciences, 7, 2959-2973, 10.5194/bg-7-2959-2010, 2010.

Weijers, J. W. H., Lim, K. L. H., Aquilina, A., Sinninghe Damsté, J. S., and Pancost, R. D.: Biogeochemical controls on glycerol dialkyl glycerol tetraether lipid distributions in sediments characterized by diffusive methane flux, Geochemistry, Geophysics, Geosystems, 12, https://doi.org/10.1029/2011GC003724, 2011.

Weijers, J. W. H., Schefuß, E., Kim, J.-H., Sinninghe Damsté, J. S., and Schouten, S.: Fractional abundance and indices for brGDGTs and crenarchaeol in dust samples, surface water samples and surface sediment samples, 2014.

Wilkinson, M. D., Dumontier, M., Aalbersberg, I. J., Appleton, G., Axton, M., Baak, A., Blomberg, N., Boiten, J.-W., da Silva Santos, L. B., Bourne, P. E., Bouwman, J., Brookes, A. J., Clark, T., Crosas, M., Dillo, I., Dumon, O., Edmunds, S., Evelo, C. T., Finkers, R., Gonzalez-Beltran, A., Gray, A. J. G., Groth, P., Goble, C., Grethe, J. S., Heringa, J., 't Hoen, P. A. C., Hooft, R., Kuhn, T., Kok, R., Kok, J., Lusher, S. J., Martone, M. E., Mons, A., Packer, A. L., Persson, B., Rocca-Serra, P., Roos, M., van Schaik, R., Sansone, S.-A., Schultes, E., Sengstag, T., Slater, T., Strawn, G., Swertz, M. A., Thompson, M., van der Lei, J., van Mulligen, E., Velterop, J., Waagmeester, A., Wittenburg, P., Wolstencroft, K., Zhao, J., and Mons, B.: The FAIR Guiding Principles for scientific data management and stewardship, Scientific Data, 3, 160018, 10.1038/sdata.2016.18, 2016.

Willard, D. A.: Arctic vegetation, temperature, and hydrology during Early Eocene transient global warming events, Global and Planetary Change, 14, 2019.

Wiltshire, G. H. and du Preez, C. C.: The effect of oven-drying on residual inorganic nitrogen in soils, South African Journal of Plant and Soil, 11, 107-109, 10.1080/02571862.1994.10634304, 1994.

Wu, J., Stein, R., Fahl, K., Syring, N., Nam, S.-I., Hefter, J., Mollenhauer, G., and Geibert, W.: Deglacial to Holocene variability in surface water characteristics and major floods in the Beaufort Sea, Communications Earth & Environment, 1, 27, 10.1038/s43247-020-00028-z, 2020.

Wuchter, C., Schouten, S., Wakeham, S. G., and Sinninghe Damsté, J. S.: Temporal and spatial variation in tetraether membrane lipids of marine Crenarchaeota in particulate organic matter: Implications for TEX 86 paleothermometry, Paleoceanography, 10.1029/2004PA001110, 2005.

Xiao, W., Wang, Y., Zhou, S., Hu, L., Yang, H., and Xu, Y.: Ubiquitous production of branched glycerol dialkyl glycerol tetraethers (brGDGTs) in global marine environments: A new source indicator for brGDGTs, Biogeosciences, 13, 5883-5894, 10.5194/bg-13-5883-2016, 2016.

Xiao, W., Wang, Y., Liu, Y., Zhang, X., Shi, L., and Xu, Y.: Predominance of hexamethylated 6-methyl branched glycerol dialkyl glycerol tetraethers in the Mariana Trench: source and environmental implication, Biogeosciences, 17, 2135-2148, 10.5194/bg-17-2135-2020, 2020.

https://doi.org/10.5194/egusphere-2025-1467
Preprint. Discussion started: 15 April 2025


Xiao, W., Xu, Y., Zhang, C., Lin, J., Wu, W., Lü, X., Tan, J., Zhang, X., Zheng, F., Song, X., Zhu, Y., Yang, Y., Zhang, H., Wenzhöfer, F., Rowden, A. A., and Glud, R. N.: Disentangling Effects of Sea Surface Temperature and Water Depth on Hydroxylated Isoprenoid GDGTs: Insights From the Hadal Zone and Global Sediments, Geophysical Research Letters, 50, e2023GL103109, https://doi.org/10.1029/2023GL103109, 2023.

Xiao, W., Xu, Y., Canfield, D. E., Wenzhöfer, F., Zhang, C., and Glud, R. N.: Strong linkage between benthic oxygen uptake and bacterial tetraether lipids in deep-sea trench regions, Nature Communications, 15, 3439, 10.1038/s41467-024-47660-3, 2024.

Xie, S., Liu, X.-L., Schubotz, F., Wakeham, S. G., and Hinrichs, K.-U.: Distribution of glycerol ether lipids in the oxygen minimum zone of the Eastern Tropical North Pacific Ocean, Organic Geochemistry, 71, 60-71, https://doi.org/10.1016/j.orggeochem.2014.04.006, 2014.

Xu, Y., Wu, W., Xiao, W., Ge, H., Wei, Y., Yin, X., Yao, H., Lipp, J. S., Pan, B., and Hinrichs, K.-U.: Intact Ether Lipids in Trench Sediments Related to Archaeal Community and Environmental Conditions in the Deepest Ocean, Journal of Geophysical Research: Biogeosciences, 125, e2019JG005431, https://doi.org/10.1029/2019JG005431, 2020.

Yang, Y., Gao, C., Dang, X., Ruan, X., Lü, X., Xie, S., Li, X., Yao, Y., and Yang, H.: Assessing hydroxylated isoprenoid GDGTs as a paleothermometer for the tropical South China Sea, Organic Geochemistry, 115, 156-165, https://doi.org/10.1016/j.orggeochem.2017.10.014, 2018.

Yedema, Y. W., Sangiorgi, F., Sluijs, A., Sinninghe Damsté, J. S., and Peterse, F.: The dispersal of fluvially discharged and marine, shelf-produced particulate organic matter in the northern Gulf of Mexico, Biogeosciences, 20, 663-686, 10.5194/bg-20-663-2023, 2023.

Zell, C., Kim, J. H., Hollander, D., Lorenzoni, L., Baker, P., Silva, C. G., Nittrouer, C., and Sinninghe Damsté, J. S.: Sources and distributions of branched and isoprenoid tetraether lipids on the Amazon shelf and fan: Implications for the use of GDGT-based proxies in marine sediments, Geochimica et Cosmochimica Acta, 139, 293-312, 10.1016/j.gca.2014.04.038, 2014.

Zeng, Z., Liu, X.-L., Farley, K. R., Wei, J. H., Metcalf, W. W., Summons, R. E., and Welander, P. V.: GDGT cyclization proteins identify the dominant archaeal sources of tetraether lipids in the ocean, Proceedings of the National Academy of Sciences of the United States of America, 116, 22505-22511, 2019.

Zhang, C., Wang, J., Wei, Y., Zhu, C., Huang, L., and Dong, H.: Production of Branched Tetraether Lipids in the Lower Pearl River and Estuary: Effects of Extraction Methods and Impact on bGDGT Proxies, Frontiers in Microbiology, 2, 10.3389/fmicb.2011.00274, 2012.

Zhang, Y. G., Zhang, C. L., Liu, X. L., Li, L., Hinrichs, K. U., and Noakes, J. E.: Methane Index: A tetraether archaeal lipid biomarker indicator for detecting the instability of marine gas hydrates, Earth and Planetary Science Letters, 307, 525-534, 10.1016/j.epsl.2011.05.031, 2011.

https://doi.org/10.5194/egusphere-2025-1467
Preprint. Discussion started: 15 April 2025


Zhang, Y. G., Pagani, M., and Liu, Z.: A 12-Million-Year Temperature History of the Tropical Pacific Ocean, Science, 344, 84-87, doi:10.1126/science.1246172, 2014.

Zhang, Y. G., Pagani, M., and Wang, Z.: Ring Index: A new strategy to evaluate the integrity of TEX 86 paleothermometry, Paleoceanography, 31, 220-232, 10.1002/2015PA002848, 2016.

Zhou, J. and Dong, L.: Molecular dynamics simulations reveal methylation in Me-GDGTs as a microbial low-temperature adaptation, Chemical Geology, 644, 121844, https://doi.org/10.1016/j.chemgeo.2023.121844, 2024.

Zhu, C., Weijers, J. W. H., Wagner, T., Pan, J.-M., Chen, J.-F., and Pancost, R. D.: Sources and distributions of tetraether lipids in surface sediments across a large river-dominated continental margin, Organic Geochemistry, 42, 376-386, https://doi.org/10.1016/j.orggeochem.2011.02.002, 2011.

Zhu, C., Wakeham, S. G., Elling, F. J., Basse, A., Mollenhauer, G., Versteegh, G. J. M., Könneke, M., and Hinrichs, K.-U.: Stratification of archaeal membrane lipids in the ocean and implications for adaptation and chemotaxonomy of planktonic archaea, Environmental Microbiology, 18, 4324-4336, https://doi.org/10.1111/1462-2920.13289, 2016.

Zhuang, G., Pagani, M., and Zhang, Y. G.: Monsoonal upwelling in the western Arabian Sea since the middle Miocene, Geology, 45, 655-658, 10.1130/g39013.1, 2017.